This is to certify that the
thesis entitled

INVESTIGATION OF THE ACUTE INJURY RESPONSE OF ARTICULAR CARTILAGE *IN VITRO* AND *IN VIVO*: ANALYSIS OF VARIOUS THERAPEUTIC TREATMENTS

presented by

Steven Anthony Rundell

has been accepted towards fulfillment
of the requirements for the

M.S. degree in Mechanical Engineering

Roger C. Haut
Major Professor's Signature

May 9, 2005
Date

INVESTIGATION OF THE ACUTE INJURY RESPONSE OF ARTICULAR CARTILAGE *IN VITRO* AND *IN VIVO*: ANALYSIS OF VARIOUS THERAPEUTIC TREATMENTS

By

Steven Anthony Rundell

A THESIS

Submitted to
Michigan State University
In partial fulfillment of the requirements
For the degree of

MASTER OF SCIENCE

Department of Mechanical Engineering

2005

ABSTRACT

INVESTIGATION OF THE ACUTE INJURY RESPONSE OF ARTICULAR CARTILAGE *IN VITRO* AND *IN VIVO*: ANALYSIS OF VARIOUS THERAPEUTIC TREATMENTS

By

Steven Anthony Rundell

Excessive mechanical loading to a joint can lead to matrix damage and chondrocyte death in articular cartilage. These injuries have been associated with the subsequent development of osteoarthritis. Understanding the mechanisms responsible for acute damage of cartilage is essential in the development of therapeutic methods to either prevent or treat these early alterations. The research presented in the current thesis uses both the *in vitro* chondral explant and *in vivo* rabbit models to examine the acute response of articular cartilage to blunt impact loading. Chapter 1 addressed the issue of injury severity in chondral explants exposed to a culture medium prior to mechanical loading versus explants taken directly from the joint. This study hypothesized that excess fluid present in explants allowed to bathe in a culture medium would result in an artificially high amount of surface fissuring and associated chondrocyte death. Chapter 2 describes experiments in which knee joints of giant Flemish rabbits were subjected to a 6 Joule intensity impact and retro-patellar cartilage was studied in terms of surface fissuring as well as chondrocyte death. This study also evaluated the efficacy of a mild non-ionic surfactant, poloxamer 188, which has been found to reduce chondrocyte death *in vitro* by repairing damaged cells after an impact. Chapter 3 evaluated the efficacy of the nutraceutical glucosamine in enhancing the mechanical integrity of cartilage explants when pre-treated for a period of 6 days prior to an injurious unconfined compression test.

DEDICATION

I would like to thank my parents who have always supported me in every decision I have made. I would also like to thank them for instilling a good work ethic in me and exposing me to so many great opportunities.

ACKNOWLEDGMENTS

I would like to acknowledge my professor, mentor and good friend Dr. Roger Haut.

I am extremely grateful to Dr. Mike Orth and Dr. Neil Wright for serving on my committee.

I would like to express my gratitude towards Clifford Becket who not only contains a vast amount of knowledge but was always willing to share it with me.

I would also like to thank Jane Walsh and Jean Atkinson for all their hard work and dedication.

I would like to thank the undergrads that supplied me with great data and did a lot of hard work: Austin McPhillamy, Aaron Stewart, Jo Ewen, Michelle Foncannon, and Zach Kaltz

Last but not least I would like to acknowledge my fellow graduate students for their help and friendship: Derek Baars, Jill Krueger, Dan Phillips, Eric Meyer, Lynn Martin, Mike Sinnot, and Eugene Kepich.

TABLE OF CONTENTS

LIST OF TABLES

LIST OF FIGURES

CHAPTER 1

CHAPTER 2

CHAPTER 3

LIST OF PUBLICATIONS

Peer Reviewed Manuscripts

Rundell, S., Haut R.C., 2004. Tissue equilibration alters the response of cartilage explants to unconfined compression. Journal of Biomechanics, In Revision

Jex, C.T., Rundell, S., Wan, C., MacDonald, B., Haut, R.C., 2004. The effect of fixation types on the biomechanical properties of the Weil osteotomy. Journal of Foot and Ankle Surgery, In Revision

Rundell, S., Baars, D., Phillips, D., Haut, R.C., 2004. Repair of damaged chondrocytes in the in vivo traumatized joint. Journal of Orthopaedic Research, In Revision.

Baars, D., Rundell, S., Haut, R.C., 2005. Treatment with the non-ionic surfactant Poloxamer p188 reduces TUNEL positive cells in bovine chondral explants exposed to injurious unconfined compression. Biomechanics and Modeling in Mechanobiology, In Review

Peer Reviewed Abstracts

Rundell, S., Haut R.C., Tissue equilibration alters the response of cartilage explants to unconfined compression. 51st Annual Meeting of the Orthopaedic Research Society, 2005

Rundell, S., McPhilamy, A., Orth, M., Haut, R.C., Glucosamine supplementation can help limit matrix damage and adjacent cell death in traumatized explants. 51st Annual Meeting of the Orthopaedic Research Society, 2005

Introduction

Lower extremity injuries account for approximately $21.5 billion each year in treatment, rehabilitation, and lost work day expenses (Miller, 1995). These injuries are a frequent outcome of automobile accidents, comprising nearly 25% of the total injuries (Luchter et al., 1995). A more recent analysis of the National Accident Sampling System database has found that 10% of these injuries involve trauma to the knee joint, while only 5% of these injuries result in fracture. The Federal Safety Standard requires that femur forces generated during a knee-instrument panel collision must not exceed 10 kN, a force that has been shown to result in gross fracture of the patella, femur, or pelvis (Melvin et al., 1975; Patrick et al., 1965; Powell et al., 1975). However, the presence of chronic joint disease has been found in patients that have only suffered from a sub-fracture knee injury (States, 1970).

Osteoarthritis (OA) is a chronic joint disease characterized by the loss of articular cartilage. Articular cartilage is the connective tissue that lines the ends of bones in diarthroidial joints. Its function is to provide a near frictionless surface on which bones can glide over, as well as absorb the shock from physical motion. Cartilage consists of a solid organic matrix and free interstitial fluid, which is mostly water. The solid matrix mainly consists of collagen (type II) and proteoglycans (PGs) (Mow et al., 1990). The PGs attract water and repel each other due to their electro-negativity. The network of collagen fibers resists this swelling (Grodzinsky et al., 1978), and gives cartilage its compressive stiffness. Chondrocytes (cartilage cells) are imbedded in the solid matrix and are responsible for synthesis and degradation of the solid matrix constituents. It has been

suggested that the pathogenesis of OA is the result of an imbalance in solid matrix turnover with degradation exceeding synthesis (Goldring, 2000; Malemud 1999).

Clinically OA is characterized by joint pain and narrowing of the joint, as diagnosed by radiological examination (Flores and Hochber, 1998). Pathologically, the disease exhibits a loss of cartilage and sclerosis of underlying bone. While the etiology of OA is not fully understood the risk of developing this disease is increased significantly in joints suffering a major injury (Felson et al., 2004). However, establishing a cause and effect relationship between joint injury and OA can be difficult as after an osteochondral injury, joint disease may not be diagnosed for 2 to 5 years, while less severe joint injuries may not be diagnosed for 10 or more years after the trauma (Wright, 1990).

Animal models have been developed in order to study the associations between blunt impact trauma to a joint and the subsequent development of chronic joint disease. In a recent study a rigid impact mass was dropped with a 6 Joule intensity onto the flexed patello-femoral joint of a giant Flemish rabbit (Ewers et al., 2002). This study documented a progressive increase in the degradation of retro-patellar surface cartilage and the thickening of underlying subchondral bone after 3 years. A separate study that used a New Zealand white rabbit model and a 10 Joule impact intensity, found significantly advanced OA-like changes in the patello-femoral joint, with fibrillation, ulceration and erosion of retro-patellar cartilage within 6 months post-contusion (Mazieres et al., 1987)). Early OA-like changes have also been described using the flexed canine patello-femoral joint subjected to approximately 2.2 kN of impact force delivered with a gravity-dropped rigid mass (Thompson et al., 1991). While these studies

indicate a link between blunt impact trauma to a joint and a subsequent degradation of joint tissue, the mechanisms responsible are still unclear.

Studies that examine the acute response of articular cartilage after a blunt impact to a joint both *in vivo* and *in situ* document gross surface lesions on the cartilage surface (Atkinson and Haut, 2001; Newberry et al., 1998). Also, *In vitro* chondral and osteochondral explant models have been developed in order to examine the acute response of injurious loading on articular cartilage. Studies that have subjected either chondral or osteochondral explants to an injurious level of unconfined compression have documented surface fissuring across the surface, as well as associated chondrocyte death (Ewers et al., 2001; Krueger et al., 2003). Acute chondrocyte death, or necrosis, has also been linked to degradation of articular cartilage after 1 year *in vivo* (Simon et al., 1976). These studies found that a severe impact to a joint will result in gross fissuring of the articular cartilage, as well as a reduction in chondrocyte viability. While the exact mechanisms responsible for long term degradation of articular cartilage after a blunt impact are not fully understood, the acute development of surface fissuring and chondrocyte death are among the suspected factors.

Matrix damage in the form of surface fissuring has been suggested to occur when the interstitial fluid pressurization in cartilage developed during loading becomes too great and exceeds the restraining capacity of the collagen network (Morel and Quinn, 2004; Pins et al., 1995). A study that exposed cartilage explants to varying rates of injurious loading documents an increased likelihood of surface fissuring at rates of loading that exceed the gel diffusion rate (Morel and Quinn, 2004). Theoretical models that simulate the effects of a blunt impact on an intact joint document the presence of

high shear (distortional) strains near the articular surface, when cartilage is modeled as transversely isotropic and biphasic (Garcia et al., 1998; Donzelli et al., 1999). Interestingly, acute chondrocyte death has been found to occur predominately around surface cracks when cartilage is loaded at a high rate (Ewers et al., 2001; Lewis et al., 2003). However, when the rate of loading is slower and closer to the gel diffusion rate a more diffuse pattern of chondrocyte death throughout the thickness has been found (Morel and Quinn, 2004: Quinn et al., 2001). In a recent study that performed confined compression on chondral explants it was documented that cell death in the superficial zone occurred only when water was allowed to flow out (Milentijevic and Torzilli, 2005). This study suggests that chondrocyte death can either occur by compaction of the superficial zone, which occurs when water flows out, or by collagen tensile failure where chondrocyte death occurs around cracks. This study also suggests that hydrostatic pressure generated during a high rate of loading has a protective effect on cells, where as at slower rates water is allowed to flow which gives rise to distortional strains.

Understanding the mechanisms responsible for acute damage of cartilage and associated chondrocyte death are essential in the future development of therapeutic methods to either prevent or treat these early alterations. The research presented in the current thesis uses both the *in vitro* chondral explant and *in vivo* rabbit models to examine the acute response of articular cartilage to blunt impact loading. Chapter 1 addressed the issue of injury severity in chondral explants exposed to a culture medium prior to mechanical loading versus explants taken directly from the joint. This study hypothesized that excess fluid present in explants allowed to bathe in a culture medium would result in an artificially high amount of surface fissuring and associated

chondrocyte death. Chapter 2 describes experiments in which knee joints of giant Flemish rabbits were subjected to a 6 Joule intensity impact and retro-patellar cartilage was studied in terms of surface fissuring as well as chondrocyte death. No previous studies have attempted to document acute chondrocyte death as a result of a blunt impact in an *in vivo* model. This study also evaluated the efficacy of a mild non-ionic surfactant, poloxamer 188, which has been found to reduced chondrocyte death *in vitro* (Phillips and Haut, 2004), in 'repairing' damaged cells after an impact *in vivo*. Chapter 3 evaluated the efficacy of the nutraceutical glucosamine in enhancing the mechanical integrity of cartilage explants when pre-treated for a period of 6 days prior to an injurious unconfined compression test.

The research presented in this thesis provides useful data in regards to the response of articular cartilage to blunt impact loading in both an *in vivo* and an *in vitro* setting. Furthermore, potential therapeutic treatments have been investigated and found to be effective in preventing damage that may result in long term degradation of articular cartilage. Future studies can utilize the data presented in this thesis to design experiments that will further help explain the mechanisms responsible for the efficacy of these treatments.

References

Atkinson PJ, Haut RC, 2001. Injuries produced by blunt trauma to the human patellofemoral joint vary with flexion angle of the knee. J Orthop Res Sep;19(5):827-33

Donzelli PS, Spilker RL, Ateshian GA, Mow VC, 1999. Contact analysis of biphasic transversely isotropic cartilage layers and correlations with tissue failure. J Biomech 32(10):1037-47

Ewers BJ, Dvoracek-Driksna D, Orth MW, Haut RC, 2001. The extent of matrix damage and chondrocyte death in mechanically traumatized articular cartilage explants depends on rate of loading. J Orthop Res 19:779-84

Ewers BJ, Weaver BT, Sevensma ET, Haut RC, 2002. Chronic changes in rabbit retro-patellar cartilage and subchondral bone after blunt impact loading of the patellofemoral joint. J Orthop Res 20:545-50

Felson DT, 2004. An update on the pathogenesis and epidemiology of osteoarthritis. Radiol Clin North Am 42:1-9

Flores R, Hochber M, 1998. Definition and classification of osteoarthritis. In: Brandt K, Doherty M, Lohmander S, editors. Osteoarthritis. Oxford: Oxford University Press: p. 1–12.

Garcia JJ, Altiero NJ, Haut RC, 1998. An approach for the stress analysis of transversely isotropic biphasic cartilage under impact load. J Biomech Eng 120(5):608-13

Grodzinsky AJ, Lipshitz H, Glimcher MJ, 1978. Electromechanical properties of articular cartilage during compression and stress relaxation. Nature 275(5679):448-50

Goldring MB, 2000. The role of the chondrocyte in osteoarthritis. Arthritis Rheum 43:1916-26

Krueger JA, Thisse P, Ewers BJ, Dvoracek-Driksna D, Orth MW, Haut RC, 2003. The extent and distribution of cell death and matrix damage in impacted chondral explants varies with the presence of underlying bone. J Biomech Eng 125:114-9

Lewis, J.L, Deloria, LB, Oyen-Tiesma, M, Thompson, RC, Jr., Ericson, M, Oegema TR, Jr., 2003. Cell death after cartilage impact occurs around matrix cracks. J Orthop Res 21, 881-7

Luchter S, Walz MC, 1995. Long-term consequences of head injury. J Neurotrauma. 12(4):517-26

Malumed CJ, 1999. Fundamental pathways in osteoarthritis: an overview. Front Biosci 15: D659-61

Mazieres B, Blanckaert A, Thiechart M, 1987. Experimental post-contusive osteo-arthritis of the knee. Quantitative microscopic study of the patella and the femoral condyles. J Rheum 14:119-21

Melvin J, Stalnaker R, Alem N, Benson J, Mohan D, 1975. Impact response and tolerance of the lower extremities. 19th annual Stapp Car Crash Conf. 19:543-559

Milentijevic D, Torzilli PA, 2005. Influence of stress rate on water loss, matrix deformation and chondrocyte viability in impacted articular cartilage. J Biomech 38, 493-502

Miller TR, Levy DT, 1995. The effect of regional trauma care systems on costs. Arch Surg 130(2):188-93.

Morel V, Quinn TM, 2004. Cartilage injury by ramp compression near the gel diffusion rate. J Orthop Res 22:145-151

Mow VC, 1990. Fundamentals of articular cartilage and meniscus biomechanics, in: Articular Cartilage and Knee Joint Function: Basic Science and Arthroscopy, J.W. Ewing, ed., Raven Press, Ltd., New York, pp1-18.

Newberry WN, Garcia JJ, Mackenzie CD, Decamp CE, Haut RC, 1998. Analysis of acute mechanical insult in an animal model of post-traumatic osteoarthrosis. J Biomech Eng 120(6):704-9

Patrick LM, Koell CK, Mertz HJ Jr., 1965. Forces on the human body in simulated crashes. 9th Annual Stapp Car Crash Conf. 12:237-259

Phillips DM, Haut RC, 2004. The use of a non-ionic surfactant (P188) to save chondrocytes from necrosis following impact loading of chondral explants. J Orthop Res 22:1135-42

Pins GD, Huang EK, Christiansen DL, Silver FH, 1995. Effects of static axial strain on the tensile properties and failure mechanisms of self-assembled collagen fibers. J Appl Polym Sci 63:1429–40

Powell WR, Ojala SJ, Advani SH, 1975. Cadaver femur responses to longitudinal impacts. 19th Annual Stapp Car Crash Conf. 19:561-579

Quinn TM, Allen RG, Schalet BJ, 2001. Matrix and cell injury due to sub-impact loading of adult bovine articular cartilage explants: effects of strain rate and peak stress. J Orthop Res 19(2):242–9

Simon WH, Richardson S, Herman W, Parsons JR, Lane J, 1976. Long-term effects of chondrocyte death on rabbit articular cartilage in vivo. J Bone Joint Surg Am 58:517-26

States JD, 1970. Traumatic arthritis: a medical dilemma, In: Proceedings of the 14th Annual Conference of the American Association for Automotive Medicine. 14:21-28

Thompson RC, Oegema T, Lewis J, Wallace L, 1991. Osteoarthritic changes after acute transarticular load. J Bone Joint Surg Am 73:990-1001

Wright V, 1990. Post-traumatic osteoarthritis- A medico-legal minefield. Br J Rheum 29:474-8

CHAPTER 1: TISSUE EQUILIBRATION ALTERS THE RESPONSE OF CARTILAGE EXPLANTS TO UNCONFINED COMPRESSION

Abstract:

Excessive mechanical loading can lead to matrix damage and chondrocyte death in articular cartilage. Previous studies on chondral explants have not clearly distinguished to what extent the degree and the distribution of cell death are dependent on the amount of free swelling seen during tissue equilibration. The current study hypothesized that increased fluid content inside equilibrated chondral explants, when subjected to injurious compression, would lead to greater matrix damage. Equilibrated and non-equilibrated chondral explants were loaded to 30MPa at a fast rate of loading (~600MPa/s) in an unconfined compression experiment. Stress-strain curves were created for each explant, and fit with a hyperelastic Ogden function using a least squares method. After 24 hours in a culture medium, matrix damage was assessed by the total length of surface fissures. The explants were also sectioned and stained for cell viability in the various layers of the cartilage. A separate group of explants was exposed to a displacement controlled unconfined compression experiment at a fast rate of loading (1200%ε/s). These explants were dried out immediately after loading in order to separate contributions of the solid and fluid phase to the mechanical response. The stiffness of the equilibrated specimens was less than non-equilibrated specimens, and it correlated with the amount of fluid taken in during equilibration. More matrix damage in the form of surface fissuring and cell death in the superficial zone was documented in equilibrated explants. Matrix damage correlated positively with fluid gained during equilibration. The amount of cell death in the deep layer of the cartilage was less in equilibrated versus non-equilibrated explants,

and also depended on the amount of fluid the specimens took in during equilibration. Correlations between peak stress and the percentage of water in the explant as well as dry weight in the displacement controlled tests were documented to decrease when explants were allowed to equilibrate. This study indicated that equilibration alters explant response to mechanical loading in terms of stiffness, matrix damage and cell viability. The alterations in response depend on percentage uptake of fluid during tissue equilibration. These data may have relevance to the applicability of experimental data from equilibrated chondral explants to the *in vivo* condition.

Introduction:

In early stages of osteoarthritis (OA), matrix damage is often seen as fissures on the articular surface (Brandt et al., 1986). Chondrocyte death, resulting from a reduction in tissue cellularity or chondrocyte malfunction, has been suggested to facilitate development of OA (Blanco et al., 1998; Buckwalter 1995). Excessive levels of mechanical load can generate acute matrix damage and chondrocyte death in articular cartilage (Ewers et al., 2001). However, establishing a cause and effect relationship between impact trauma and development of OA has been difficult as joint injuries with bone fracture may require 2-5 years to develop clinical symptoms, while less severe injuries may not be diagnosed for 10 or more years after trauma (Wright, 1990). Therefore, animal models have been used to study the potential association of trauma and disease. For example, blunt impact to the rabbit patello-femoral joint has indicated acute surface fissuring and a subsequent chronic degradation of the traumatized articular cartilage with thickening of the underlying subchondral bone (Newberry et al., 1998). Computational models of the joint have been developed to help investigate correlations

between the acute state of stress and strain with the subsequent changes in joint tissues (Newberry et al., 1998), but these models are complex and not yet validated.

To help clarify potential associations between mechanical events and early alterations in joint tissue, chondral (Ewers et al., 2001; Milentijevic et al., 2003; D'Lima et al., 2001) and osteochondral (Kreuger et al., 2003; Clements et al., 2001) explant models have also been developed for the laboratory setting. While these experimental models provide more ideal geometries for mechanical analyses, they are in vitro models that may not adequately represent the in vivo situation. In a study that compared the amounts of matrix damage and cell death in chondral versus osteochondral explants when exposed to 30 MPa of pressure, the presence of underlying bone reduced matrix damage and cell death (Krueger et al., 2003). Similarly in situ cadaveric human joint studies show minimal surface fissuring at contact pressures in the range of 20 to 30 MPa (Atkinson and Haut 2001, Atkinson and Haut 1995). Also, an in vivo rabbit study documented minimal or no occurrence of surface fissuring on the retropatellar surface at pressures of approximately 30 MPa delivered in roughly 50 milliseconds (Ewers et al., 2002). A study which used similar rates and amplitudes of loading on chondral explants documented excessive fissuring throughout the whole explant surface (Ewers et al, 2001). Even studies using osteochondral explants exposed to the same level of high rate unconfined compression experienced substantial surface damage (Krueger et al., 2003). One possible explanation for differences in the extent of surface fissuring in in situ and in vitro models may be the amount of tissue fluid present in the in situ joint cartilage versus that of explanted tissue bathed for a period of time in a standard culture medium. This procedure is common in cartilage explant studies (Borelli et al., 1997; Bush and Hall,

2003; DiMicco et al., 2004: Sauerland et al., 2003) and is typically referred to as tissue equilibration.

Interstitial fluid pressurization has been shown to contribute to the functional response of articular cartilage (Mansour and Mow, 1976; Mow et al. 1980; Zarek and Edward, 1963). This pressurization is the result of polyanionic glycosaminoglycans which create an electrostatic tissue swelling and resistance to compression. When collagen fibers are damaged, they lose their ability to resist swelling. This phenomenon has been documented in a number of studies. Grushko and co-workers (1989) noted that damaged or fibrillated human cartilage plugs swelled when placed in physiological saline. Sah and co-workers (1989) showed a swelling of excised bovine articular cartilage when placed in physiologic saline. Swelling of articular cartilage has been observed to be non-uniform and anisotropic (Myers et al., 1984, Maroudas et al., 1986) which characterizes the non-uniform organization of collagen (Clark, 1991; Clark, 1990) and the non-uniform distribution of negatively charged proteoglycans (Maroudas et al 1969). It follows that when explanting cartilage from a joint, the collagen matrix is disrupted allowing for changes in fluid content that arises when the tissue is bathed in a standard culture medium.

Articular cartilage consists of a solid and fluid phase which, due to their interation, determines the mechanical characteristics of the tissue. Theoretical and computational analyses have separated the contributions of the fluid and solid phase in load bearing, and found that the fluid phase is responsible for approximately 90% of the load bearing (Ateshian et al., 1994; Ateshian and Wang, 1995; Macirowski et al., 1994). It is believed that interstitial fluid pressurization is the dominant mechanism of load

support (Park et al., 2003). Current studies, which induce or inhibit cartilage swelling by varying levels of NaCl concentrations in tissue baths (Maroudas, 1975; Lee et al., 1981), find significant effects occur in the tissue's mechanical response characteristics. Given that the fluid content and the associated interstitial fluid pressurization has such a large effect on the load bearing capacity of this tissue, any changes in these parameters may result in an altered mechanical response during blunt impact. In addition, matrix damage in the form of surface fissuring, has been attributed to fluid pressurization and a subsequent tensile damage to the collagen network when the tissue is subjected to blunt impact loading (Morel and Quinn, 2004). Increases in cartilage explant fluid contentresulting from tissue equilibration, could potentially result in increased surface fissuring during high rates of unconfined compression. A previous study has shown that cell death in an intact bovine patella occurs exclusively around impact induced surface cracks (Lewis et al., 2003) suggesting that if in fact increased fluid results in a higher incidence of surface fissuring there will likely be an associated increase in chondrocyte death.

The hypothesis of the current study was that excised chondral explants would swell in the medium during equilibration and the increase in fluid content would then alter the mechanical response of the explants resulting in greater matrix damage for equilibrated explants versus non-equilibrated tissue when exposed to a high rate of injurious compression.

Methods and Materials:

Three pairs of skeletally mature (12-24 months) bovine forelegs were obtained from a local abattoir within 3 hours of slaughter. The legs were cut proximal to the

metacarpal surface leaving the joint intact. The legs were rinsed with distilled water, skinned, and rinsed again prior to opening the joint under a laminar flow hood. A 6-mm biopsy punch was used to make 52 cartilage plugs. These plugs were removed from the underlying bone with a scalpel and divided evenly into two groups, equilibrated and non-equilibrated. All explants were weighed immediately after removal from the joint.

Twenty-six explants were assigned to a so-called "equilibrated" group. These were placed in Dulbecco's Modified Eagle's Medium (DMEM): F12 (Gibco, USA #12500-039) supplemented with 10 % fetal bovine serum, additional amino acids, and antibiotics (penicillin 100 units/ml, streptomycin 1μg/ml, amphotericin B 0.25 μg/ml). They were then washed three times, and allowed to equilibrate for one day in a humidity-controlled incubator (37° C, 7.2% CO_2, NuAire, Plymouth, MN). After equilibration these specimens were subjected to mechanical loading and returned to incubation for another 24 hours. They were then evaluated in terms of surface damage and cell viability.

Another group of twenty-six were assigned to the "non-equilibrated" group. These explants were taken directly to a servo-hydraulic machine (Instron, model 1331 with 8500 upgraded electronics) for immediate mechanical testing of the explants. Tests were performed immediately after removal from the bone for each explant in order to avoid potential drying out. These specimens were then placed in supplemented DMEM:F12 and incubated for twenty-four hours before being examined for cell viability and matrix damage. Six equilibrated and non-equilibrated specimens were chosen as non-impact controls. These explants followed the same procedure as their respective groups with the exception of receiving impact.

The unconfined compression experiments were performed with a high rate of loading (50 ms to peak, ~600MPa/s). Each explant was placed between two highly polished stainless steel plates (figure 1). Prior to the test, the plates were pressed together at 100 N and the location of the machine actuator was recorded. The thickness of each specimen was determined by finding the difference in the actuator's location at 5 N of load during the test and when the plates were pressed together prior to loading. Each specimen received a 0.5 N preload before being compressed to a peak load of 857N (~30MPa) using a single haversine load-time pulse. This protocol has been established in previous experiments from this laboratory (Ewers et al., 2001; Krueger et al., 2003). The load, time, and actuator displacement were recorded during each experiment with an accuracy of 0.1 N, 0.001 s, and 0.01 mm, respectively. After loading, each explant was washed three times in media before being returned to pre-assigned wells with one ml of supplemented media and incubated for an additional 24 hours.

Twenty-four hours after the mechanical compression experiment, each explant was examined for matrix damage and cell viability. The surface of each explant was wiped with India ink. The explants were immediately photographed at 25X under a dissection microscope (Wild M5A, Wild Heerbrugg Ltd., Switzerland) to determine the total length of the surface fissures (figure 2). The total fissure length was measured with digital imaging software (Sigma Scan, SPSS Inc., Chicago, IL). One observer (AM) digitally recorded the length of the surface fissures in each photograph.

For cell viability, two 0.5-mm slices were taken through the thickness at the center of each explant using a customized cutting tool (Ewers et al., 2001). The sections were stained with a kit containing calcein and ethidium bromide homodimer (Live/Dead

&Viability/Cytotoxity, Molecular Probes, Oregon). Each section was viewed under a fluorescence microscope at 100X (Lecia DM LB (frequency: 50-60 Hz), Lecia Mikroskopie and Systeme GmgH, Germany). Full thickness, digital images were taken of a 2.5-mm length at the center of each explant. These images were partitioned into the superficial zone (top 20%), intermediate zone (middle 50%), and deep zone (bottom 30%). The viable (green) and dead (red) cells were manually counted by one observer (AS) using image software (Sigma Scan, SPSS Inc., Chicago, IL) (Figure 3). The percent of cell death was computed for each layer.

Stress-strain curves were determined using the collected load and displacement data from the unconfined compression tests of the equilibrated and non-equilibrated explants (Figure 4). Compressive stress and corresponding strain were determined at 1, 5, 10, 15, and 20 MPa and used to generate an average response curve for each group of explants. To help quantify the overall responses of each group of explants during unconfined compression the stress-strain data were curve fit to a hyperelastic Ogden function using a least squares method,

$$\sigma(\mu,\alpha,\varepsilon) = \frac{2\mu}{\alpha}\left[(1+\varepsilon)^{\alpha-1} - (1+\varepsilon)^{-0.5\alpha-1}\right]$$

where σ is the compressive stress, ε is compressive strain, μ is a shear modulus parameter, and α is the stiffening factor. In order to ensure that the values for μ and α converged, the initial guesses, determined from a preliminary analysis, were multiplied by a random constant between 0.1 and 10 before conducting the curve fitting procedure. The process was repeated 100 times for each curve fit in order to obtain a guess that resulted in the minimum amount of error (Abramowitch and Woo, 2004). All guesses

tried in this range resulted in the same values for μ and α. R squared values were calculated for each curve in order to quantify the goodness of fit. The overall error (SSE) was calculated by subtracting the theoretical stress from the actual stress at 1, 5, 10, 15, and 20 MPa and summing all the values. In order to quantify the goodness of fit of the curve, the r squared value was calculated. The r squared value (R^2) was calculated by taking the ratio of the sum of squares of the regression (*SSR*) and the total sum of squares (*SST*).

$$SSR = \sum_{i=1}^{n} (\sigma_{th}(\mu, \alpha, \varepsilon)_i - \sigma_{avg})^2$$

$$SST = \sum_{i=1}^{n} (\sigma_{(actual)_i} - \sigma_{avg})^2$$

$$R^2 = \frac{SSR}{SST}$$

Unpaired t-tests were used to compare the peak strain, fissure length, μ, α, and total cell death for equilibrated and non-equilibrated explants. Repeated factors ANOVA was used to compare cell death between the different layers through the thickness. Pearson correlation tests were performed in order to determine statistical significance of correlations between parameters within each group of explants. All data were reported as mean $\pm$ one standard deviation. Statistical significance was indicated at $p<0.05$.

Controlled Displacement Tests

A separate group of a total of 96 (48 equilibrated and 48 un-equilibrated) explants from 4 bovine forelegs were subjected to a displacement controlled unconfined

compression experiment. The unconfined compression experiments were performed with a high rate of loading (50 ms to peak displacement, ~1200%ε/s). Each explant was placed between two highly polished stainless steel plates (Figure 1). Prior to the test, the plates were pressed together at 100 N and the location of the machine actuator was recorded. The thickness of each specimen was determined by finding the difference in the actuator's location at a preload of -0.5 N and when the plates were pressed together. Using the thickness of each explant the actuator arm was programmed to travel a total displacement corresponding to 60% strain (ε) for each individual explant. Each specimen received a 0.5 N preload before being compressed to a peak strain of 60% using a single haversine load-time pulse. The load, time, and actuator displacement were recorded during each experiment with an accuracy of 0.1 N, 0.001 s, and 0.01 mm, respectively. After loading, each explant was dried out in a vacuum oven for 24 hours in order to determine the dry weight (DW).

Besides differences in mechanical loading equilibrated and non-equilibrated explants used in these tests underwent the same procedure as previously described. Dry weights were obtained for these specimens in order to calculate the percentage of fluid present in the explant at the time of mechanical loading. Data from these tests was used to separate contributions of the fluid and solid phase to the mechanical response of cartilage explants. Chondrocyte viability and matrix damage were not assessed because this does not allow for the full explant to be dried out after mechanical loading. Pearson correlation tests were performed to find correlations between peak stress and explant thickness, explant weight, dry weight, percent fluid content, and percent fluid gained during equilibration. Statistical significance was indicated at $p<0.05$.

Results:

The peak stress generated during loading for the equilibrated group (28.86 ± 0.71 MPa, n=20) was not significantly different than that for the non-equilibrated group (29.08± 0.32 MPa, n=20). Nonlinear stress-strain curves were generated for explants with and without equilibration. Equilibration decreased the explant stiffness by producing a shift in the response curves to the right (Figure 5). The maximum strain for the equilibrated explants (62 ± 13 %, n=20) was significantly different than that for the non-equilibrated explants (56 ± 6 %, n=20). There was no significant differences in the average thickness of the equilibrated explants (0.56 ± 0.11 mm, n=20) versus that of the non-equilibrated explants (0.59 ± 0.09 mm, n=20). The Ogden function fit the data with a high degree of accuracy. The r^2 values for both the equilibrated and non-equilibrated explant response curves were 0.99 ± 0.01 (n=20). All r^2 values for individual tests were above 0.95. The shear modulus parameter, μ, for the equilibrated group (2.0 ± 0.9 MPa, n=20) was significantly different than for the non-equilibrated group (2.9 ± 0.9 MPa, n=20). The value of α for the equilibrated group (-2.1 ± 0.8 MPa, n=20) was not significantly different than that for the non-equilibrated group (-2.5 ± 0.7 MPa, n=20).

The average fluid gain for the equilibrated group was 13 ± 5 % (n=20). All values were positive. The shear modulus parameter, μ, significantly correlated inversely (r^2 = 0.44, p = 0.001) with fluid gain for the equilibrated group (Figure 6). The peak strain, on the other hand, significantly correlated positively (r^2 = 0.53, p < 0.001) with fluid gain in the equilibrated group (Figure 7).

Equilibration of the chondral explants also significantly increased the degree of surface fissuring for a 30 MPa unconfined compression compared to non-equilibrated specimens (Figure 8). The total length of surface fissuring for the equilibrated group was 57.6 ± 15.2mm (n=20) versus 45.1 ± 17.8mm (n=20) for the non-equilibrated group (p=0.022). In the equilibrated group, there was a significant positive correlation (r^2 = 0.40, p = 0.003) between the length of surface fissuring and the amount of fluid gained by the explant (Figure 9). There were no visible surface fissures observed on the surfaces of the non-impacted specimens for either group of chondral explants.

There was no significant difference (p = 0.53) in the percentage of total cell death in equilibrated (17 ± 6 %, n=20) and non-equilibrated groups of explants (19 ± 9 %, n=20). Significantly (p=0.006) less cell death, however, was noted in the deep zone of the equilibrated explants (12 ± 10 %, n=20) (Figure 10) versus the non-equilibrated explants (25 ± 17 %, n=20) (Figure 11). In contrast, a significant increase (p=0.016) in the percentage of cell death was documented in the superficial zone of the equilibrated group of explants (36 ± 12 %, n=20) versus the non-equilibrated group (27 ± 10 %, n=20). There was also a significant inverse correlation (r^2 = 0.36, p = 0.005) between fluid gain and the percentage of cell death in the deep zone for the equilibrated group of explants (Figure 12). No cell death was documented in the non-impacted explants from either group.

Controlled Displacement Tests

The peak strain generated during loading for the equilibrated group (62.5 ± 3.7 %, n=48) was not significantly different than that for the non-equilibrated group (61.4 ± 3.2 %, n=48). The average fluid gain for the equilibrated group was 12 ± 9 % (n=48). The

average thickness of the equilibrated explants (0.71 ± 0.11 mm, n=48) was significantly higher ($p<0.001$) versus that of the non-equilibrated explants (0.62 ± 0.10 mm, n=48). Significant correlations were found between peak stress and thickness, explant weight, dry weight, and percent fluid content for the non-equilibrated explants (Figure 13). Significant correlations were found between peak stress and thickness, dry weight, percent fluid content, and percent fluid gain for the equilibrated explants (Figure 14). The strength of the correlations, as determined by the r value, decreased in all instances for the equilibrated group of explants. The significance ($p<0.001$) of the correlation between explant weight and peak stress documented in the non-equilibrated explants was lost ($p=0.167$) in the equilibrated explants.

Discussion:

The objective of this study was to document differences in the biomechanical responses of chondral explants subjected to 30 MPa of unconfined compression that were either taken directly from the joint or equilibrated in a standard culture medium for 24 hours before impact loading. The hypothesis of the study was that excised chondral explants would swell in the medium during equilibration, and the increase in fluid content would then alter the mechanical response of the explants resulting in greater matrix damage for equilibrated explants versus non-equilibrated tissue during a high rate of unconfined compression. The current study confirmed that equilibration of chondral explants in a standard culture medium resulted in a significant uptake of fluid over 24 hours. The study also confirmed that the increased fluid content resulted in more matrix damage resulting from a 30 MPa unconfined compression, as documented by an increased extent of surface fissuring in equilibrated versus non-equilibrated explants.

All equilibrated explants gained weight during the 24 hour period of equilibration despite that the standard culture media used was hypertonic (300 mosM) with regards to an isotonic osmolarity of 150 mosM. Parsons and Black (1979) documented an increase in cartilage thickness in intact rabbit femoral condyles in hypotonic solutions (<150 mosM) and a corresponding decrease in hypertonic solutions (>150 mosM). However, many explant studies document swelling at both physiological and hypertonic osmolarities. A study by Torzilli et al. (1997), for example, shows that bovine chondral explants swell 10.2 ± 11.0% in the thickness direction and approximately 3.31 ± 2.67% radially when exposed to physiological saline (~150 mosM) for 30 minutes. In another study on calf cartilage disks swelling was observed axially 25-40% above the cut tissue thickness of 1.0 mm, when incubated in culture media (~300 mosM) for 6 days (Sah et al., 1989). In the current study the controlled displacement test equilibrated specimens experienced approximately a 14% increase in thickness during 24 hours in culture media. The current study documented a range in the amount of weight from 3 – 22% of the original wet weight. This large range of swelling was similar to the variations mentioned above in the previous studies by others. A study by Appleyard et al. (2003) documents site-specific trends in the contents of collagen and proteoglycans across the surface of articular cartilage on the ovine tibia. Similar findings were documented by Brama et al. (2000) for mature equine metacarpophalangeal joints. Areas of cartilage rich in collagen may better restrain tissue swelling in the bovine explant, but additional studies are needed to more completely explain variations in the percentage of fluid gain for various explants taken from different areas on the same joint surface.

The percent of dead cells in the deep zone following impact loading for equilibrated explants was substantially lower than that for non-equilibrated explants. This difference in deep zone cell death contrasted with a higher percentage of cell death in the superficial zone for the equilibrated versus non-equilibrated explants. Previous studies have documented the appearance of dead cells predominately around surface cracks (Ewers et al., 2001; Lewis et al., 2003) resulting from high rates of injurious compression. In the current study the increased length of surface fissures documented in the equilibrated explants helps explain the increase in the percentage of dead cells noted in the superficial zone. This, however, does not explain the seemingly protective effect of an increase in fluid volume on cells in the deep zone of equilibrated explants. Unfortunately, the mechanisms responsible for cell damage resulting from a blunt impact are yet unclear. The current data, in combination with previous studies that document zonal dependencies on the amount of free swelling in articular cartilage (Narmoneva et al., 1999), infer that susceptibility to cell death throughout the thickness of chondral explants during blunt impact may, in part, depend on local fluid content (Morel and Quinn, 2004). However, more research in this area is required in order to validate this hypothesis. The current study did suggest that changes in fluid content arising from 24 hours of equilibration in culture media had an effect on the levels of cell death throughout the thickness of chondral explants, but additional studies on mechanisms of cell death via blunt impact loading are warranted.

On average, the total length of surface fissuring on equilibrated explants was greater than that on non-equilibrated explants. Previous studies correlate the onset of surface fissures with the development of high tensile strains in the collagen fibril network

(Morel and Quinn, 2004; Askew and Mow, 1978; Eberhardt et al., 1991). Studies that have modeled *in situ* blunt impact loading have documented high tensile strains near the surface of the cartilage (Li et al., 1995; Atkinson et al., 1998). The compressive strain at a given stress (Figure 1), and consequently the in-plane tensile strain, based on the Poisson effect, was less for non-equilibrated cartilage possibly explaining the occurrence of more surface fissuring in the equilibrated explants. This, however, does not explain why equilibrated explants exhibited a less stiff response to high rates of mechanical loading. The precise reasons as to why an increased fluid content would result in softening of the tissue is not clear, however, it is possible that swelling created geometric differences in the collagenous microstructure. A study by Wilson et al. (2004) used a poroviscoelastic fibril reinforced model to show that local stress and strain fields in cartilage are highly influenced by collagen orientation. Interestingly the softening of the equilibrated explants was observed to occur in the initial response to loading. This was exhibited by a significant decrease in the instantaneous shear modulus (μ) with no significant difference in the stiffening factor (α) for equilibrated versus non-equilibrated explants. A possible explanation may be that fluid taken on by the explant during equilibration was more easily expelled during the initial phase of loading. Although theoretical models show that under impact loading cartilage responds as an incompressible elastic material (Armstrong et al., 1984; Mak et al., 1987), i.e., fluid cannot flow out, fluid taken on by chondral explants during equilibration may have substantially increased the initial permeability of the cartilage. Future studies may wish to observe swelling in the thickness direction and how it correlates to deformation during the initial loading phase. The current study suggests that the increased length of surface fissures documented in the equilibrated

versus non-equilibrated explants may have resulted from greater tensile stresses generated near the surface of equilibrated explants as a result of fluid gained during equilibration.

A high fluid content, as a result of a damaged collagen network, is one of the early alterations documented in osteoarthritis (Buckwalter, 1995; Bank et al., 2000). Equilibrated explants displayed a reduction in dynamic stiffness exhibited by a greater peak strain and a lower shear modulus parameter μ. Both of these quantities were correlated with the amount of fluid gained during tissue equilibration. Osteoarthritic cartilage has also been shown to exhibit a softening effect (Ateshian et al., 1994; Mow et al., 1992; Setton et al., 1993) associated with tissue "edema" (Maroudas et al., 1986; Mankin and Thrasher 1975). The present results may suggest that damage to the collagenous network and associated tissue matrix swelling that occurs in early stages of OA make diseased tissue more vulnerable to a blunt mechanical injury. Blunt mechanical loads on a joint exhibiting early stages of disease may help accelerate the disease process in these individuals. While additional studies are needed to validate this hypothesis, the result may have important implications in forensic biomechanics. Additionally, tissue swelling could make joint tissues relatively more susceptible to blunt impact injury following a surgical procedure.

In the controlled displacement tests significant correlations were documented between the peak stress generated during unconfined compression and various parameters. In all cases the correlations were stronger for non-equilibrated versus equilibrated explants. In the case of explant weight, a significant correlation was lost in the equilibrated group of explants. Previous studies that have determined the mechanical

properties of cartilage across the surface of an intact joint document changes in stiffness parameters that correlate with site-specific collagen and proteoglycan content (Appleyard et al., 2003; Brama et al., 2000). In the current study the decrease in the strength of correlations in the equilibrated explants may indicate that relationships between solid matrix constituents and the mechanical response of articular cartilage are shrouded by an artificially high amount of fluid acquired during 'tissue equilibration'. Furthermore, the peak stress was found to significantly decrease as fluid gained during equilibration increased suggesting that increased fluid leads to a less stiff response. These data agree with the data obtained from the load controlled explant group.

In conclusion, cartilage explant studies that allow for a period of tissue equilibration in standard culture media should consider the possible effects this may have on the tissue's mechanical characteristics. Severe levels of matrix damage and associated cell death occurring in chondral explants exposed to injurious levels of compression may be in part due to an artificially high level of interstitial fluid due to the experimental protocol. Changes in the explant stiffness, resulting from tissue swelling, have an effect on chondrocyte viability throughout the thickness, as well as an increased susceptibility for surface fissuring. In order to help understand the large amount of variation in fluid gain between explants from the same joint surface noted in this study, additional studies are needed.

Acknowledgements: This study was supported by grants from The National Center for Injury Control and Prevention, The Centers for Disease Control and Prevention (R49/CCR503607) and The TRW Automotive Fund. Its contents are solely the responsibility of the authors and do not necessarily represent the official views of the

CDC or The TRW Automotive Fund. The authors wish to gratefully acknowledge the help of Clifford Beckett, Austin McPhillamy, and Aaron Stewart (AS) for technical assistance during this study.

References

Abramowitch, S.D., Woo, S.L.Y., 2004. An improved method to analyze the stress relaxation of ligaments following a finite ramp time based on the quasi-linear viscoelastic theory. Journal of Biomechanical Engineering 126, 92-97.

Appleyard, R.C., Burkhardt, D., Ghosh, P., Read, R., Cake, M., Swain, M.V., Murrell, G.A. 2003. Topographical analysis of the structural, biochemical and dynamic biomechanical properties of cartilage in an ovine model of osteoarthritis. Osteoarthritis and Cartilage 11, 65-77.

Armstrong, C.G., Lai, W.M., Mow, V.C., 1984. An analysis of the unconfined compression of articular cartilage. Journal of Biomechanical Engineering 106, 165-173.

Askew, M., Mow, V.C., 1978. The biomechanical function of the collagen fibril ultrastructure of articular cartilage. Journal of Biomechanics 100, 105-115.

Ateshian, G.A., Lai, W.M., Zhu, W.B., Mow, V.C., 1994. An asymptotic solution for the contact of two biphasic cartilage layers. Journal of Biomechanics 27, 1347-1360.

Ateshian, G.A., Wang, H., 1995. A theoretical solution for the frictionless rolling contact of cylindrical biphasic articular cartilage layers. Journal of Biomechanics 28, 1341-1355.

Atkinson, P.J., Haut, R.C., 2001. Injuries produced by blunt trauma to the human patellofemoral joint vary with flexion angle of the knee. Journal of Orthopaedic Research 19, 827-833.

Atkinson, P.J., Haut, R.C., 1995. Subfracture insult to the human cadaver patellofemoral joint produces occult injury. Journal of Orthopaedic Research 13, 936-944.

Atkinson, T.S., Haut, R.C., Altiero, N.J., 1998. Impact-induced fissuring of articular cartilage: an investigation of failure criteria. Journal of Biomechanical Engineering 120, 181-187.

Bank, R.A., Soudry, M., Maroudas, A., Mizrahi, J., TeKoppele, J.M., 2000. The increased swelling and instantaneous deformation of osteoarthritic cartilage is highly correlated with collagen degradation. Arthritis and Rheumatism 43, 2202-2210.

Blanco, F.J., Guitian R., Vazquez-Martul E, de Toro F.J., Galdo F., 1998. Osteoarthritis chondrocytes die by apoptosis: A possible pathway for osteoarthritis pathology. Arthritis and Rheumatology 41, 284-289.

Borrelli, J., Torzilli, P.A., Grigiene, R., Helfet, D.L., 1997. Effect of impact load on articular cartilage: development of an intra-articular fracture model. Journal of Orthopaedic Trauma 11, 319-326

Brama, P.A., Tekoppele, J.M., Bank, R.A., Barneveld, A., van Weeren, P.R., 2000. Functional adaptation of equine articular cartilage: the formation of regional biochemical characteristics up to age one year. Equine Veterinary Journal 2000 May;32(3):217-21.

Brandt, K.D., Mankin H.J., Shulman L.E., 1986. Workshop on etiopathogenesis of osteoarthiritis. Journal of Rheumatology 13, 1126-1160.

Buckwater, J.A., 1995. Osteoarthritis and articular cartilage use, disuse, and abuse: Experimental studies. Journal of Rheumatology Supplement 43,13-15.

Bush, P.G., Hall, A.C., 2003. The volume and morphology of chondrocytes within non-degenerate and degenerate human articular cartilage. Osteoarthritis and Cartilage. 11, 242-251.

Clark, J.M., 1990. The organisation of collagen fibrils in the superficial zones of articular cartilage. Journal of Anatomy. 171, 117-130.

Clark, J.M., 1991. Variation of collagen fiber alignment in a joint surface: a scanning electron microscope study of the tibial plateau in dog, rabbit, and man.

Journal of Orthopaedic Research 9, 246-257.

Clements, K.M., Bee, Z.C., Crossingham, G.V., Adams, M.A., Sarif, M., 2001. How severe must repetitive loading be to kill chondrocytes in articular cartilage? Osteoarthritis and Cartilage 9, 499-507.

DiMicco, M.A., Patwari, P., Siparsky, P.N., Kumar, S., Pratta, M.A., Lark, M.W., Kim, Y.J., Grodzinsky, A.J., 2004. Mechanisms and kinetics of glycosaminoglycan release following in vitro cartilage injury. Arthritis and Rheumatology. 50, 840-848.

D'Lima, D.D., Hashimoto, S., Chen, P.C., Colwell, C.W. Jr., Lotz, M.K., 2001. Impactof mechanical trauma on matrix and cells. Clinical Orthopaedics and Related Research 391, S90-S94

Eberhardt, A.W., Lewis, J.L., Keer, L.M., 1991. Normal contact of elastic spheres with two elastic layers as a model of joint articulation. Journal of Biomechanical Engineering 113, 410-417.

Ewers, B.J., Dvoracek-Driksna, D., Orth, M.W., Haut, R.C., 2001. The extent of matrix damage and chondrocyte death in mechanically traumatized articular cartilage explants depends on rate of loading. 19(5), 779-784.

Ewers, B.J., Jayaraman, V.M., Banglamaier, R.F., Haut, R.C., 2002. Rate of blunt impact loading affects changes in retropatellar cartilage and underlying bone in the rabbit patella. Journal of Biomechanics 35, 747-755.

Krueger, J.A., Thisse, P., Ewers, B.J., Dvoracek-Driksna, D., Orth, M.W., Haut, R.C., 2003. The extent and distribution of cell death and matrix damage in impacted chondral explants varies with the presence of underlying bone. Journal of Biomechanical Engineering 125, 114-119.

Lee, R.C., Frank, E.H., Grodzinsky, A.J., Roylance, D.K., 1981. Oscillatory compressional behaviour of articular cartilage and the associated electromechanical properties. Journal of Biomechanical Engineering 103, 280-292.

Lewis, J.L., Deloria, L.B., Oyen-Tiesma, M., Thompson, R.C., Jr., Ericson, M., Oegema, T.R., Jr., 2003. Cell death after cartilage impact occurs around matrix cracks.

Journal of Orthopaedic Research 21, 881-887.

Li, X., Haut, R.C., Altiero, N.J., 1995. An analytical model to study blunt impact response of the rabbit P-F joint. Journal of Biomechanical Engineering 117, 485-491.

Macirowski, T., Tepic, S., Mann, R.W., 1994. Cartilage stresses in the human hip joint. Journal of Biomechanical Engineering 116, 10-18.

Mak, A.F., Lai, W.M., Mow, V.C., 1987. Biphasic indentation of articular cartilage--I. Theoretical analysis. Journal of Biomechanics 20, 703-714.

Mankin, H.J., Thrasher, A.Z., 1975. Water content and binding in normal and osteoarthritic human cartilage. Journal of Bone and Joint Surgery 57A, 76-80.

Maroudas, A., 1975. Biophysical chemistry of cartilaginous tissues with special reference to solute and fluid transport. Biorheology 12, 233-248.

Maroudas, A., Mizrahi, J., Katz, E.P., Wachtel, E.J., Soudry, M., 1986. Physiochemical properties and functional behavior of normal and osteoarthritic human cartilage. In: Kuettner, K., et al. (Eds.), Articular Cartilage Biochemistry. Raven Press, New York, pp. 311-329.

Maroudas, A., Muir, H., Wingham, J., 1969. The correlation of fixed negative charge with glycosaminoglycan content of human articular cartilage.Biochimica et Biophysica Acta 177, 492-500.

Mansour, J.M., Mow, V.C., 1976. The permeability of articular cartilage under compressive strain and at high pressures. Journal of Bone and Joint Surgery 58, 509-16.

Milentijevic, D., Helfet, D.L., Torzilli, P.A., 2003. Influence of stress magnitude on water loss and chondrocyte viability in impacted articular cartilage. Journal of Biomechanical Engineering 125, 594-601.

Morel, V., Quinn, T.M., 2004. Cartilage injury by ramp compression near the gel diffusion rate. Journal of Orthopaedic Research 22, 145-151.

Mow, V.C., Kuei, S.C., Lai, W.M., Armstrong, C.G., 1980. Biphasic creep and stress relaxation of articular cartilage in compression? Theory and experiments. Journal of Biomechanical Engineering 102, 73-84.

Mow, V.C., Ratcliffe, A., Poole, A.R., 1992. Cartilage and diarthrodial joints as paradigms for hierarchical materials and structures. Biomaterials 13, 67-97.

Myers, E.R., Lai, W.M., Mow, V.C., 1984. A continuum theory and an experiment for the ion-induced swelling behavior of articular cartilage. Journal of Biomechanical Engineering 106, 151-158.

Narmoneva, D.A., Wang, J.Y., Setton, L.A., 1999. Nonuniform swelling-induced residual strains in articular cartilage. Journal of Biomechanics 32, 401-408.

Newberry, W.N., Garcia, J.J., Mackenzie, C.D., Decamp, C.E., Haut, R.C., 1998. Analysis of acute mechanical insult in an animal model of post-traumatic osteoarthrosis. Journal of Biomechanical Engineering 120, 704-709.

Newberry, W.N., Mackenzie C.D., Haut R.C., 1998. Blunt impact causes changes in bone and cartilage in a regularly exercised animal model. Journal of Orthopaedic Research 16, 348-354.

Park, S., Krishnan, R., Nicoll, S.B., Ateshian, G.A., 2003. Cartilage interstitial fluid load support in unconfined compression. Journal of Biomechanics 36, 1785-1796.

Parsons, J.R., Black, J., 1979. Mechanical behavior of articular cartilage: quantitative changes with alteration of ionic environment. Journal of Biomechanics 12, 765-773.

Sah, R.L., Kim, Y.J., Doong, J.Y., Grodzinsky, A.J., Plaas, A.H., Sandy, J.D., 1989. Biosynthetic response of cartilage explants to dynamic compression. Journal of Orthopaedic Research 7, 619-636.

Sauerland, K., Raiss, R.X., Steinmeyer, J., 2003. Proteoglycan metabolism and viability of articular cartilage explants as modulated by the frequency of intermittent loading. Osteoarthritis and Cartilage. 11, 343-350.

Setton, L.A., Zhu, W.B., Mow, V.C., 1993. The biphasic poroviscoelastic behavior of articular cartilage: role of the surface zone in governing the compressive behavior. Journal of Biomechanics 26, 581-592.

Torzilli, P.A., Grigiene, R., Huang, C., Friedman, S.M., Doty, S.B., Boskey, A.L., Lust, G., 1997. Characterization of cartilage metabolic response to static and dynamic stress using a mechanical explant test system. Journal of Biomechanics 30, 1-9.

Wilson, W., van Donkelaar, C.C., van Rietbergen, B., Ito, K., Huiskes, R., 2004. Stresses in the local collagen network of articular cartilage: a poroviscoelastic fibril-reinforced finite element study. Journal of Biomechanics 37, 357-366.

Wright, V., 1990. Post-traumatic osteoarthritis—A medico-legal minefield. British Journal of Rheumatology 29, 474-478.

Zarek, J.M., Edward, J., 1963. The stress-structure relationship in articular cartilage. Medical Electroncs and Biological Engineering 1, 497-507.

Figure Captions

Figure 1

(a) Photograph of servo-hydraulic testing machine set up. Explant specimens were placed between the actuator arm and the lower platen which is attached to a load cell. (b) A two dimensional drawing showing the loading scenario created by the servo-hydraulic testing machine.

Figure 2

Photographs taken at 25X magnification were analyzed using digital imaging software. Manual digital pixel overlays were drawn along the length of all visible surface cracks. The software counted the total number of pixels. Pixel amounts were converted into units of millimeters by calibrating the software with a photograph of a ruler at the same magnification.

Figure 3

Fluorescence images taken at 100X were separated into superficial, middle, and deep zones. The dead (red) and viable (green) cells were manually counted in digital imaging software. Dead cell counts were divided by total cell counts in each zone in order to yield a percentage of dead cells.

Figure 4

Non-linear stress versus strain curves were generated for all of the impacted explants. Values of strain were interpolated from stress values of 1, 5, 10, 15, and 20 mega Pascals. The curves were fit with a hyper-elastic Ogden function.

Figure 5

Average stress-strain plots for equilibrated and non-equilibrated chondral explants were constructed following blunt impact mechanical loading. Non-equilibrated explants exhibited a stiffer response resulting in a shift to the left on the graph.

Figure 6

A plot of the shear modulus parameter μ vs. water gain for the equilibrated explants fit with a least squares linear regression line showing a statistically significant negative correlation between this mechanical parameter and fluid intake during equilibration using a Pearson correlation coefficient test.

Figure 7

A plot of peak strain vs. water gain for the equilibrated explants fit with a least squares linear regression line showing a statistically significant positive correlation between explant strain and fluid intake during equilibration using a Pearson correlation coefficient test.

Figure 8

Gross photographs were used to determine the average total fissure length for cartilage explants following blunt impacts. Less fissuring was documented in non-equilibrated explants (a) compared to equilibrated specimens (b).

Figure 9

A plot of the length of surface fissuring vs. water gain during 24 hours of equilibration fit with a least squares linear regression line showing a statistically significant positive correlation between the total length of surface cracks and fluid intake during equilibration using a Pearson correlation coefficient test.

Figure 10

Gross inspection of flouresence cell viability pictures taken at 100X show a higher occurrence of deep zone cell death in the non-equilibrated (b) versus equilibrated group (a).

Figure 11

Comparison bar graph showing percentages of cell death in the various zones of equilibrated and non-equilibrated chondral explants after 30 MPa of unconfined compression. Significant differences (*) in cell death were noted in both deep and superficial zones between goups ($p<0.05$).

Figure 12

A plot of the percentage of dead cells in the deep zone vs. water gained in the equilibrated explants fit with a least squares linear regression line showing a statistically significant negative correlation between cell death in the deep zone and fluid intake during equilibration using a Pearson correlation coefficient test.

Figure 13

Pearson correlation tests revealed significant correlations between the peak compressive stress generated during unconfined compression and thickness (a), explant weight (b), dry weight (c), and the percentage of water content (d) in the non-equilibrated explants.

Figure 14

Pearson correlation tests revealed significant correlations between the peak compressive stress generated during unconfined compression and thickness (a), dry weight (c), the percentage of water content (d), and the percentage of fluid gained during equilibration. A significant correlation was not documented between explant weight and peak compressive stress (b).

Figures

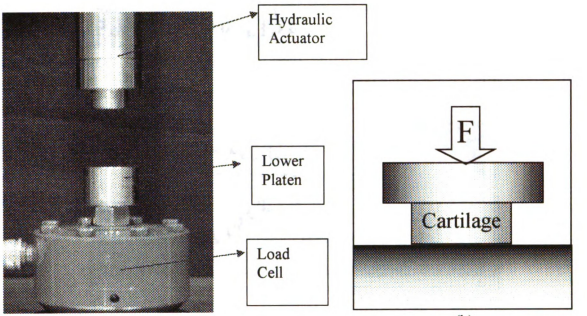

Figure 1

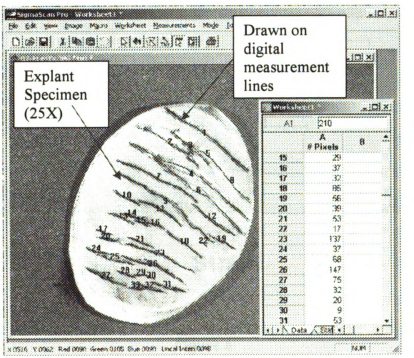

Figure 2

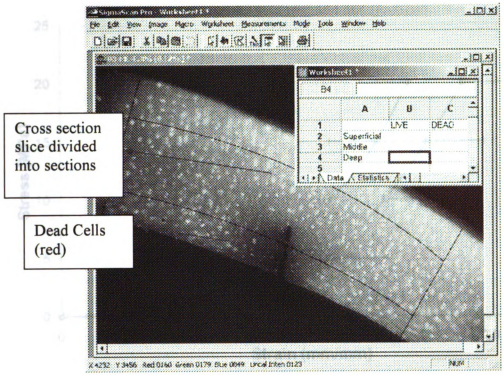

Figure 3

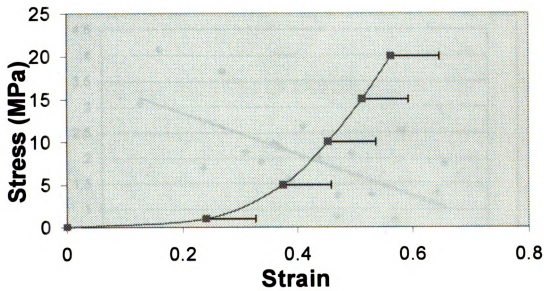

Figure 4

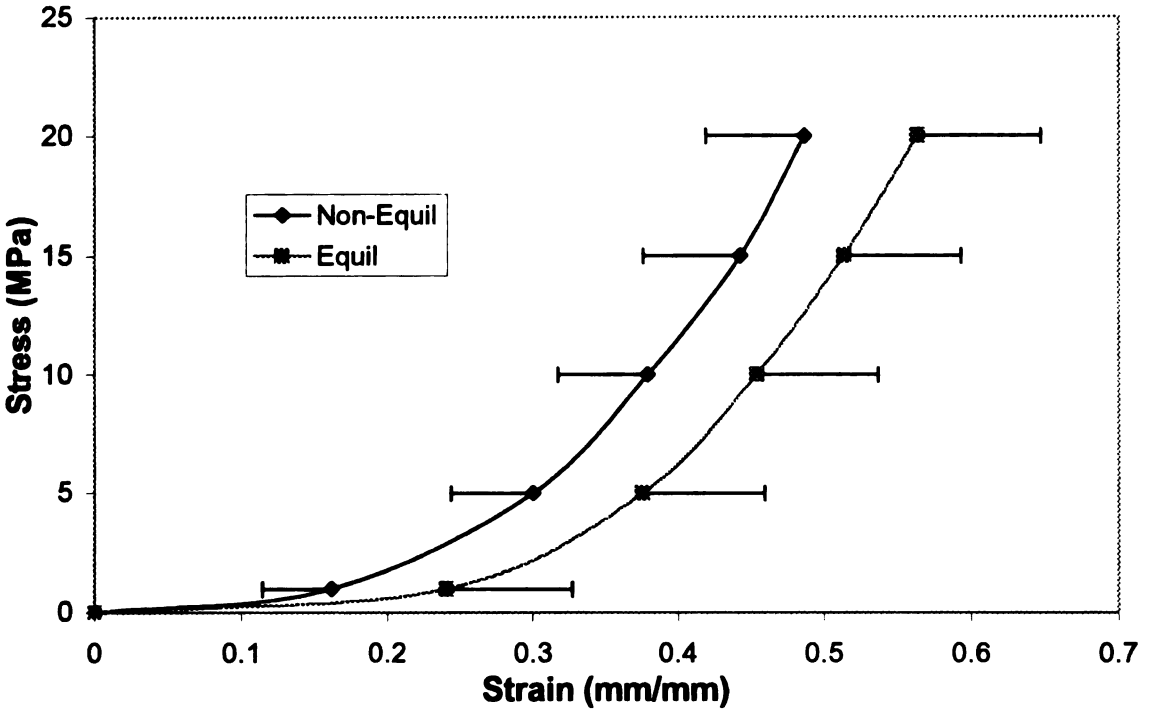

Figure 5

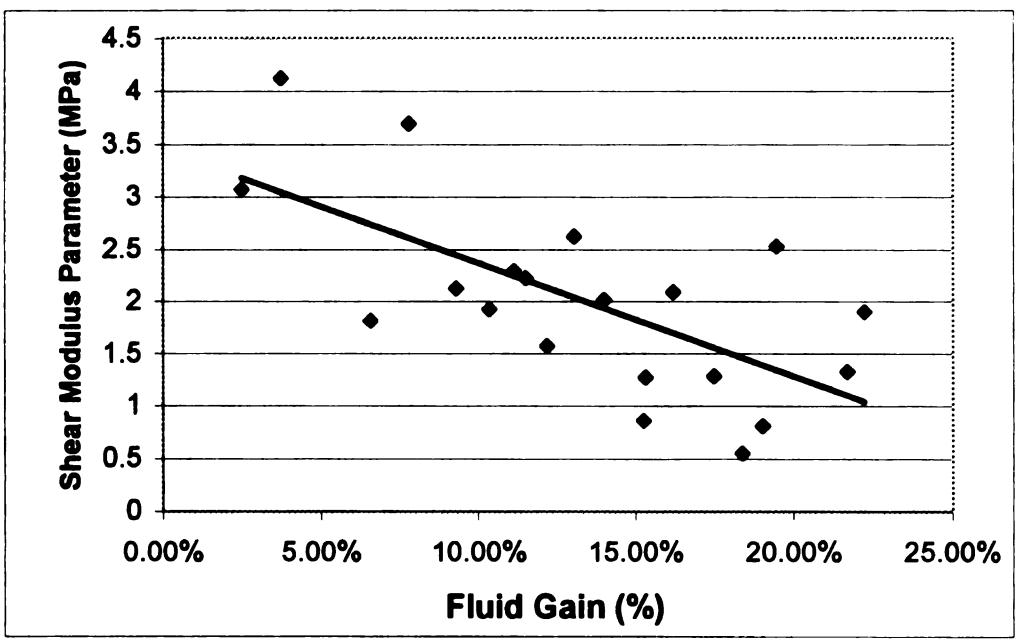

Figure 6

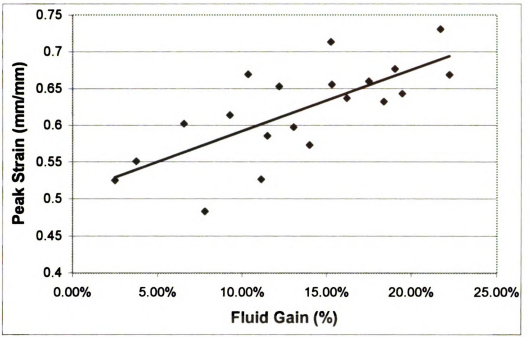

Figure 7

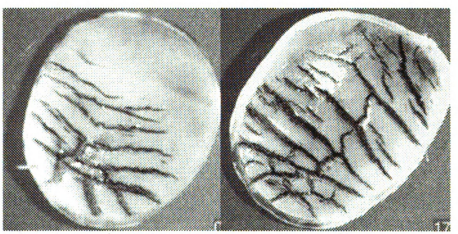

a) b)

Figure 8

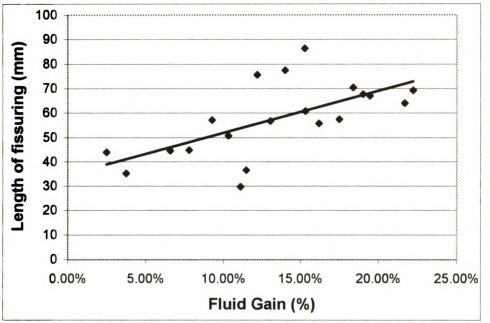

Figure 9

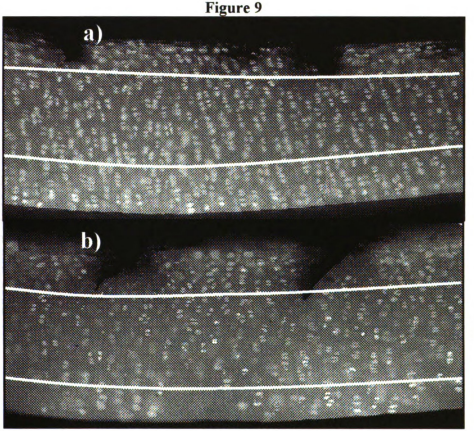

Figure 10

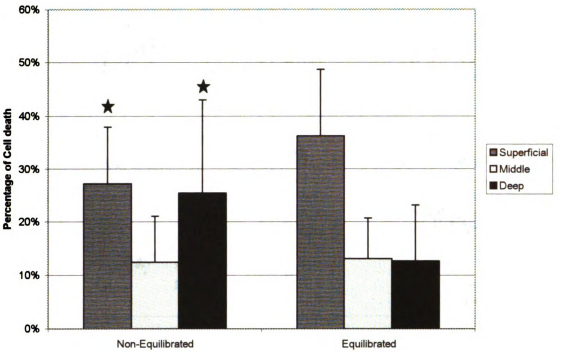

Figure 11

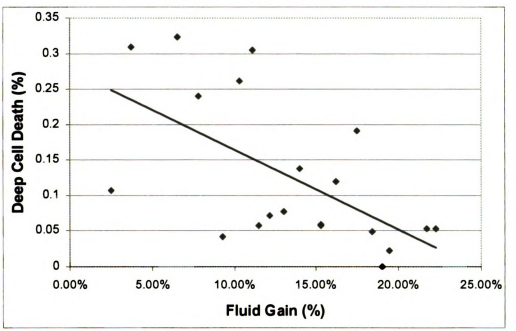

Figure 12

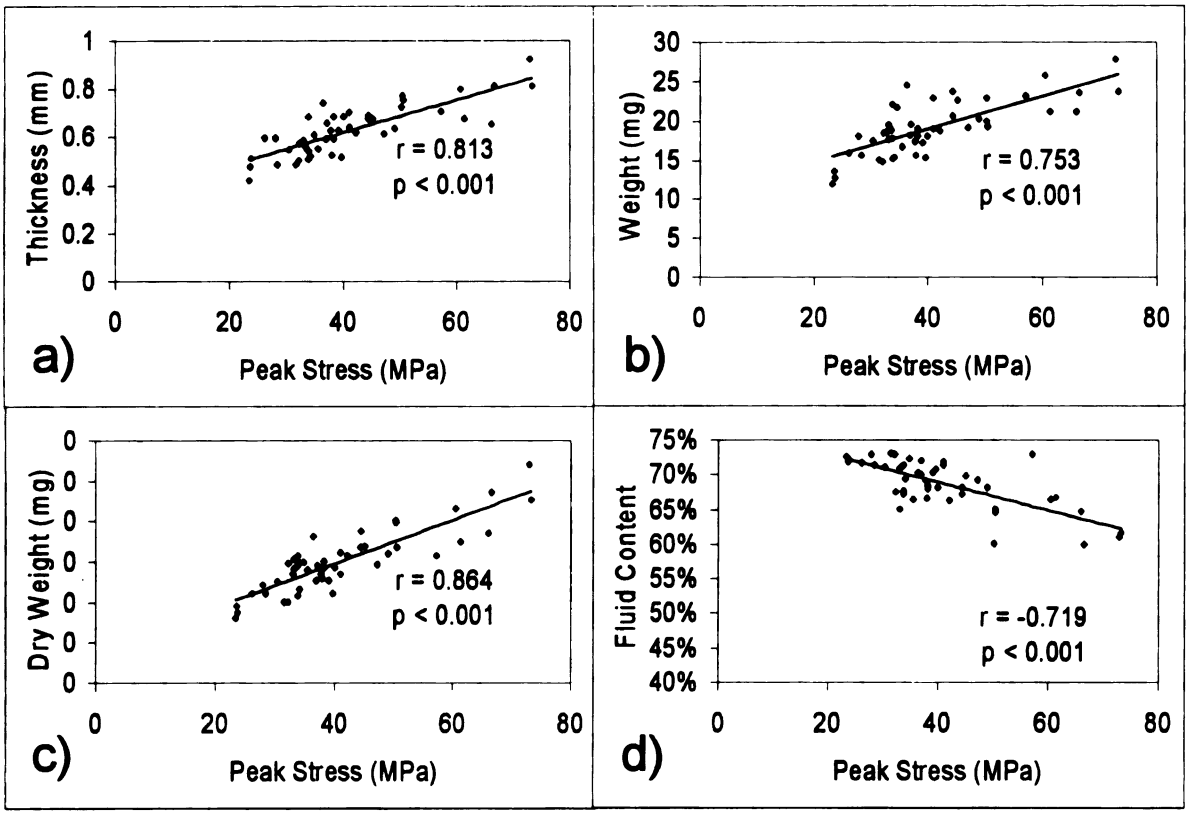
Thickness (mm)
1
0.8
0.6
0.4
0.2
0
0
20
40
60
80
r = 0.813
p < 0.001
a)
Peak Stress (MPa)
Weight (mg)
30
25
20
15
10
5
0
r = 0.753
p < 0.001
b)
Peak Stress (MPa)
Dry Weight (mg)
r = 0.864
p < 0.001
c)
Peak Stress (MPa)
Fluid Content
75%
70%
65%
60%
55%
50%
45%
40%
r = -0.719
p < 0.001
d)
Peak Stress (MPa)

Figure 13

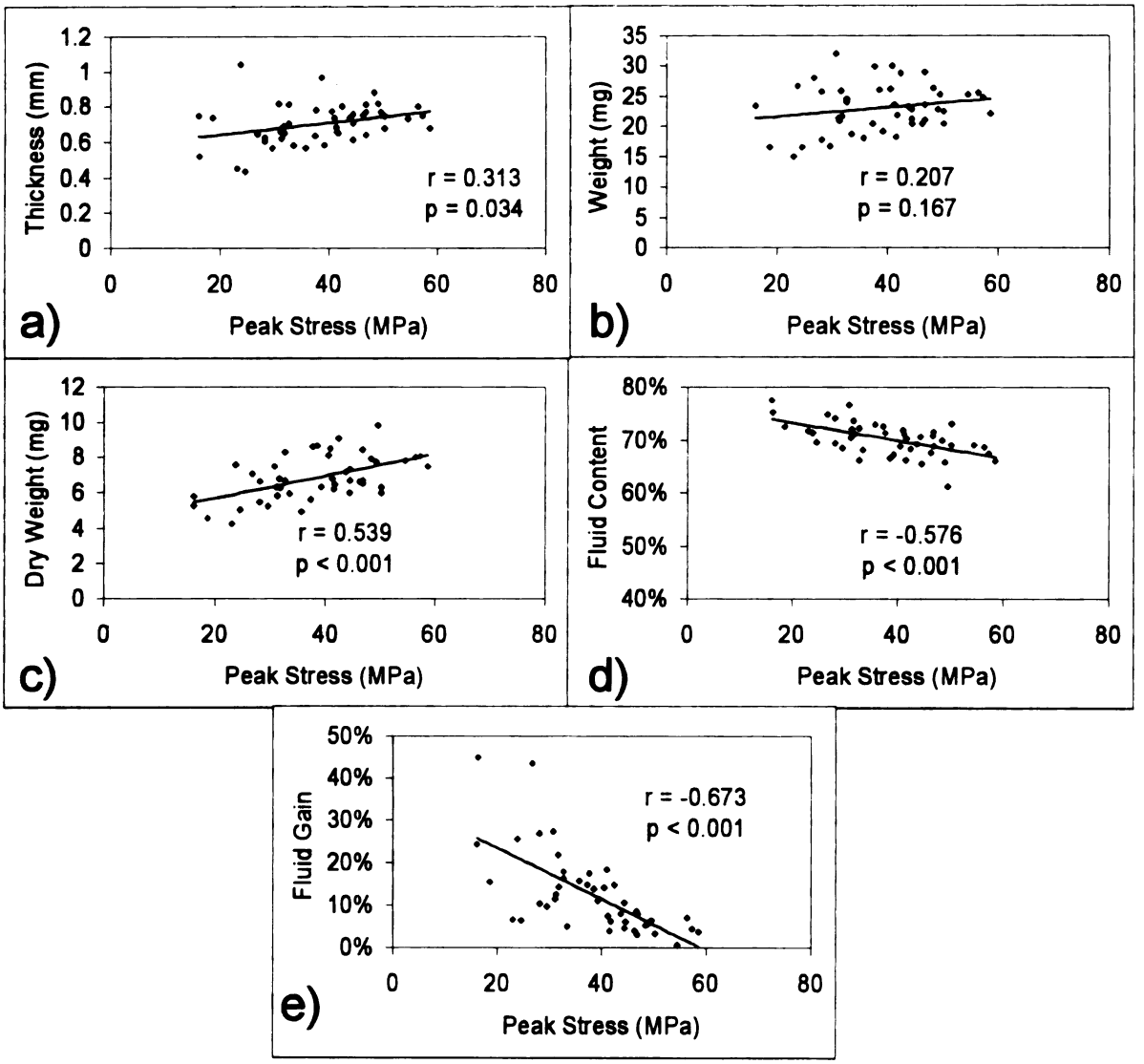
Thickness (mm)
1.2
1
0.8
0.6
0.4
0.2
0
r = 0.313
p = 0.034
0
20
40
60
80
Peak Stress (MPa)
a)
Weight (mg)
35
30
25
20
15
10
5
0
r = 0.207
p = 0.167
Peak Stress (MPa)
b)
Dry Weight (mg)
12
10
8
6
4
2
0
r = 0.539
p < 0.001
Peak Stress (MPa)
c)
Fluid Content
80%
70%
60%
50%
40%
r = -0.576
p < 0.001
Peak Stress (MPa)
d)
Fluid Gain
50%
40%
30%
20%
10%
0%
r = -0.673
p < 0.001
Peak Stress (MPa)
e)

Figure 14

CHAPTER 2: THE LIMITATION OF ACUTE NECROSIS IN RETRO-PATELLAR CARTILAGE AFTER A SEVERE BLUNT IMPACT TO THE *IN VIVO* RABBIT PATELLO-FEMORAL JOINT

Abstract:

Our laboratory has previously shown that severe levels of blunt mechanical load, generating contact pressures greater than 25 MPa, on chondral and osteochondral explants produce surface lesions and acute necrosis of chondrocytes. In vivo studies by our laboratory have also found surface lesions and chronic degradation of retro-patellar cartilage within 3 years following a 6 Joule impact intensity with an associated average pressure of 25 MPa in the rabbit patello-femoral joint. A hypothesis of the current study was that cellular necrosis is produced acutely in the retro-patellar cartilage of the aforementioned rabbit model as a result of a 6 Joule impact. Another hypothesis of the study was that an early injection of the non-ionic surfactant, poloxamer 188 (P188) would significantly reduce the percentage of necrotic cells in the traumatized retro-patellar cartilage.

In the current study eighteen rabbits were equally divided into 3 groups. One group was termed 'time zero', and the other groups were carried out for 4 days. One '4 day' group was administered a 1.5 ml injection of P188 into the impacted joint immediately after trauma, while the other was injected with a placebo solution. Impact trauma produced surface lesions on retropatellar cartilage in all groups. Approximately 15% of retro-patellar chondrocytes suffered acute necrosis in the 'time zero' and '4 day no poloxamer' groups. In contrast, significantly fewer (7%) cells suffered necrosis in the '4 day poloxamer' group. The effect of this treatment was most significant in the superficial layer of the cartilage.

The study indicated the potential use of P188 surfactant in the acute repair of mechanically damaged cell membranes in the in vivo setting. Its use early after severe trauma to articular cartilage may allow sufficient time for damaged cells to heal, which may in turn mitigate the potential for a post-traumatic osteoarthritis in the joint. Additional studies are needed to improve the efficacy of this surfactant and to determine the long-term health of joint cartilage after P188 intervention.

Introduction:

Osteoarthritis (OA) affects over 21 million Americans and is the leading cause of disability in the United States (Wright, 1990). While the mechanisms responsible for this disease are unknown, the risk of OA is increased significantly in joints suffering a major injury (Felson, 2004). However, establishing a cause and effect relationship between joint injury and OA can be difficult as after an osteochondral injury joint disease may not be diagnosed for 2 to 5 years, while less severe joint injuries may not be diagnosed for 10 or more years after the trauma (U.S. Census Bureau, 2000). Clinically this disease is characterized by joint pain and narrowing of the joint, as diagnosed by radiological examination (Flores and Hochber, 1998). Pathologically, the disease exhibits a loss of cartilage and sclerosis of underlying bone.

Experimental studies with animal models have been conducted in attempts to understand the potential association between acute joint injury and the chronic pathogenesis of OA. This laboratory has developed a model of post-traumatic OA using the Flemish Giant rabbit (Haut et al., 1995). In a recent study a rigid impact mass was dropped with 6 Joule of energy onto the flexed patello-femoral joint, using this model (Ewers et al., 2002). The study found surface fissures acutely with a progressive increase

in the degradation of retro-patellar surface cartilage and the thickening of underlying subchondral bone after 3 years. Another study found that during this impact event patello-femoral contact pressures reach approximately 25 MPa (Newberry et al., 1998). A study by another laboratory, using the New Zealand white rabbit subjected to a 10 Joule impact intensity, found significantly advanced OA-like changes in the patello-femoral joint, with fibrillation, ulceration and erosion of retro-patellar cartilage within 6 months post-contusion (Mazieres et al., 1987). Early OA-like changes have also been described using the flexed canine patello-femoral joint subjected to approximately 2.2 kN of impact force delivered with a gravity-dropped rigid mass (Thompson et al., 1991). The study acutely found surface fissures on retro-patellar cartilage with clefts in the underlying subchondral bone and calcified cartilage. After 6 months the surface fissures had loss of safranin-O staining and new bone formation in the underlying subchondral bone. While the studies described above found an association between blunt impact trauma to a joint and the subsequent development of OA-like changes in the traumatized cartilage, the mechanisms of acute damage leading to these pathological changes are yet unclear.

Excessive mechanical loads resulting from a single blunt impact have been found to result in surface fissures and necrotic cell death in chondral (Ewers et al., 2001; Torzilli et al., 1999) and osteochondral explants (Krueger et al., 2003; Morel and Quinn, 2004). Forty megapascals (MPa) of unconfined compression on bovine chondral explants results in significant surface fissuring of the tissue with approximately 50% of cells acutely necrotic (Ewers et al., 2001). Necrotic cells have been found in the superficial zone (upper 20%) located near fissures and in the middle zone (next 50% of thickness)

zone, with a few dead cells found in the deepest zone of the cartilage, especially in osteochondral explants (Krueger et al., 2003). A critical threshold stress of 15-20 MPa was found for cell death and collagen matrix damage in unconfined compression using the bovine chondral explant (Torzilli et al., 1999)). A later study using osteochondral explants found that significant surface fissuring with adjacent cellular necrosis occurs when impact rates of loading exceed the gel diffusion rate of the cartilage (Morel and Quinn, 2004). This study also documented cell death largely in the superficial zone adjacent to fissures. Necrotic cell death has also been found in situ using the bovine patella subjected to a single impact of 53 MPa (Lewis et al., 2003)). In that study cell death occurred around surface cracks, but not in impacted areas away from these cracks. The authors suggested "that early stabilization of damaged areas of the cartilage may prevent late sequelae that lead to OA." Other studies have also associated the physiopathology of articular cartilage in OA with the death of chondrocytes (Hashimoto et al., 1998).

Few in vivo experimental studies, however, have been conducted that specifically associate cell death with the development of OA. In one study significant necrosis of chondrocytes was induced in the patello-femoral joint of rabbits by localized freezing of the tissue in vivo (Simon et al., 1976). After 1 year the affected cartilage had changes that were consistent with early signs of OA. These tissue changes were similar to those documented by our laboratory using the impacted joint model (Ewers et al., 2001). A hypothesis of the current study was that a 6 Joule blunt impact onto the rabbit patello-femoral joint would induce acute necrosis of chondrocytes in the retro-patellar cartilage.

A defining feature of cell death by necrosis is damage to the plasma membrane, and the inability of the cell to maintain ionic gradients across its membrane resulting in swelling with subsequent rupture of the cell (Duke et al., 1996). Due to the nature of necrotic cell death, mild surfactants have been used to restore integrity to cells after physical and chemical stresses (Clarke and McNeil, 1992; Papoutsakis, 1991). Specifically, poloxamer 188 (P188) has been found to 'save' neurons from early necrotic death after severe mechanical loading (Marks et al., 2001; Borgens et al., 2004). A recent study by our laboratory also found that P188 surfactant was able to 'save' chondrocytes from acute necrotic death in bovine chondral explants subjected to 25 MPa of unconfined compression (Phillips and Haut, 2004). A second hypothesis of the current study was that injection of P188 surfactant into the in vivo patello-femoral joint capsule shortly after a 6 Joule blunt impact would significantly reduce the percentage of necrotic cells in retro-patellar cartilage in the acute setting (4 days post trauma).

Methods:

Eighteen skeletally mature, Flemish Giant rabbits (aged 6-8 months) were used in this study. The project was approved by the All-University Committee on Animal Use and Care. The blunt impact experiments have been described previously (Haut et al., 1995). Briefly, a 1.33 kg mass with a flat 25 mm diameter aluminum impact interface was dropped from 0.46 m (6 Joules of impact energy) onto the right patellofemoral joint of anesthetized animals (2% Isoflurane and oxygen) (Figure 1). The opposite limb was not impacted and used as a paired, un-impacted control. A load transducer (2.225-kN capacity) (model 31/432; Sensotec, Columbus, OH, U.S.A.) was attached behind the rigid

interface to record impact loads. Peak contact load, time to peak, and total contact duration were collected at 10 kHz. The mass was arrested electronically after the first impact, preventing multiple impacts.

Six rabbits were randomly selected as 'time zero' animals. These were sacrificed immediately after impact. The remaining 12 animals were sacrificed 4 days post impact. During these 4 days the animals were exercised 10 minutes a day at 0.3 mph on a treadmill (Oyen-Tiesma et al., 1998). The exercise protocol was initiated on the first day approximately 4 hours after impact. Animals were housed in individual cages (122 cm x 61 cm x 49 cm) when not exercising. Six of the animals (4 day poloxamer group) received a single 1.5 ml injection of an 8mg/ml concentration of P188 surfactant in sterile phosphate-buffered saline (PBS) injected into the traumatized patello-femoral joint capsule shortly (within approximately 2 minutes) after impact. The remaining six animals (4 day no poloxamer group) received a sham injection of 1.5 mL sterile PBS into the impacted joint shortly after trauma. The combination P188 in PBS and the PBS sham solutions were filter sterilized prior to injection in the joints using a 0.2 mm vacuum filter (Nalgene, Nalge Nunc Int., Rochester, New York, USA). After injection, the animal's limb was exercised manually to help distribute the P188 surfactant and PBS solutions in the joint.

Patellae from the impacted and the opposite un-impacted limbs were excised immediately after sacrifice from each animal. The retro-patellar surface was wiped with India ink to highlight surface defects and was photographed using a digital camera (Polaroid DMC2, Polaroid Corporation, Waltham, MA, USA) under a dissecting

microscope (Wild TYP 374590, Heerbrugg, Switzerland). Each patella was then wrapped in PBS soaked gauze and prepared for cell viability analyses.

Osteochondral sections from the impacted and opposite un-impacted patella from each animal were prepared for cell viability analyses. A low speed bone saw (model# 11-1180-170, Buehler, Inc., Lake Bluff, IL) was used to remove trabecular bone from the overlying retro-patellar cartilage, leaving approximately 0.5 mm of subchondral bone (Figure 2). Full depth sections (0.5 mm thick) of retropatellar cartilage and subchondral bone were cut using a specialized cutting device (Ewers et al., 2001) from the area of known patello-femoral contact during blunt impact to the joint (Haut et al., 1995). The sections were stained with Calcein AM and Ethidium Homodimer, according to the manufacturer's specifications (Live/Dead Cytotoxicity Kit, Molecular Probes, Eugene, OR). Approximately 8 sections from each patella were viewed near the midline of the patella using a fluorescence microscope (Leitz Dialux 20 (frequency: 50-60 Hz), Leitz Mikroskopie und Systeme GmgH, Wetlzar, Germany). The sections were photographed with a digital camera (Polaroid DMC2, Polaroid Corporation, Waltham, MA, USA). Each photographic section was divided into two zones: superficial (top 20% of the cartilage depth) and a deep zone (bottom 80%), using an established protocol (Phillips and Haut, 2004). A blinded observer (A.S.) manually counted live and dead cells of in each section using image analysis software (Sigma Scan, SPSS INC., Chicago, IL, USA). The percentage cell death in each zone and the total percentage cell death were determined for each section. The individual section data was averaged to yield the percentage of cell death in each zone and the total percentage of cell death for each limb. The length of surface fissuring was measured on 4 randomly selected impacted and un-impacted pairs

of patellae from each group using the same image analysis software, according to an established protocol (Ewers et al., 2001).

Two factor repeated measures ANOVA and Student-Newman-Keuls post-hoc tests were used to detect statistical differences in the percentage of cell death, percentage of cell death in each zone, and the average total fissure length between impacted and un-impacted limbs, as well as between treatment groups. A two factor (time and limb) ANOVA was performed to detect differences between and within the 'time zero' and '4-day no poloxamer' groups, while a separate two factor (P188 treatment and time) ANOVA was performed to detect differences between and within the '4-day no poloxamer' and '4-day poloxamer' groups. A single factor ANOVA was used to detect differences in peak impact loads and time to peak loads between treatment groups. Statistical significance in these tests was set at $p<0.05$. All experimental data are presented as mean ± one standard deviation.

Results:

There were no statistical differences in the times to peak impact load or the magnitudes of peak load between the treatment groups. The peak impact load developed on the patello-femoral joint was 675.7±134.4 N, and the time to peak load was 3.5±1.0 ms for this study. The animals did not appear to favor one limb over the other during the 4 days of treadmill exercise, per observations by the licensed veterinary animal technician (J.A.).

Gross inspections of the impacted and un-impacted patellae indicated surface fissures on the retro-patellar surfaces (Figure 3). On the impacted patellae there were more fissures with a proximal to distal orientation that were located near the mid-line of the patella. This resulted in a statistically significant difference in the length of surface fissuring on the impacted versus the un-impacted patellae for each group (Figure 4). No significant differences in the length of surface fissures were detected between treatment groups for either impacted or un-impacted patellae, however with the small sample size of the current study the statistical power between groups for this analysis was below the desired level of 0.8.

Magnification of the stained chondral sections showed the presence of necrotic cells in both the superficial and deep zones of impacted and the opposite, un-impacted retro-patellar cartilage (Figure 5). Analyses of the cell viability across the depth of the retro-patellar cartilage showed statistically significant differences in the percentages of dead cells between the impacted and un-impacted patellae for the 'time 0' ($p<0.001$) and for the '4 day no poloxamer' treatment groups ($p=0.002$)(Figure 6). In contrast, there was not a statistically significant difference ($p=0.072$, power = 0.947) in the percentage of total cell death between the impacted and un-impacted patellae for the '4 day poloxamer' group. The effect of P188 injections into the joint shortly after impact trauma was also evident in a significant difference ($p=0.027$) in the percentage of total cell death between the impacted limbs of the '4 day no poloxamer' group and the '4 day poloxamer' group. In contrast, there was not a significant difference in the percentage of total cell death in the impacted ($p=0.195$) or the un-impacted ($p=0.899$) retro-patellar cartilage between the 'time 0' and the '4 day no poloxamer' groups.

Gross inspection of the cartilage sections indicated a large amount of cell death in the superficial zone (Figure 5b). While there were statistically significant differences between the percentages of cell death in the superficial zones of impacted versus un-impacted retropatellar cartilage for the 'time zero' ($p=0.002$) and the '4 day no poloxamer' ($p=0.008$) groups, there was no significant difference (power = 0.994) recorded in the percentage of cell death in this zone for the '4 day poloxamer' ($p=0.095$) group (Figure 7). In contrast, however, there were significant differences in the percentages of cell death in the deep zones between impacted and un-impacted patellae in all treatment groups. Statistical differences were not detected for the superficial or deep zones between groups in this study, but with the small sample size the statistical power between groups was again less than 0.8.

Discussion

An objective of this study was to test the hypothesis that 6 Joules of impact energy delivered to the flexed rabbit patello-femoral joint, via a rigid impact interface, would cause a significant amount of cell death in the retro-patellar cartilage. Impact to the joint produced surface lesions, or fissures, on the retro-patellar cartilage. The proximal to distal orientation of the impact-induced surface fissures have previously been associated with the impact event (Haut et al., 1995). In the current study impact trauma resulted in the acute death of chondrocytes throughout the depth of the retro-patellar cartilage by approximately 15% more in the impacted versus the opposite un-impacted patella. A second objective of the study was to test the hypothesis that an immediate post-trauma injection of P188 surfactant into the joint would significantly reduce the percentage of dead cells in the retro-patellar cartilage. The current study found that the

percentage of total dead cells in the impacted versus the un-impacted retro-patellar cartilage was not statistically different for the '4 day poloxamer' group. While the zonal layer data showed statistically significant differences in the percentage of dead cells in the superficial and deep zones of impacted versus un-impacted patella for the 'time zero' and '4-day no poloxamer' groups, in the '4-day poloxamer' group the effect was only statistically significant in the deep zone. These data suggest that P188 was most effective in 'saving' cells from necrotic death in the superficial zone in the current study.

The current study verified that a blunt impact to the rabbit patello-femoral joint with a 6 Joule intensity produced statistically significant cell death in the retro-patellar cartilage. A defining feature of cell death by necrosis is swelling, due to the injured cell being unable to maintain ionic gradients across a damaged plasma membrane (Duke et al., 1996). In the current study the percentage of dead cells was measured by membrane disruption, as membrane damage was documented by the ability of EthD-1 (ethidium homodimer) to only pass through a damaged cell membrane. This particular mechanism of damage was also supported by the efficacy of P188 surfactant to repair these cells in this study. A previous study showed that this surfactant specifically inserts into only damaged areas of a cell membrane (Marks et al., 2001).

In a similar, in vivo study by D'Lima et al. (2001) which used New Zealand White rabbits, a 3 Joule intensity blunt impact to the patello-femoral joint resulted in a 14% increase in apoptotic (TUNEL positive) cells in retro-patellar cartilage versus the un-impacted limb at 4 days post trauma (D'Lima et al., 2001). The study verified cellular apoptosis by examining attributes of nuclear morphology indicative of apoptosis. Chondrocyte apoptosis has also been shown in human biopsy tissue near sites of chondral

fracture (Kim et al., 2002). Canine cartilage explants subjected to 5 MPa of cyclic compression at 0.3 Hz exhibited the development of both cellular necrosis and apoptosis progressively increasing with load duration and time. Necrosis was observed 2 hours after cessation of loading, whereas apoptosis (TUNEL-positive cells) was not significant until 48 or more hours after loading stopped. Apoptosis was verified in some cells using transmission electron microscopy (Chen et al., 2001). A study that induced osteochondral wounding of a joint also found significant percentages of necrotic and apoptotic cells in the tissue (Tew et al., 2000). These data suggest that mechanical injury to a joint may result in both necrotic and apoptotic cell death. The D'Lima et al. study (2001) also found 34% of chondrocytes in human chondral explants die via apoptosis when exposed to14 MPa of unconfined compression. Administration of z-VAD.fmk, a pan-caspase inhibitor, reduced cell death to 25% in these explants. A limitation of the current study was that cell death by other mechanisms, for example by apoptosis, was not examined following P188 intervention. An influx of Ca2+, for example, into the chondrocyte prior to membrane resealing by P188 may trigger an early programmed cell death (Aigner and Kim, 2002). A previous study on neuronal cells has also found P188 to be effective in limiting apoptosis as detected by TUNEL staining (Serbest, 2003). It is likely that after trauma, interventions like z-VAD.fmk could be used in combination with P188 to more effectively reduce chondrocyte death or dysfunction in the longer term.

The current study found that early administration of P188 surfactant into the joint resulted in a decrease in the percentage of total dead cells in retro-patellar cartilage from approximately 18% to 7%. In a previous study by our laboratory using bovine chondral explants, 25 MPa of unconfined compression applied in 1 second resulted in

approximately 34% of the cells necrotic 24 hours after impact (Phillips and Haut, 2004). Immediate treatment of these explants after impact with an 8 mg/ml concentration of P188 surfactant reduced cell death to approximately 14 % at 24 hours post trauma. Differences in total cell death between the previous and current studies may have been due to the presence of underlying bone in the in vivo model that stiffened the articular cartilage and prevented excessive deformation during impact to the joint (Krueger et al., 2003). Furthermore, in contrast to the current study in which P188 surfactant appeared more effective in 'saving' cells in the superficial zone of the retro-patellar cartilage, the treatment of chondral explants in the previous study with this same concentration of surfactant significantly reduced cell death in all layers of the tissue. One explanation for the more limited efficacy of the treatment in the current study may relate to the penetration of the P188 surfactant. In the previous study the chondral explants were 'pumped' immediately after administration of the surfactant and approximately 22 hours after impact with 10 cycles of unconfined compression at 1 MPa pressure and a frequency of 1 Hertz. In the current study the animal joint was flexed approximately 10 times immediately after injection of the surfactant, and the animals were exercised daily beginning on the day of blunt impact to the joint. It was assumed that post trauma exercise would help 'pump' the surfactant into the cartilage. The 'pumping' of surfactant into the tissue, while not verified in the previous or current studies, may have been less effective in the in vivo joint due to differences in the intensity of the pressure and the unknown loading of the joint during treadmill exercise. Penetration of the surfactant into the cartilage may have also been limited by the underlying subchondral bone in the in vivo joint. The efficacy of this treatment, on the other hand, may be enhanced by a

reduction in the concentration of the surfactant solution, after the relationship between efficacy and solution concentration is established in future in vitro studies with both chondral and osteochondral explants. Another limitation of the current study was that the quantity of surfactant solution was limited to 1.5 ml. There was no basis for choosing this quantity other than to limit the amount of fluid in the small rabbit knee, and that in a previous study this quantity of polysulfated glycosaminoglycan solution was injected into the rabbit joint (Ewers and Haut, 2000). The relationships between optimization of the surfactant concentration, the quantity of fluid, and the timing of the intervention post impact should be determined in future studies using the established rabbit model, or possibly another larger, yet undeveloped in vivo animal model.

The current study used a small sample size (n=6) and an in vivo model which yielded large variations in both surface fissure and chondrocyte viability data. This resulted in an insufficient amount of statistical power between treatment groups. The average total length of surface fissures in the '4-day poloxamer' group was approximately 4 times greater in the un-impacted and approximately 2 times greater in the impacted patellae than the '4-day no poloxamer' group on average. A statistically significant difference was not detectable due to the low power. The greater length of surface fissuring in the '4-day poloxamer group' resulted from two animals that exhibited large amounts of base-line surface fissuring on their un-impacted retropatellar surface. These animals were not disregarded due to the already small sample size. Furthermore, previous studies have documented chondrocyte death around surface cracks (Ewers et al., 2001; Lewis et al., 2002), but the '4-day poloxamer' group exhibited significantly less percentage of dead cells on average in the impacted patellae versus the '4-day no

poloxamer' group. These data suggest that the increased, baseline surface fissuring documented in the '4-day poloxamer' group did not adversely affect the results of the study.

In summary, 6 Joules of blunt impact to the flexed rabbit patello-femoral joint was found to result in a significant percentage of necrotic cells in the retro-patellar cartilage immediately after insult. It is hypothesized that the chronic degradation of this cartilage, which has been documented by our laboratory in a 3 year post trauma study (Ewers et al., 2002), may be due, at least in part, to the death of these chondrocytes. The current study also found, in concert with earlier studies on chondral explants (Phillips and Haut, 2004), that immediate administration of the traumatized joint with P188 surfactant resulted in a statistically significant decrease in the percentage of necrotic cells. The above hypothesis on a mechanism of post traumatic osteoarthritis may be tested in the future with injection of P188 surfactant into the joint immediately after blunt insult. The long term consequences of 'saving' these cells from early necrotic death, in terms of them ultimately becoming apoptotic and producing degradation enzymes into the joint tissue (Pickvance et al., 1993) must be investigated in future studies. This intervention with P188 surfactant, however, may also allow sufficient time to evaluate the biological condition of these and other cells in the traumatized tissue and utilize additional pharmacological treatments, such as the caspase inhibitor mentioned earlier, if needed, for the long term survival of the joint cartilage.

Acknowledgements: This study was supported by grants from The Centers for Disease Control and Prevention, The National Center for Injury Control and Prevention

(R49/CCR503607) and The TRW Automotive Fund. Its contents are solely the responsibility of the authors and do not necessarily represent the official views of the CDC or the TRW Corporation. The authors wish to gratefully acknowledge the help of Clifford Beckett, Aaron Stewart (A.S.), and Jean Atkinson (J.A.) for technical assistance during this study.

References

Aigner T, Kim HA. Apoptosis and cellular vitality: issues in osteoarthritic cartilage degeneration. Arthritis Rheum 2002;46:1986-96

Borgens RB, Bohnert D, Duerstock B, Spomar D, Lee RC. Subcutaneous tri-block copolymer produces recovery from spinal cord injury. J Neurosci Res 2004;76:141-54.

Chen CT, Burton-Wurster N, Borden C, Huegger K, Bloom SE, Lust G. Chondrocyte necrosis and apoptosis in impact damaged articular cartilage. J Orthop Res. 2001;19:703-11

Clarke MSF, McNeil PL. Syringe loading introduces macromolecules into living mammalian cell cytosol. J Cell Sci 1992;102:533-41

Costouros JG, Dang AC, Kim HT. Inhibition of chondrocyte apoptosis in vivo following acute osteochondral injury. Osteoarthritis Cartilage 2003;11:756-9

D'Lima DD, Hashimoto S, Chen PC, Colwell CW, Lotz MK. Impact of mechanical trauma on matrix and cells. Clin Orthop Rel Res 2001;391S:90-9

Duke RC, Ojcius DM, Young JDE. Cell suicide in health and disease. Sci Am 1996;275:80-7

Ewers BJ, Dvoracek-Driksna D, Orth MW, Haut RC. The extent of matrix damage and chondrocyte death in mechanically traumatized articular cartilage explants depends on rate of loading. J Orthop Res 2001;19:779-84

Ewers BJ, Haut RC. Polysulphated glycosaminoglycan treatments can mitigate decreases in stiffness of articular cartilage in a traumatized animal joint. J Orthop Res 2000;18:756-61

Ewers BJ, Weaver BT, Sevensma ET, Haut RC. Chronic changes in rabbit retro-patellar cartilage and subchondral bone after blunt impact loading of the patellofemoral joint. J Orthop Res 2002;20:545-50

Felson DT. An update on the pathogenesis and epidemiology of osteoarthritis. Radiol Clin North Am 2004;42:1-9

Flores R, Hochber M. Definition and classification of osteoarthritis. In: Brandt K, Doherty M, Lohmander S, editors. Osteoarthritis. Oxford: Oxford University Press: 1998. p. 1–12.

Hashimoto S, Ochs RL, Komiya S, Lotz M. Linkage of chondrocyte apoptosis and cartilage degradation in human osteoarthritis. Arthritis Rheum 1998;41:1632-8

Haut RC, Ide TM, DeCamp CE. Mechanical responses of the rabbit patello-femoral joint to blunt impact. J Biomech Eng 1995;117:402-8

Kim HT, Lo MY, Pillarisetty R. Chondrocyte apoptosis following intraarticular fracture in humans. Osteoarthritis Cartilage 2002;10:747-9

Krueger JA, Thisse P, Ewers BJ, Dvoracek-Driksna D, Orth MW, Haut RC. The extent and distribution of cell death and matrix damage in impacted chondral explants varies with the presence of underlying bone. J Biomech Eng 2003;125:114-9

Lewis JL, Deloria LB, Oyen-Tiesma M, Thompson RC, Ericson M, Oegema TR. Cell death after cartilage impact occurs around matrix cracks. J Orthop Res 2003;21:881-7

Marks JD, Pan CY, Bushell T, Cromie W, Lee RC. Amphiphilic, tri-block copolymers provide potent membrane-targeted neuroprotection. FASEB 2001;15:1107-9

Mazieres B, Blanckaert A, Thiechart M. Experimental post-contusive osteo-arthritis of the knee. Quantitative microscopic study of the patella and the femoral condyles. J Rheum 1987;14:119-21

Morel V, Quinn TM. Cartilage injury by ramp compression near the gel diffusion rate. J Orthop Res 2004;22:145-51

Morel V, Quinn TM. Short-term changes in cell and matrix damage following mechanical injury of articular cartilage explants and modelling of microphysical mediators. Biorheology 2004;41:509-19

Newberry WN, Garcia JJ, Mackenzie CD, DeCamp CE, Haut RC. Analysis of acute mechanical insult in an animal model of post-traumatic osteoarthrosis. J Biomech Eng 1998;120:704-9

Oyen-Tiesma M, Atkinson J, Haut RC. A method for promoting regular rabbit exercise in orthopaedics research. Contempy Top Lab Anim Sci 1998;37:77-80

Papoutsakis ET. Media additives for protecting freely suspended animal cells against agitation and aeration damage. TIBTECH 1991;9:316-24

Phillips DM, Haut RC. The use of a non-ionic surfactant (P188) to save chondrocytes from necrosis following impact loading of chondral explants. J Orthop Res 2004;22:1135-42

Pickvance EA, Oegema TR, Thompson RC. Immunolocalization of selected cytokines and proteases in canine articular cartilage after transarticular loading. J Orthop Res 1993;11:313-23

Serbest G. In vitro neuronal cell injury model: characterization and treatment strategies. Ph.D. dissertation, Drexel University, 2003;103-42

Simon WH, Richardson S, Herman W, Parsons JR, Lane J. Long-term effects of chondrocyte death on rabbit articular cartilage in vivo. J Bone Joint Surg Am 1976;58:517-26

Tew SR, Kwan APL, Hann A, Thomson BM, Archer CW. The reactions of articular cartilage to experimental wounding. Role of apoptosis. Arthritis Rheum 2000;43:215-25

Thompson RC, Oegema T, Lewis J, Wallace L. Osteoarthritic changes after acute transarticular load. J Bone Joint Surg Am 1991;73:990-1001

Torzilli PA, Grigiene R, Borrelli J, Jr., Helfet DL. Effect of impact load on articular cartilage. Cell metabolism and viability, and matrix water content. J Biomech Eng 1999;121:433-41

U.S.Census Bureau. State and County Quickfacts. 2000. U.S. Public Information Office.

Wright V. Post-traumatic osteoarthritis- A medico-legal minefield. Br J Rheum 1990;29:474-8

Figure Captions

Figure 1

(a) Photograph of the rabbit impact set-up (b) Sketch of the setup depicting the load alignment with the knee joint.

Figure 2

Patellae were glued to cylindrical block (a,b) in order to align the surface parallel with the Isomet gravity saw blade (c). The saw was used to create osteochondral sections of the retro-patellar surface.

Figure 3

Digital photographs (25X) of un-impacted (a) and impacted (b) retro-patellar surfaces were taken for each rabbit. Impact induced fissures were stained with India ink. The fissures were digitally measured and recorded with digital imaging software.

Figure 4

Digitally measured and recorded surface fissure lengths were averaged and depicted in a bar chart. Brackets indicate significant differences between groups using a 2 factor repeated measures ANOVA . There was a statistically significant greater average length of surface fissuring in impacted versus un-impacted patellae in all of the groups.

Figure 5

Impacted (a) and un-impacted (b) patellar cross sectional slices were stained for cell viability. Live cells were stained green and dead cells were stained red. The impacted patellae were subjected to a 6 Joule impact and stained with calcein AM and ethidium homodimer either immediately following impact or 4 days post-impact. Images (a) and

(b) show patellae that were untreated and viewed immediately after impact. The impacted patella (b) shows extensive areas of cell death in the surface zone after trauma.

Figure 6

Statistically greater amounts of cell death were documented in the impacted versus un-impacted patellae of both the "time 0" and the "4-day no poloxamer" groups. A significantly greater amount of cell death was recorded in the impacted patellae of the '4 day no poloxamer' group versus the '4 day poloxamer' group. The brackets denote statistical significance by a 2 factor repeated measures ANOVA.

Figure 7

There was a statistically greater percentage of cell death in the superficial and deep zones of the impacted versus un-impacted patellae in both the "time 0" and "4 day no poloxamer" groups. There was also a significant difference in the total percentage of cell death in the deep zones of impacted versus un-impacted patellae in the "4 day poloxamer" group. The brackets denote statistical differences using a 2 factor repeated measures ANOVA performed separately for the superficial and deep zones.

Figures

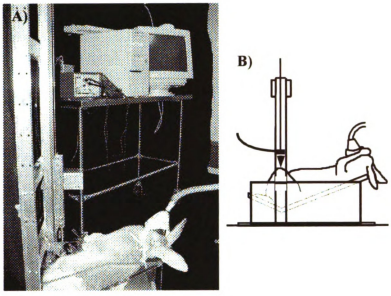

Figure 1

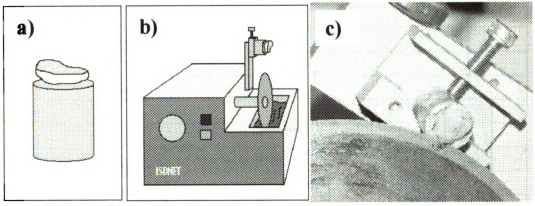

Figure 2

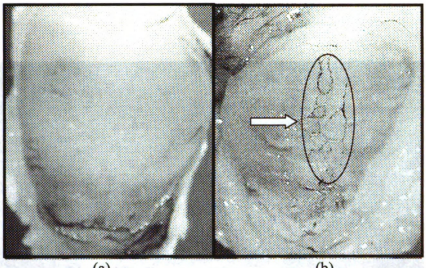

Figure 3

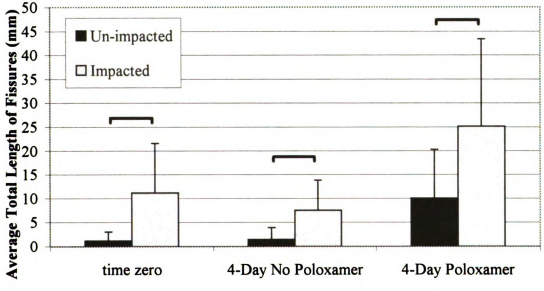

Figure 4

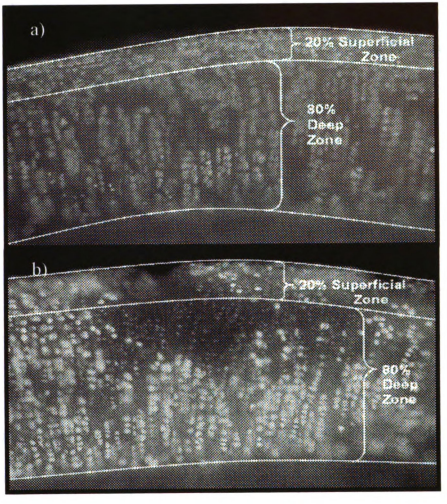
a)
20% Superficial Zone
80% Deep Zone
b)
20% Superficial Zone
80% Deep Zone

Figure 5

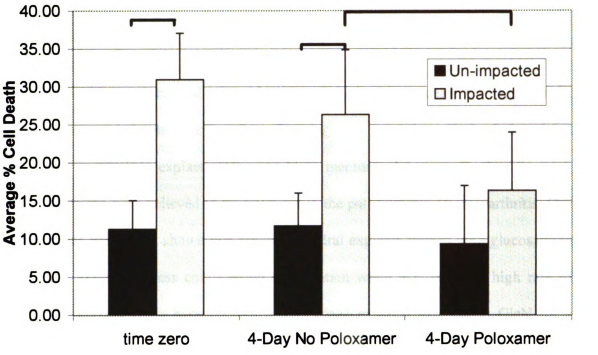

Figure 6

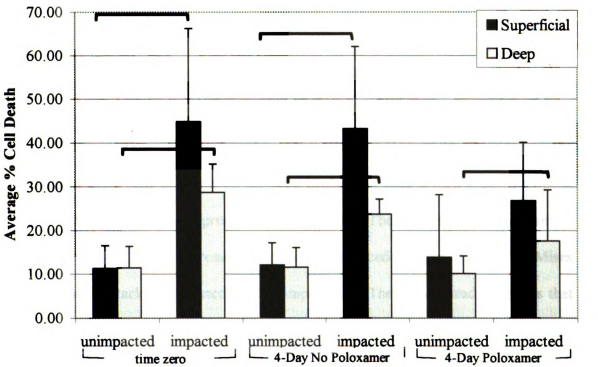

Figure 7

CHAPTER 3: GLUCOSAMINE SUPPLEMENTATION CAN HELP LIMIT MATRIX DAMAGE AND ADJACENT CELL DEATH IN TRAUMATIZED EXPLANTS

Abstract

Severe blunt mechanical trauma has been linked with the onset of osteoarthritis. Matrix damage in the form of surface fissuring and necrotic cell death has been documented in cartilage explants following blunt mechanical trauma. Surface fissuring and cell death are both believed to be pathways in the pathogenesis of osteoarthritis. Our laboratory has previously shown that bovine chondral explants treated with glucosamine (GlcN) will experience less compressive deformation when exposed to a high rate of impact. The current study hypothesized that cartilage explants exposed to GlcN for a period of 6 days will develop an extracellular matrix richer in glycosaminoglycans (GAG). These GAGs will reduce the permeability which will in turn result in hydrostatic pressure generated during loading to help limit distortional strains which have been suggested to be responsible for chondrocyte death. A finite element model, using a transversely isotropic biphasic material model for articular cartilage was developed in order to test the effects of permeability on the stress field in a chondral explant under unconfined compression. The results indicate that GlcN supplementation help reduce the percentage of dead cells in impacted cartilage explants at both a high (~50ms to peak pressure) and low (~1 s to peak pressure) rate of loading. The study also showed, using a finite element model, that a decrease in permeability reduced the area of high Von Mises stresses around a crack during unconfined compression. The current study suggests that pretreating chondral explants with GlcN can help limit impact induced cell death.

Introduction:

Excessive mechanical loading to a joint has been linked to the long term chronic degradation of articular cartilage (Ewers et al., 2000). *In situ* studies that examine the acute response of a blunt impact to human knee joints document the appearance of surface lesions on the retro-patellar cartilage resulting from pressures of approximately 30 MPa (Atkinson and Haut, 2001). *In vivo* studies using the giant Flemish rabbit also document the appearance of surface fissures on retro-patellar cartilage as the result of a 6 Joule blunt impact to the knee at pressures of approximately 25 MPa (Newberry et al., 1998). This same *in vivo* rabbit model has been used to document significant degradation of articular cartilage 3 years post impact (Ewers et al., 2002). A similar study that looked at the acute response of a 6 Joule impact to the rabbit knee found surface lesions and associated chondrocyte death acutely in the retro-patellar cartilage (Baars et al., 2005). *In vitro* studies that subject bovine chondral explants to 30 MPa of unconfined compression find excessive surface fissuring and associated chondrocyte death (Ewers et al., 2000; Krueger et al., 2003; Phillips and Haut 2004). In an *in vivo* study significant necrosis of chondrocytes was induced in the patello-femoral joint of rabbits by localized freezing of the tissue *in vivo* (Simon et el., 1976). After 1 year the affected cartilage shows changes that are consistent with early signs of OA. The tissue changes appear similar to those documented by our laboratory using the impacted joint model (Ewers et al., 2002). These data suggest that the association between blunt impact trauma to a joint and a subsequent degradation of articular cartilage may be the result of impact induced surface damage and associated chondrocyte death.

Previous studies correlate the onset of surface fissures with the development of high tensile strains in the collagen (Morel and Quinn 2004, Askew and Mow1978, Eberhardt et al., 1991). One study found that surface fissures in cartilage explants could not be induced when the loading rate was equal or less than the gel diffusion rate suggesting that fluid pressurization generated during loading causes collagen fiber failure (Morel and Quinn, 2004). While chondrocyte death has been documented to occur predominately around surface cracks at high rates (Ewers et al., 2000; Lewis et al., 2003), other studies have found chondrocyte death to occur throughout the thickness without the presence of surface cracks (Millentejivic and Torzilli, 2005; Morel and Quinn, 2004). A study by Ewers et al. (2000) compared the effects of high and low rates of loading and found chondrocyte death to occur around surface cracks at both rates, but with a greater diffusion of cell death away from cracks in lower rate of loading experiments. It has been suggested that chondrocyte death may be limited in areas away from cracks if fluid flow is prevented, thus increasing the hydrostatic pressure and limit cell deformations during loading (Millentejivic and Torzilli, 2005). These data suggest that an increase in glycosaminoglycan content, and thus an increase in interstitial fluid pressurization and decrease in tissue permeability could potentially limit chondrocyte deformation during loading.

Some studies have documented an upregulation of glycosaminoglycan production both *in vivo* (Oegema et al., 2002) and in cultured human chondrocytes (Dodge and Jimenez 2003) as a result of treatment with the nutraceutical glucosamine (GlcN). A study by this laboratory found that treating bovine chondral explants with GlcN prior to a high rate of blunt impact loading significantly reduced cartilage deformation, matrix

damage, and nitric oxide production post impact (Kreuger et al., 2000). A study by Lippiello (2003) found bovine cartilage explants exposed to GlcN experienced a 1000% increase in cell metabolism. In clinical trials GlcN has been shown to significantly reduce the progression of joint space narrowing (Reginster et al., 1999), decrease pain, and improve joint mobility in patients suffering from OA (Camarada and Dowless, 1998; Rovat, 1992; Vaz, 1982; Pujalte et al., 1980). *In vitro* studies, which chemically induce cartilage degradation via exposure to interleukin-1 (IL-1) or lipopolysaccharide (LPS), have documented significant decreases in the tissue's subsequent production of degradation enzymes when exposed to GlcN (Fenton et al., 2000; Fenton et al., 2002). These data suggest that GlcN can improve the quality of the cartilage matrix by reducing the presence of degradation enzymes, as a well as promoting the synthesis of tissue glycosaminoglycans.

The aim of the current study was to further investigate the effects of preconditioning chondral explants with GlcN prior to a severe blunt impact. The hypothesis was that chondral explants pretreated with GlcN and exposed to injurious unconfined compression will possess a less permeable matrix richer in glycosaminoglycans which will in turn resist fluid movement and result in less chondrocyte death around surface cracks. To test the hypothesis a transversely isotropic biphasic model of cartilage was developed in order to determine whether tissue permeability affects stress fields around the area of a crack in a chondral explant exposed to unconfined compression. Also, bovine chondral explants were exposed to GlcN for a period of six days prior to an unconfined compression of 30 MPa at both at high and low rates. These explants were then studied in regards to their mechanical response under

compression, the presence of surface cracks, and chondrocyte death both throughout the thickness as well as number of dead cells adjacent to surface lesions.

Methods

Experimental

Four pairs of bovine forelegs were obtained from a local abattoir within 6 hours of slaughter. The legs were cut just above the knee joint leaving the metacarpal joints intact. The forelegs were cleaned and skinned prior to opening the joint under a laminar flow hood. A 6.35 mm punch with a smooth edge was used to make 120 plugs. Fifteen plugs were taken from each limb. The cartilage plugs were removed from the underlying bone with a scalpel. Sixty explants were placed in individual wells containing Dulbecco's Modified Eagle's Medium (DMEM):F12 (Gibco, USA #12500-039) supplemented with 10% fetal bovine serum and antibiotics (penicillin 100 units/ml, streptomycin 1μg/ml, amphotericin B 0.25 μg/ml), while the remaining sixty specimens were placed in the same media supplemented with 1 mg/ml glucosamine (GlcN) (FCHG49®).

After 48 hours of equilibration, all explants were subjected to manual cyclic loads of 0.5 MPa at 1 Hz. Ten consecutive cycles were applied once each day for four days. The media was replaced every 48 hours. Manual cyclic loading was applied with a custom solid stainless steel cylinder placed in series with a 50 pound load cell (model 31/1432: Sensotec, Columbus, OH). The load cell was connected to a computer with an analog to digital converter. LabView (National Instruments Corp., Austin, TX) software was used to monitor the amplitude and frequency of the intermittent loading.

After four days of intermittent loading, 56 explants from each group were subjected to unconfined compression. Twenty-eight low- and 28 high-rate of loading

experiments were conducted to a peak of 30 MPa in 1s or 50ms, respectively, using a haversine impact load function. Each explant was placed between two highly polished stainless steel plates. Prior to the test, the plates were pressed together at 100 N and the location of the machine actuator was recorded. The thickness of each specimen was determined by finding the difference in the actuator's location at 5 N of load during the test and when the plates were pressed together prior to loading. Each specimen received a 0.5 N preload before being compressed. This protocol has been established in previous experiments from this laboratory (Ewers et al., 2001, Krueger et al., 2003). The load, time, and displacement were recorded during each experiment with an accuracy of 0.1 N, 0.001 s, and 0.01 mm, respectively. Four explants from each media group were not impacted and used for positive and negative controls of cell viability. After the load cycled to approx. 30 MPa each explant was washed three times in media before being returned to pre-assigned wells with one ml of supplemented media and incubated for another 24 hours.

Approximately 24 hours after each mechanical compression experiment, each explant was examined for matrix damage and cell viability. The surface of each explant was wiped with India ink. The explants were immediately photographed with a digital camera (Polaroid DMC2, Polaroid Corporation, Waltham, MA, USA) at 25X under a dissection microscope (Wild M5A, Wild Heerbrugg Ltd., Switzerland) to determine the total length of the surface fissures. The total fissure length was calculated with digital imaging software (Sigma Scan, SPSS Inc., Chicago, IL). One observer (AM) digitally measured the length of the surface fissures in each of the photographs.

For cell viability, two 0.5-mm slices were taken through the thickness at the center of each explant using a customized cutting tool (Ewers et al., 2001). The sections were cut perpendicular to the preferred orientation of surface fissures. The sections were stained with a kit containing calcein and ethidium bromide homodimer (Live/Dead &Viability/Cytotoxity, Molecular Probes, Oregon). Positive controls were put through three freeze-thaw cycles in order to kill all of the cells. Each section was viewed under a fluorescence microscope at 100X (Lecia DM LB (frequency: 50-60 Hz), Lecia Mikroskopie and Systeme GmgH, Germany). Full thickness, digital images were taken of a 2.5-mm length at the center of each explant. These images were partitioned into the superficial zone (top 20%), intermediate zone (middle 50%), and deep zone (bottom 30%). The viable (green) and dead (red) cells were manually counted by one observer (SR) using image software (Sigma Scan, SPSS Inc., Chicago, IL). The percent of cell death was computed for each layer. Also, in order to test whether or not potential differences in cell death were a result of differences in surface fissuring, a blinded observer (AM) manually measured the depth of each surface fissure on each section and counted the number of dead cells in the zone adjacent to each fissure. The ratios of dead cells per fissure and per unit fissure depth were documented.

Unpaired t-tests were used to compare the total length of surface fissures, peak strain, peak stress, time to peak, cartilage thickness, and strains at given stresses between "with GlcN" and "no GlcN" groups for both high and low rates of loading tests. Two factor ANOVAs were performed to evaluate effects of glucosamine treatment and rates of loading on the percentage of cell death for each cartilage tissue layer (superficial, middle, and deep) as well as for the total overall percentage of cell death. Two factor

ANOVAs were also used to evaluate significant differences in the amount of dead cells recorded per fissure as well as per unit depth of fissure. The two factors or independent variables were glucosamine treatment and rate of loading while the dependent variable was percentage of cell death or number of dead cells. All data were reported as mean ± one standard deviation. Statistical significance was indicated at $p<0.05$.

Theoretical

A transversely isotropic biphasic model of articular cartilage was developed using a commercial finite element software package (Abaqus v 6.1, Abaqus Inc., Providence, Rhode Island). The cartilage material model consisted of six independent material constants including Young's modulus in the one and three directions (E_1 and E_3), shear modulus in the one-three plane (G_{13}), Poisson's ratio for the one-three plane (υ_{13}), and hydraulic permeability in both the one and three directions (k_1 and k_3) (Figure 1a). For transverse isotropy, material properties in the two direction were set equal to properties in the one direction. Material properties were assigned based on data from indentation testing of rabbit retro-patellar cartilage (Newberry et al., 1998) (Table 1).

An axisymmetric model of unconfined compression of a chondral explant was constructed (Figure 1b). An arbitrary load of 10 Newtons was applied to a rigid platen in contact with the top surface of the explant. In order to ensure a uniform boundary pressure the platen was not allowed to rotate during loading. Boundary conditions for explant displacement were set to be zero in the axial direction along the bottom side of the explant. Transverse displacement was set at zero along the symmetric axis. Pore pressure was set to zero along the unrestricted edge of the explant in order to allow water flow at the edges.

Two separate models of the unconfined compression experiment were created. One model used an intact cartilage explant and the other had a pre-existing crack, in order to evaluate stress fields around a crack during loading (Figure 1c). Validation of the model was performed by compressing an intact explant at two different rates of loading. The high rate of loading experiment required peak load to be reached in 50ms, and a low rate required peak load to be reached at 1 second. Loading was applied using a ramp. A previous study that applied these rates of loading to bovine chondral explants documented a higher overall strain in the low rate of loading experiments (Ewers et al., 2001). In the current study total distance traveled by the platen was documented and regarded as axial deformation and compared between the high and low rate experiments.

In order to simulate the effects of GlcN treatment the material properties of the cartilage were altered. The permeability for GlcN treated cartilage was decreased an amount that the permeability of rabbit retro-patellar articular cartilage decreased in a separate study where the rabbits were orally administered GlcN (unpublished data) (Table 1). In this study rabbits were fed GlcN for a period of two months prior to indentation testing of the retro-patellar cartilage. Unconfined compression experiments were ran at both high and low rates for GlcN treated cartilage with a pre-existing crack. Von Mises stress patterns were documented around the crack for an explant with normal and reduced permeability. Von Mises stress, is used to estimate yield criteria for ductile materials. It is calculated by combining stresses in two or three dimensions, with the result compared to the tensile strength of the material loaded in one dimension. The formula for the Von Mises stress is given below (http://en.wikipedia.org/wiki/Von_Mises_stress).

$$\sigma_v = \sqrt{\frac{(\sigma_1 - \sigma_2)^2 + (\sigma_2 - \sigma_3)^2 + (\sigma_3 - \sigma_1)^2}{2}}$$

Where σ_1, σ_2, and σ_3 are the principal stresses at a point in the material. The current study evaluated Von Mises stresses since it is a measure of the distortional strain energy and distortional strains have been suggested as a potential mechanism for impact induced chondrocyte death (Millentejivic and Torzilli, 2005).

Results:

Experimental

In high rate of loading experiments there was no difference in the peak pressures between the "no GlcN" group (28.5 ± 0.5MPa, n=28) and the "with GlcN" group (28.4 ± 0.6MPa, n=28). The time to reach peak load for the "with GlcN" group (44 ± 4ms, n=28) was not significantly different from that of the "no GlcN" group (43 ± 4ms, n=28) in the high rate experiments. There was, however, a significant difference in peak strain for the "no GlcN" group (55 ± 6%, n=28) versus the "with GlcN" group (51 ± 6%, n=28) (p=0.043). There were no significant differences in cartilage explant thickness between the "with GlcN" group (0.68 ± 0.1mm, n=28) versus the "no GlcN" group (0.67 ± 0.1mm, n=28). From the data recorded during the high rate tests, nonlinear stress-strain curves were generated for explants from both groups. The "with GlcN" group experienced an increase in explant stiffness by producing a shift in the response curves to the left. There were significant differences in the amount of strain seen by the explant at 20 (p = 0.022), 15 (p = 0.025), 10 (p = 0.029), and 5 (p = 0.033) MPa between the "with GlcN" and "no GlcN" groups (Figure 2).

In the low rate of loading experiments there was also no difference in peak pressures between the "no GlcN" group (28.9 ± 0.5MPa, n=28) and the "with GlcN" group (28.8 ± 0.5MPa, n=28). The time to reach peak load for the "with GlcN" group (0.89 ± 0.05s, n=28) was not significantly different from that of the "no GlcN" group (0.89 ± 0.04s, n=28) in the low rate experiments. There were no significant differences seen in the peak strain between the "with GlcN" group (61 ± 6%, n=28) versus the "no GlcN" group (59 ± 6%, n=28). There were no significant differences in cartilage explant thickness between the "with GlcN" group (0.65 ± 0.1mm, n=28) versus the "no GlcN" group (0.66 ± 0.1mm, n=28). The non-linear stress-strain curves were very similar for both groups during low rate loading, and showed no significant differences in strain at 5, 10, 15, or 20 MPa.

Supplementation of the culture medium with GlcN significantly reduced the amount of surface fissuring in the "with GlcN" group for explants exposed to high rates of loading (Figure 3). Digital analysis of stained explant photographs indicated that for explants in the "no GlcN" group, the total length of fissuring in the high rate tests was 42.8 ± 15.3mm (n=28). In contrast, for "with GlcN" explants the total length of fissures was 31.5 ± 13.3mm (n=28) ($p = 0.003$) (Figure 4). The low rate explants showed no significant differences in total surface fissuring between "with GlcN" (48.3 ± 19mm, n=28) versus "no GlcN" (46.4 ± 11mm, n=28).

For high rates of loading there was a significant difference ($p < 0.001$) in the percentage of total cell death in the "with GlcN" (20 ± 11 %, n=28) group versus "no GlcN" (35 ± 17 %, n=28) group of explants (Figure 5a,b). There was also a significant difference ($p = 0.017$) in the total percentage of cell death in the low rate of loading

experiments between the "with GlcN" (25 ± 10 %, n=28) and "no GlcN" (34 ± 12 %, n=28) groups (Figure 5c,d). Zonal analysis revealed that significantly less cell death was recorded in both the superficial and middle zones in the "with GlcN" groups versus the "no GlcN" groups in both the high and low rates of loading (Figure 6). There were no significant differences found in the percentage of cell death of the deep zone as a result of treatment or rate of loading. The percentage of cell death in the superficial zone for the high rate of loading "with GlcN" group (32 ± 16 %, n=28) was significantly less ($p < 0.001$) than that for the low rate of loading "with GlcN" group (49 ± 15 %, n=28). Cell death typically appeared adjacent to surface lesions in a butterfly wing-like pattern (Figure 7). There was a significantly greater amount of dead cells per fissure in the "no GlcN" group versus the "with GlcN" group at both high and low rates of loading (Figure 8). There was also a significantly greater amount of dead cells per millimeter fissure depth in the "no GlcN" group versus the "with GlcN" group at both rates of loading (Figure 9). The positive and negative controls showed virtually all dead and all live cells, respectively (Figure 10).

Theoretical

The total axial deformation of the explant in the finite element, unconfined compression model was greater for a low rate versus a high rate of loading. The peak axial deformation for the low rate experiment was 6.354×10^{-5} m and 6.554×10^{-5} m for the high rate. These data display a rate effect on tissue stiffness that is consistent with previous studies (Ewers et al., 2001; Krueger et al., 2003). The pattern of Von Mises stress gradients around the crack tip were similar to the patterns of chondrocyte death observed in explants around surface lesions (Figure 11). For the high rate of loading

simulation the explant with a decreased permeability, or rather the 'with GlcN' explant, experienced a higher range of Von Mises stresses (0.259 – 0.766 MPa) versus the explant with normal permeability (0.257 – 0.741 MPa). However, the stress field was different between explants with different permeabilities. Thee explant with with a smaller permeability experienced higher Von Misses stresses concentrated locally around the crack as to where the normal permeability explant experienced a more diffuse pattern of high Von Mises stress around the crack (Figure 11). Similar trends were observed for the low rate of loading simulation, however, the differences in both stress range and pattern were not as strong (Figure 12).

Discussion:

This study confirmed some of the results of a previous study (Krueger et al., 2000), showing that supplementation of the culture medium with glucosamine reduced peak explant strain and the degree of matrix damage during a high rate of unconfined compression. The current study was able to show these results with a concentration of 1 mg/mL versus 2.5 mg/mL, which was used in the previous study (Krueger et al., 2000). The current study documented stiffening in the high rate of loading "with GlcN" explants as observed by a shifting to the left of the stress versus strain response curve (Figure 2). A separate study found the compressive stiffness of articular cartilage to correlate with glycosaminoglycan (GAG) content as determined by magnetic resonance imaging (MRI) techniques (Kurkijarvi et al., 2004). A previous study, which measured the dynamic shear modulus of ovine articular cartilage found it to correlate with cartilage thickness, collagen organization, and GAG content (Oakley et al., 2004). Previous studies have documented an upregulation of GAGs in cartilage exposed to GlcN both *in vivo* and *in*

vitro (Lippiello et al., 2000; Lippiello 2003).. These data, as well as data from the previously mentioned studies, suggest that GlcN treatment may have had an affect on proteoglycan content and/or collagen organization that in turn affected the mechanical response of explants during a high rate of loading. A limitation of the current study was that collagen organization and proteoglycan content was not quantified. Further studies are needed to examine the affects of GlcN treatment on collagen organization and proteoglycan content.

The current study reported a significant reduction in the average total length of surface fissures in GlcN treated explants exposed to a high rate of loading. This phenomenon was not, however, documented in explants exposed to a lower rate of loading. Previous studies correlate the onset of surface fissures with the development of high tensile strains in the collagen fibril network (Morel and Quinn 2004; Askew and Mow, 1978; Eberhardt et al., 1991). Theoretical models of *in situ* cartilage loading scenarios suggest that a potential mechanism for surface fissuring could be the development of high tensile strains near the surface of cartilage during loading (Li et al., 1995; Atkinson et al., 1998). It has been documented that the development of surface fissures occurs at fast rates of loading that don't allow for fluid movement through the semi-permeable solid matrix (Morel and Quinn, 2004). This inability of fluid to escape from the matrix results in interstitial fluid pressurization generated during loading that exceeds the restraining capacity of the collagen network (Pins et al., 1995). The maximum compressive strain was less, on average, in the high rate of loading "with GlcN" group of explants suggesting that the in-plane strain, based on the Poisson affect, was also less. There were no significant differences in maximum compressive strain

documented in the low rate of loading explants between the "with GlcN" versus the "no GlcN" explants, possibly helping to explain no significant differences in average surface fissure length between groups. The data from the current study suggest that the reduction in surface fissuring in the high rate of loading "with GlcN" group may have resulted from the stiffened response as documented by a shift to the left of the stress versus strain curve (Figure 2).

A significantly less amount of total cell death was documented in explants pretreated with GlcN for both high and low rates of loading tests. These findings are in contrast with those from a previous study which did not document any significant differences in cell death between GlcN treated and untreated explants exposed to a blunt impact (Krueger et al., 2000). Potential causes for the contrast in data may have been from differences in the GlcN pretreatment incubation period, GlcN concentration, and the introduction of intermittent cyclic loading prior to impact. The previous study exposed explants to a concentration of 2.5 mg/ml of GlcN, as opposed to the current study which used 1 mg/mL GlcN. Recent studies have found that high concentrations of GlcN have cytotoxic effects at high concentrations (Mello et al., 2004). Furthermore, the previous study pretreated explants for a period of 48 hours, as opposed to the current study which used a 6 day incubation period. Other *in vitro* studies that have shown an increase in cartilage matrix synthesis as a result of GlcN treatment have used incubation periods as long as 10 days (Lippiello, 2003; Fenton et al., 2004). Also, the introduction of intermittent low level cyclic loading throughout the incubation period may have also contributed to the differences in cell viability in the current versus the previous study. In a separate study that examined the effects of a mild surfactant on chondrocyte viability

low level cyclic loading after treatment was necessary in order for the treatment to be effective. The protocol was suggested to have allowed for the surfactant to be 'pumped' into the tissue (Phillips and Haut, 2004). A separate study found a 1000% increase in cartilage metabolism in GlcN treated explants exposed to 24 hours of static stress, as opposed to a 40% increase in those that were not stressed. The data from the current study suggests that GlcN dosage concentration, pretreatment time duration, and mechanical stress may play a role in GlcN's ability to prevent chondrocyte death as a result of a blunt impact *in vitro*. The increased benefits of GlcN on traumatized cartilage in explants that were exposed to low level cyclic loading prior to injury may also suggest co-benefits to the cartilage that may arise from exercise in combination with GlcN in an *in vivo* situation.

A reduction in impact induced surface cracks, as a result of less compressive strain in the GlcN treated, high rate of loading group of explants may have been responsible for the reduction in chondrocyte death in the superficial zone. This agrees with previous studies that document the presence of cell death primarily around surface cracks in explant studies (Lewis et al., 2003; Ewers et al., 2000). However, there was also a significant decrease in chondrocyte death in the "with GlcN" versus "no GlcN" explants for low rates of loading. In order to eliminate the effects of surface fissuring on chondrocyte viability the number of dead cells per surface fissure, and dead cells per unit depth of surface fissure were quantified. Results from this data showed a significant reduction in dead cells per fissure and dead cells per unit fissure depth in GlcN supplemented groups for both rates of loading versus their respective "no GlcN" groups. While the mechanism for the action of GlcN on cell death near surface cracks is yet

unclear, upregulation of tissue PGs in the pericellular matrix (Quinn et al., 1998) may help limit shearing strains in chondrocytes near the cracks. The effect could, as well, be that GlcN increases the yield stress and reduces post-yield strains in articular cartilage. Both of these alterations can reduce the zone of plastic strain adjacent to surface fissures (Mendelson 1968). The zone of plastic strain around a crack tip resembles the zone of dead cells in an impacted cartilage explant (Figure 13). The data from the current study indicate that pre-treatment with GlcN can help reduce the zone of plastic strain perhaps by increasing the yield strength of the tissue. Previous studies have documented cell death to occur predominately around surface cracks when loaded at a high rate (Lewis et al., 2003; Ewers et al., 2001) and away from cracks and further into the depth of the cartilage when loaded at slower rates (Morel and Quinn 2004). It has been suggested that large distortional strains developed in the cartilage matrix during loading may contribute to acute cell death (Milentejivic and Torzilli, 2005). The same study suggested that hydrostatic pressure developed during loading could help limit cell deformations. A decrease in permeability, to model GlcN treatment, was shown to reduce the zone of high Von Mises stresses around a crack in the theoretical model of unconfined compression. These data may suggest a mechanism whereby GlcN treatment may help limit the potential for developing a post-traumatic osteoarthritis by decreasing cartilage permeability, perhaps as a result of an up-regulation of tissue GAGs, to increase a hydrostatic pressure effect in the cartilage during impact loading and limit chondrocyte death. More studies need to be performed in order to validate this hypothesis. Further experimental and theoretical analyses are needed to better explain the chondroprotective effect of glucosamine for blunt impact situations.

In conclusion, in the current study bathing cartilage explants in GlcN supplemented culture media prior to a blunt impact had some significant beneficial effects. Impact induced chondrocyte death was found to be significantly reduced in explants that were pretreated with GlcN. This reduction in cell death was found to occur predominately around surface lesions with fewer dead cells per lesion in the GlcN supplemented explants. However, the mechanism by which GlcN was able to reduce cell death around these traumatized areas cannot be deduced based on the collected data from the current study. Future investigations should explore potential mechanisms of this phenomenon.

Acknowledgement: This research was supported by a grant from the Cendter for Disease Control (R49/ CCR503607). Nutramax Laboratories, Inc., Edgewood, MD provided the supplement. The Authors would like to thank Clifford Beckett for his technical assistance.

References

Askew M, Mow V: The biomechanical function of the collagen fibril ultrastructure of articular cartilage. Journal of Biomechanical Engineering 100:105-115, 1978

Atkinson TS, Haut RC, Altiero NJ: An investigation of biphasic failure criteria for impact-induced fissuring of articular cartilage. Journal of Biomechanical Engineering 120:536-537, 1998

Atkinson PJ, Haut RC: Injuries produced by blunt trauma to the human patellofemoral joint vary with flexion angle of the knee. Journal of Orthopaedic Research 19, 827-833, 2001

Baars D, Phillips DM, Haut RC: Repair of damaged chondrocytes in the *in vivo* traumatized joint. Transactions of the 51st Annual meeting of Orthopaedic Research Society 2005

Camara, CC, Dowless GV: Glucosamine sulfate for osteoarthritis. Annals of Pharmacotherapeutics 32(5), 580-587, 1998

Dodge GR, Jimenez SA: Glucosamine sulfate modulates the levels of aggrecan and matrix metalloproteinase-3 synthesized by cultured human osteoarthritis articular chondrocytes. Osteoarthritis and Cartilage 11(6): 424-432, 2003

Eberhardt AW, Lewis JL, Keer LM: Normal contact of elastic spheres with two elastic layers as a model of joint articulation. Journal of Biomechanical Engineering 113, 410-417, 1991

Ewers B, Dvoracek-Driksna D, Orth M, Altiero N, Haut R: Matrix damage and chondrocyte death in articular cartilage depends upon loading rate. Transactions of the 46th Annual meeting of Orthopaedic Research Society. 2000

Ewers BJ, Dvoracek-Driksna D, Orth MW, Haut RC: The extent of matrix damage and chondrocyte death in mechanically traumatized articular cartilage explants depends on rate of loading. Journal of Orthopaedic Research 19:779-784, 2001

Ewers BJ, Weaver BT, Sevensma ET, Haut RC: Chronic changes in rabbit retro-patellar cartilage and subchondral bone after blunt impact loading of the patellofemoral joint. Journal of Orthopaedic Research 20:545-550, 2002

http://en.wikipedia.org/wiki/Von_Mises_stress

Krueger J, Dvoracek-Driksna D, Ewers B, Haut R, Orth M. Effects of pretreatment with glucosamine on mechanically traumatized cartilage explants. 47, 257. 2001. Transactions of the 47th Annual Meeting of the Orthopaedic Research Society. 2001.

Krueger JA, Thisse P, Ewers BJ, Dvoracek-Driksna D, Orth MW, Haut RC: The extent and distribution of cell death and matrix damage in impacted chondral explants varies with the presence of underlying bone. Journal of Biomechanical Engineering 125(1):114-119, 2003

Kurkijarvi JE, Nissi MJ, Kiviranta I, Jurvelin JS, Nieminen MT: Delayed gadolinium-enhanced MRI of cartilage (dGEMRIC) and T2 characteristics of human knee articular cartilage: topographical variation and relationships to mechanical properties. Magnetic Resonance in Medicine 52(1):41-6, 2004

Lewis JL, Deloria LB, Oyen-Tiesma M, Thompson RC, Ericson M, Oegema TR: Cell death after cartilage impact occurs around matrix cracks. Journal of Orthopaedic Research 21:881-887, 2003

Li X, Haut RC, Altiero NJ: An analytic model to study blunt impact response of the rabbit P-F joint. Journal of Biomechanical Engineering 117:485-491, 1995

Lippiello L, Han MS. Dose and stress response characteristics of articular cartilage chondrocytes to glucosamine and chondroitin sulfate. 49th Annual Meeting of the Orthopaedic Research Society, 2003

Lippiello L, Woodward J, Karpman R, Hammad T: In vivo chondroprotection and metabolic synergy of glucosamine and chondroitin sulfate. Clinical Orthopaedics and Related Research 381:229-240, 2000

Mello DM, Nielsen BD, Peters TL, Caron JP, Orth MW: Comparison of inhibitory effects of glucosamine and mannosamine on bovine articular cartilage degradation in vitro. American Journal of Veterinary Research 65(10):1440-5, 2004

Milentijevic, D., Helfet, D.L., Torzilli, P.A., 2005. Influence of stress rate on water loss, matrix deformation and chondrocyte viability in impacted articular cartilage. Journal of Biomechanics 38, 493-502.

Morel V, Quinn TM: Short-term changes in cell and matrix damage following mechanical injury of articular cartilage explants and modeling of microphysical mediators. Biorheology 41(3-4):509-519, 2004

Newberry, W.N., Garcia, J.J., Mackenzie, C.D., Decamp, C.E., Haut, R.C., 1998. Analysis of acute mechanical insult in an animal model of post-traumatic osteoarthrosis. Journal of Biomechanical Engineering 120, 704-709.

Oakley SP, Lassere MN, Portek I, Szomor Z, Ghosh P, Kirkham BW, Murrell GA, Wulf S, Appleyard RC: Biomechanical, histologic and macroscopic assessment of articular cartilage in a sheep model of osteoarthritis. Osteoarthritis and Cartilage. 12(8):667-79, 2004

Oegema TR, Deloria LB, Sandy JD, Hart DA: Effect of oral glucosamine on cartilage and meniscus in normal and chymopapain-injected knees of young rabbits. Arthritis and Rheumatism 46(9):2495-2503, 2002

Phillips DM, Haut RC: The use of a non-ionic surfactant (P188) to save chondrocytes from necrosis following impact loading of chondral explants. Journal of Orthopaedic Research 22:1135-42, 2004

Pins GD, Huang EK, Christiansen DL, Silver FH: Effects of static axial strain on the tensile properties and failure mechanisms of self-assembled collagen fibers. Journal of Applied Polymer Science 63:1429–40, 1995

Pujalte JM, Llavore EP, Ylescupidez FR: Double-blind clinical evaluation of oral glucaosamine sulphate in the basic treatment of osteoarthrosis. Current Medical Research and Opinion 7:110-114, 1980

Quinn TM, Grodzinsky AJ, Hunziker EB, Sandy JD: Effects of injurious compression on matrix turnover around individual cells in calf articular cartilage explants. Journal of Orthopaedic Research 16:490-499, 1998

Reginster J, Dacre J, Rovati L, Gosset C: Glucosamine sulfate significantly reduces progression of knee osteoarthritis over 3 years: A large randomized, placebo-controlled, double-blind, prospective trial. Osteoarthritis and Cartilage 8(2):151-152, 2001

Rovati LC: Clinical research in osteoarthritis: Design and results of short-term and long-term trials with disease-modifying drugs. International Journal of Tissue Reaction 14:243-251, 1992

Simon WH, Richardson S, Herman W, Parsons JR, Lane J: Long-term effects of chondrocyte death on rabbit articular cartilage in vivo. Journal of Bone and Joint Surgery 58(4):517-526, 1976

Vaz AL: Double-blind clinical evaluation of the relative efficacy of ibuprofen and glucosamine sulphate in the management of osteoarthrosis of the knee in out-patients. Current Medical Research and Opinion 8:145-149, 1982

Tables

Table 1. Transversely isotropic and **biphasic** material properties values for the theoretical cartilage material model

	"no GlcN"	"with GlcN"
E_1 (MPa)	7.835	7.835
E_3 (MPa)	1.53	1.53
k_1 ($*10^{-13}$ m^2)	5.95	3.149
k_3 ($*10^{-13}$ m^2)	1.222	0.858
υ_1	0.5	0.5
υ_3	0	0
G_{13} (MPa)	0	0

Figure Captions

Figure 1. An axisymmetric finite element model of an unconfined compression of a chondral explant was developed. Cartilage was modeled as being transversely isotropic biphasic (a). Two separate geometries were used; one was an intact cartilage explant (b) while the other was cartilage with a pre-existing crack(c)

Figure 2. Stress vs. Strain response curves for high rate of loading tests for both the "with GlcN" and "no GlcN" groups. Stress and strain data was collected during unconfined compression tests. Stars indicate statistically significant different amounts of strain at the same pressure ($p<0.05$

Figure 3. Gross photographs were used to determine the average total fissure length for cartilage explants following blunt impacts. In the high rate of loading groups, less fissuring was documented in GlcN treated explants (a) compared to non-treated specimens (b).

Figure 4. The total length of surface fissuring was quantified using digital imaging software. Bar graphs of average values of total fissure length both high rate and low rate tests were made. Error bars represent the standard deviation. "*" indicates statistically significant ($p<0.05$) difference from corresponding "no GlcN" group

Figure 5. Explants cross sections were stained with calcein and ethidium homodimer. Photographs were taken at 100X with a digital camera attached to a flouresence microscope. Viable cells are indicated via a green stain and dead cells a red stain. (a) low

rate "with GlcN" (b) high rate "with GlcN" (c) low rate "no GlcN" (d) high rate "no GlcN"

Figure 6. Cross section chondrocyte viability photographs were divided into superficial, middle, and deep zones. Amount of dead and live cells were manually counted in each zone using digital imaging software. Percentages of chondrocyte death were placed in bar charts for both (a) high rate and (b) low rate of loading tests. A * indicates a statistical difference versus respective 'No GlcN' group. A ** indicates a statistical difference in % cell death between rates of loading.

Figure 7. Fluorescence photographs of explant cross sections reveal a greater area of chondrocyte death around impact induced cracks for both rates of loading. (a) "No GlcN" high rate, (b) "With GlcN" high rate (c) "No GlcN" low rate (d) "With GlcN"Low rate.

Figure 8. The number of dead cells around individual fissures were manually counted, recorded, and averaged for each group. "*" indicates a statistical difference from corresponding "no GlcN" groups.

Figure 9. The number of dead cells around individual fissures were manually counted and divided by the depth of the fissure in millimeters. "*" indicates a statistical difference from corresponding "no GlcN" groups.

Figure 10. Half of the un-impacted explants were put through three freeze-thaw cycled and revealed virtually all dead cells (a). Other un-impacted explants showed virtually no cell death (b).

Figure 11. The Von Mises stress paterns were examined after a high rate of load application to a cracked explant in a finite element model of unconfined compression. GlcN modeled cartilage was given a lower permeability based on a hypothesized increase in glycosaminoglycan content. The area of increased Von Mises stresses appeared to be greater in the "No GlcN" modeled cartilage versus the "with GlcN" modeled cartilage.

Figure 12. The Von Mises stress patterns were examined after a low rate of load application to a cracked explant in a finite element model of unconfined compression. There did not appear to be any differences in Von Mises stress patterns between the 'with GlcN' and 'no GlcN' groups.

Figure 13. (a) The area of plastic strain around a crack tip resembles the shape of a butterfly wing. (b) The pattern of plastic strain around a crack superimposed over a fluorescence image of a cartilage explant cross section exposed to 30 MPa of unconfined compression. The pattern of cell death is falls within the bounds of the plastic strain.

Figures

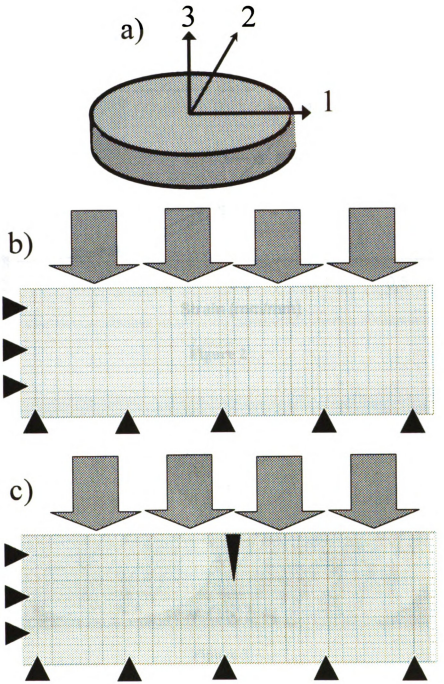

Figure 1

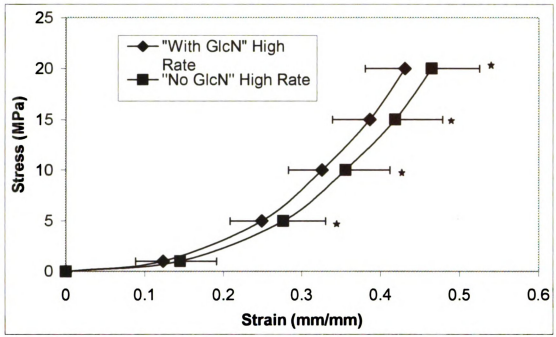

Figure 2

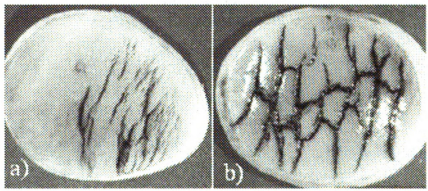

Figure 3

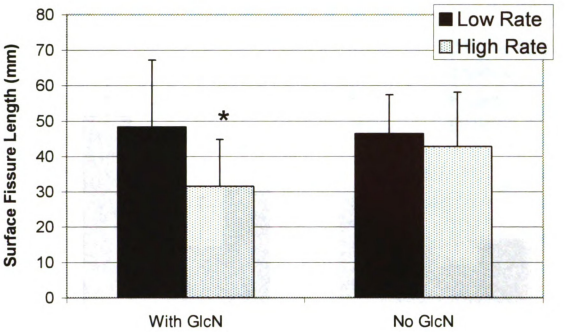

Figure 4

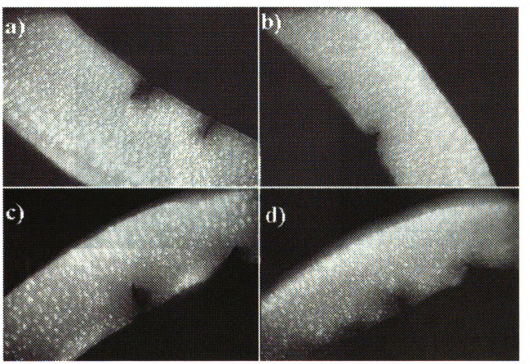

Figure 5

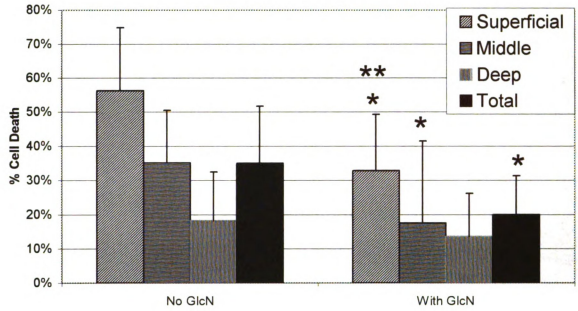
80%
70%
60%
50%
40%
30%
20%
10%
0%
% Cell Death
Superficial
Middle
Deep
Total
**
*
*
*
No GlcN
With GlcN

(a)

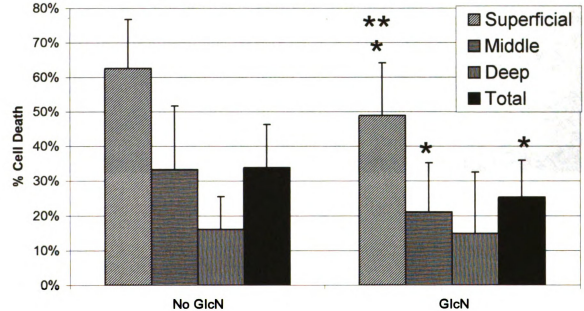
80%
70%
60%
50%
40%
30%
20%
10%
0%
% Cell Death
Superficial
Middle
Deep
Total
**
*
*
*
No GlcN
GlcN

(b)

Figure 6

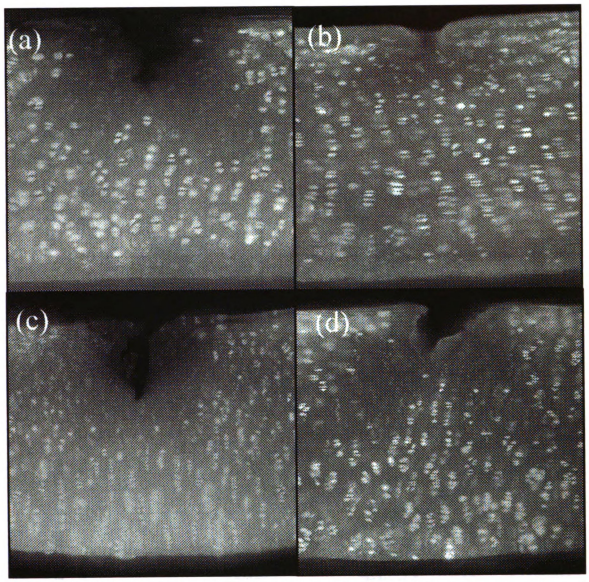

Figure 7

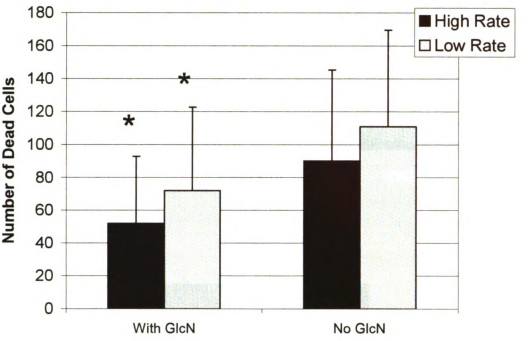

Figure 8

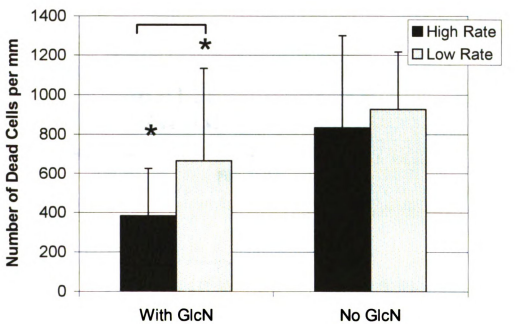

Figure 9

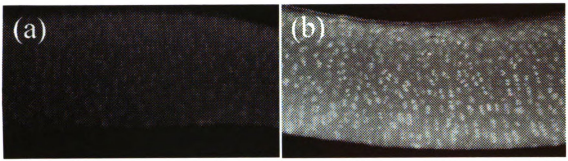

Figure 10

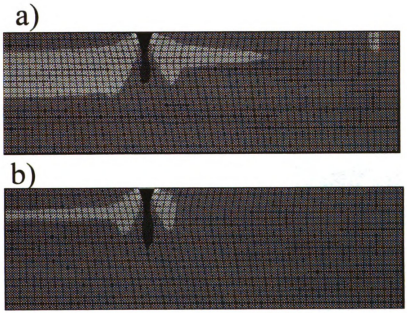

Figure 11

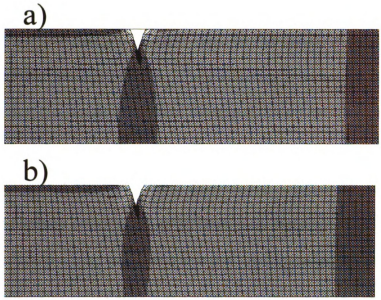

Figure 12

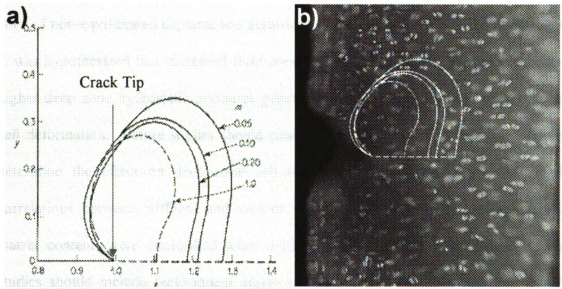

Figure 13

Conclusions and Recommendations for Future Work

The previous chapters describe the results of an injurious blunt impact load to articular cartilage in terms of matrix damage and chondrocyte viability using both *in vitro* and *in vivo* models. Potential therapeutic treatments that can help limit cell death, either by membrane resealing or matrix strengthening were studied.

In Chapter 1 'tissue equilibration' of chondral explants prior to an injurious unconfined compression experiment was found to result in a greater overall length of surface fissuring versus explants that were impacted immediately after removal from the joint. This corresponded to a greater percentage of cell death in the superficial zone for the equilibrated explants. In contrast, the percentage of chondrocyte death in the deep zone of non-equilibrated explants was significantly greater then for equilibrated explants. It was hypothesized that increased fluid present in the equilibrated explants resulted in higher deep zone hydrostatic pressures generated during loading, which in turn limited cell deformation. Future studies should consider the presence of underlying bone, and determine the effect on deep zone cell death. Additionally, it was observed that correlations between stiffness and various parameters, indicative of water and solid matrix content, were diminished when explants were allowed to equilibrate. Future studies should include biochemical assays in order to determine correlations between mechanical characteristics and various matrix constituents, and whether or not these correlations are also diminished as a result of equilibration. Future studies that wish to compare theoretical models with experimental data should be aware of the effects that 'tissue equilibration' might have on the mechanical properties of the tissue.

Chapter 2 described a study on rabbit patello-femoral joints subjected to a 6 Joule intensity impact. The major findings of this study were the presence of acutely necrotic cells in the retro-patellar cartilage and a reduction in the percentage of these dead cells with the administration of poloxamer 188 (P188) directly into the joint immediately after impact. The methods used in this chapter did not account for the long term viability of cells 'saved' by P188. The possibility that these cells, which were saved within the first 4 days after impact, may not function properly or die by apoptosis at a later time needs further investigation. Future studies should acknowledge this possibility and document chondrocyte viability over a longer time period. Methods for determining apoptosis, such as TUNEL staining, should also be included in future studies. Also, a small sample size (n=6) was used in this study, which resulted in a lack of statistical power in numerous analyses. Unfortunately, biologically meaningful differences may have existed, but they were unable to be detected due to the lack of statistical power in the current study. Furthermore, two rabbits in the '4-day poloxamer' group had very high base-line levels of surface fissuring, resulting in average total fissure lengths approximately twice as great as that documented in the other treatment groups. This compromised the current database. The concentration of P188 and the amount of exercise of the rabbit were chosen arbitrarily and should be studied more specifically in future studies. The ability of the P188 to penetrate into the deep zone of the tissue was not recorded in the current study. Future studies may wish to 'tag' the P188 and track the presence of it throughout the thickness of the cartilage.

In Chapter 3 the effects of bathing chondral explants in culture media supplemented with the nutraceutical glucosamine (GlcN) were examined. This study

found that explants treated with GlcN experienced less compressive strain when impacted at a high rate. This limited the amount of surface fissuring. The study also found that the percentage of chondrocyte death was reduced in the group of explants treated with GlcN, in both the superficial and middle zones of the tissue. This affect appeared due to a smaller dispersion of dead cells in the vicinity of impact induced cracks with GlcN supplementation of the medium. A transversely isotropic, biphasic theoretical model of the cartilage explant exposed to unconfined compression found the area of high Von Mises stresses around a crack reduced if the permeability of the tissue was reduced. My study was limited by the fact that no independent measure of permeability was performed to determine if GlcN supplementation, indeed, decreased tissue permeability. Future studies should incorporate mechanical testing of explants both treated and not treated with GlcN to deduce hydraulic permeability. Furthermore, it was suggested that GAGs produced by chondrocytes as the result of GlcN treatment might have been deposited in the pericellular matrix, in turn having a protective effect on the cells. However, in a companion study no significant increase in GAG was documented in explants treated with the same concentration of GlcN used in the current study over a 6 day period. Future studies may wish to examine GAG contents in the immediate vicinity of the chondrocyte, as there may be a rather small, localized effect yielding these results. Also, the current study exposed all explants to manual cyclic loading during pre-treatment with GlcN. Future studies should further examine the potentially synergistic affects of cyclic mechanical loading and GlcN treatment on cartilage explants.

While the current studies find effects of tissue equilibration, P188, and GlcN pre-treatment on the injury response of articular cartilage, they do not fully explain their

mechanisms. Future studies should incorporate other experimental methods such as biochemical assays, molecular magnetic resonance imaging techniques, and apoptotic cell death detection methods to further investigate these findings.

Appendix A: Chapter 1 Raw Data

Load Controlled Experiments

Table 1. Mechanical data for the non-equilbrated explants

Specimen	Time to Peak	Peak Stress	Peak Strain	Thickness	μ	α
	[s]	[MPa]		[mm]		
1	0.041	29.55	0.5932	0.70	2.723	-2.408
2	0.033	29.13	0.5798	0.59	2.258	-2.5
3	0.041	29.00	0.4294	0.67	5.333	-3.632
4	0.042	29.24	0.5203	0.70	3.422	-3.08
5	0.04	29.15	0.6268	0.66	2.078	-2.313
6	0.041	28.60	0.5427	0.51	3.336	-2.672
7	0.035	28.84	0.5346	0.56	3.813	-2.318
8	0.04	29.05	0.5475	0.73	2.403	-3.492
9	0.037	28.82	0.5532	0.73	1.816	-3.853
10	0.042	28.73	0.5376	0.66	3.57	-2.668
11	0.029	28.88	0.4994	0.50	3.149	-2.749
12	0.025	29.48	0.5595	0.51	2.831	-2.462
13	0.038	29.06	0.5755	0.40	3.579	-1.779
14	0.026	28.85	0.6334	0.42	1.794	-1.803
15	0.036	28.91	0.6703	0.45	1.815	-1.532
16	0.034	28.75	0.6622	0.50	1.963	-1.418
17	0.021	29.36	0.5386	0.40	3.336	-2.313
18	0.013	29.96	0.5931	0.46	2.002	-2.218
19	0.025	29.10	0.6654	0.40	1.614	-1.816
20	0.026	29.11	0.4423	0.64	4.274	-3.68
Average	**0.03325**	**29.08**	**0.5652**	**0.56478597**	**2.85545**	**-2.5353**
Std. Dev.	**0.008245413**	**0.323**	**0.0665**	**0.11829986**	**0.9870341**	**0.714273**

Table 2. Mechanical data fro the equilibrated explants

Specimen	Time to Peak	Peak Stress	Peak Strain	Thickness	μ	α
	[s]	*[MPa]*		*[mm]*		
21	0.028	28.76	0.483135075	0.68602437	3.696	-3.457
22	0.03	28.39	0.636599281	0.5911175	2.086	-1.746
23	0.024	29.11	0.551089931	0.63070628	4.124	-1.897
24	0.032	28.13	0.597155084	0.51655235	2.624	-1.874
25	0.028	28.38	0.573146548	0.74151165	2.013	-3.17
26	0.028	28.60	0.659859868	0.68541583	1.289	-2.638
27	0.019	27.96	0.652667409	0.82900104	1.572	-1.968
28	0.026	28.08	0.525510225	0.60141453	3.071	-2.957
29	0.029	27.86	0.602277073	0.61117848	1.817	-3.04
30	0.018	29.04	0.64280617	0.6410789	2.53	-0.896
31	0.028	28.01	0.585485859	0.4954436	2.228	-2.517
32	0.028	28.83	0.6137	0.43598885	2.126	-1.775
33	0.022	29.76	0.6684	0.57511755	1.905	-0.866
34	0.017	29.46	0.6765	0.44708819	0.813	-2.015
35	0.026	29.63	0.7311	0.6264876	1.329	-0.822
36	0.023	28.59	0.7135	0.62121262	0.863	-1.418
37	0.026	29.16	0.5268	0.6110233	2.292	-2.946
38	0.016	30.43	0.6321	0.66077322	0.554	-2.745
39	0.027	29.35	0.6692	0.53320697	1.927	-1.032
40	0.025	29.52	0.6554	0.45653088	1.277	-1.916
Average	**0.025**	**28.84**	**0.619822144**	**0.59984369**	**2.0068**	**-2.08475**
Std. Dev.	**0.004507304**	**0.701**	**0.064593511**	**0.09968538**	**0.9138422**	**0.820396**

Table 3. Equilibrated explant weights and fluid gain

Specimen	Time 0 Weight	Time 24 Weight	Fluid Gain
	*[g*10^-5]*	*[g*10^-5]*	
21	2090	2253	7.80%
22	1420	1650	16.20%
23	1768	1834	3.73%
24	1418	1603	13.05%
25	2106	2401	14.01%
26	1504	1767	17.49%
27	2116	2374	12.19%
28	1850	1896	2.49%
29	1523	1623	6.57%
30	1762	2105	19.47%
31	1453	1620	11.49%
32	1519	1660	9.28%
33	2028	2479	22.24%
34	1445	1720	19.03%
35	1885	2294	21.70%
36	1966	2266	15.26%
37	2021	2246	11.13%
38	2236	2647	18.38%
39	1749	1930	10.35%
40	1666	1921	15.31%
Average	**1776.25**	**2014.45**	**13.36%**
Std. Dev.	**271.215757**	**332.5921281**	**5.62%**

Table 4. Surface fissure data in pixels and millimeters for non-equilibrated (specimens 1-20) and equilibrated (specimens 21-40).

Specimen	Matrix Damage	Matrix Damage	Specimen	Matrix Damage	Matrix Damage
	Pixels	mm		Pixels	mm
1	7071	75.35	21	4209	44.85612789
2	5573	59.39	22	5229	55.72646536
3	2604	27.75	23	3308	35.25399645
4	5383	57.36	24	5320	56.69626998
5	5528	58.91	25	7266	77.43516874
6	3190	33.99	26	5386	57.39964476
7	6983	74.41	27	7098	75.64476021
8	3707	39.50	28	4118	43.88632327
9	5137	54.74	29	4179	44.53641208
10	6129	65.31	30	6290	67.03374778
11	1184	12.61	31	3432	36.57548845
12	5203	55.44	32	5360	57.12255773
13	3387	36.09	33	6496	69.22912966
14	3285	35.00	34	6351	67.68383659
15	3964	42.24	35	6005	63.9964476
16	3721	39.65	36	8105	86.37655417
17	2881	30.70	37	2786	29.69094139
18	3350	35.70	38	6609	70.43339254
19	5016	53.45	39	4759	50.71758437
20	1299	13.843	40	5711	60.86323268
Average	**4229.75**	**45.077**	**Average**	**5400**	**57.55790409**
Std. Dev.	**1667.918964**	**17.775**	**Std. Dev.**	**1425**	**15.18769892**

Table 5. Cell viability data for non-equilibrated (specimens 1-20) and equilibrated (specimens 21-40). The percentage of dead cells was recorded in each zone.

Specimen	% Dead Super	% Dead Middle	% Dead Deep	% Dead ALL
1	12.24%	2.70%	5.56%	5.61%
2	13.22%	7.20%	14.04%	10.70%
3	22.64%	4.40%	17.76%	12.03%
4	24.76%	8.31%	15.02%	14.37%
5	37.93%	30.38%	52.73%	37.56%
6	30.34%	12.20%	6.76%	13.74%
7	18.12%	10.33%	53.68%	20.08%
8	23.47%	23.43%	24.30%	23.68%
9	23.08%	4.54%	24.04%	12.82%
10	26.57%	13.37%	31.17%	19.97%
11	34.95%	6.56%	44.86%	22.03%
12	16.00%	5.12%	5.93%	7.39%
13	23.01%	21.97%	52.94%	29.05%
14	39.08%	20.09%	37.37%	28.10%
15	21.80%	11.93%	14.81%	15.90%
16	43.88%	16.74%	24.19%	24.83%
17	16.48%	3.85%	11.61%	8.21%
18	44.55%	29.21%	52.94%	36.47%
19	47.92%	13.86%	7.97%	18.44%
20	24.53%	3.13%	11.88%	9.40%
Average	**27.23%**	**12.47%**	**25.48%**	**18.52%**
Std. Dev.	**10.73%**	**8.63%**	**17.51%**	**9.27%**

Specimen	% Dead Super	% Dead Middle	% Dead Deep	% Dead All
21	25.96%	11.45%	24.00%	16.99%
22	35.06%	12.73%	12.00%	15.99%
23	46.58%	14.51%	30.87%	26.01%
24	22.34%	8.30%	7.76%	11.16%
25	30.61%	8.12%	13.73%	13.56%
26	29.90%	12.33%	19.05%	17.35%
27	31.30%	5.60%	7.11%	10.55%
28	19.44%	2.28%	10.71%	8.66%
29	36.36%	18.75%	32.29%	26.80%
30	49.37%	1.63%	2.26%	9.38%
31	61.25%	25.21%	5.71%	25.55%
32	48.72%	13.07%	4.26%	14.89%
33	36.36%	20.96%	5.41%	16.33%
34	29.82%	3.39%	0.00%	9.42%
35	36.07%	10.31%	5.41%	12.41%
36	26.92%	22.91%	5.79%	16.87%
37	34.85%	21.36%	30.51%	26.24%
38	67.16%	16.03%	4.90%	21.35%
39	27.50%	26.92%	26.09%	26.74%
40	29.10%	6.12%	5.93%	12.27%
Average	**36.23%**	**13.10%**	**12.69%**	**16.93%**
Std. Dev.	**12.47%**	**7.65%**	**10.49%**	**6.37%**

Displacement Controlled Experiments

Table 6. Mechanical and weight data for all un-equilibrated explants

Specimen	Time to Peak	Peak Stress	Peak Strain	Thickness	Initial Weight	Dry Weight	Percent Water
	[s]	*[MPa]*		*[mm]*	*[g]*	*[g]*	
1	0.048	60.607	0.608	0.801	0.02581	0.00864	66.52%
2	0.046	30.466	0.618	0.549	0.01753	0.00507	71.08%
3	0.046	49.009	0.567	0.635	0.02017	0.00642	68.17%
4	0.046	40.033	0.626	0.684	0.01807	0.00574	68.23%
5	0.045	27.980	0.624	0.597	0.01803	0.00488	72.93%
6	0.044	41.043	0.621	0.704	0.02300	0.00647	71.87%
7	0.046	28.458	0.573	0.488	0.01556	0.00444	71.47%
8	0.046	31.563	0.540	0.485	0.01509	0.00405	73.16%
9	0.044	33.857	0.644	0.685	0.0221	0.00631	71.45%
10	0.046	34.799	0.626	0.612	0.0217	0.00599	72.40%
11	0.043	33.752	0.584	0.548	0.01892	0.0061	67.76%
12	0.044	33.062	0.600	0.587	0.01871	0.00544	70.92%
13	0.043	37.060	0.605	0.660	0.01952	0.00584	70.08%
14	0.048	36.487	0.645	0.742	0.02462	0.00728	70.43%
15	0.045	23.802	0.613	0.514	0.01275	0.00353	72.31%
16	0.045	23.391	0.552	0.422	0.01195	0.00326	72.72%
17	0.044	66.081	0.535	0.653	0.02118	0.00745	64.83%
18	0.045	72.917	0.629	0.923	0.02784	0.01085	61.03%
19	0.046	73.336	0.578	0.815	0.02370	0.00909	61.65%
20	0.044	66.630	0.590	0.813	0.02357	0.00945	59.91%
21	0.046	61.414	0.548	0.675	0.02118	0.00702	66.86%
22	0.044	50.341	0.602	0.724	0.02001	0.00799	60.07%
23	0.048	57.210	0.568	0.709	0.02328	0.00630	72.94%
24	0.047	42.209	0.589	0.620	0.01876	0.00631	66.36%
25	0.045	34.214	0.563	0.521	0.01529	0.00467	69.46%
26	0.045	35.504	0.566	0.555	0.01676	0.00561	66.53%
27	0.042	38.019	0.537	0.526	0.01561	0.00521	66.62%
28	0.044	33.159	0.571	0.567	0.01764	0.00615	65.14%
29	0.046	44.463	0.570	0.678	0.02060	0.00676	67.18%
30	0.045	45.197	0.568	0.678	0.02261	0.00681	69.88%
31	0.044	38.309	0.607	0.687	0.01809	0.00571	68.44%
32	0.044	33.879	0.556	0.543	0.01785	0.00585	67.23%
33	0.045	39.708	0.567	0.519	0.01539	0.00448	70.89%
34	0.046	47.223	0.594	0.616	0.01918	0.00589	69.29%
35	0.046	50.515	0.633	0.754	0.01930	0.00673	65.13%
36	0.046	41.078	0.624	0.641	0.01897	0.00542	71.43%
37	0.046	26.137	0.627	0.596	0.01586	0.00447	71.82%
38	0.045	23.639	0.574	0.476	0.01358	0.00381	71.94%
39	0.043	50.356	0.572	0.775	0.02290	0.00809	64.67%
40	0.044	33.198	0.572	0.565	0.01960	0.00567	71.07%
41	0.046	32.308	0.595	0.575	0.01845	0.00597	67.64%
42	0.045	44.453	0.579	0.691	0.02380	0.00756	68.24%

43	0.043	33.885	0.531	0.508	0.01520	0.00435	71.38%

Table 6 (cont.)

Specimen	Time to Peak	Peak Stress	Peak Strain	Thickness	Initial Weight	Dry Weight	Percent Water
	[s]	*[MPa]*		*[mm]*	*[g]*	*[g]*	
44	0.046	36.975	0.570	0.592	0.01820	0.00509	72.03%
45	0.045	39.134	0.575	0.627	0.01722	0.00511	70.33%
46	0.043	32.184	0.531	0.505	0.01486	0.00402	72.95%
47	0.042	37.827	0.569	0.629	0.01743	0.00539	69.08%
48	0.045	38.276	0.539	0.593	0.01901	0.00607	68.07%
Average	**0.045**	**40.940**	**0.623**	**0.626**	**0.01909**	**0.00602**	**0.68783**
Std. Dev.	**0.001**	**12.403**	**0.031**	**0.103**	**0.00346**	**0.00155**	**0.03470**

Table 7. Mechanical and weight data for all equilibrated explants

Sp.	Time to Peak	Peak Stress	Peak Strain	Thick ness	Initial Weight	24hr Weight	Dry Weight	Final Water	Water Gain
	[s]	*[MPa]*		*[mm]*	*[g]*	*[g]*	*[g]*		
101	0.04	29.6132	0.6101	0.5705	0.01517	0.01666	0.00524	68.55%	9.82%
102	0.043	30.7522	0.6939	0.8176	0.02511	0.03199	0.00749	76.59%	27.40%
103	0.038	31.3075	0.6260	0.6205	0.01856	0.02089	0.00585	72.00%	12.55%
104	0.037	31.0925	0.6375	0.6574	0.01916	0.02135	0.00630	70.49%	11.43%
105	0.034	28.1859	0.6108	0.6242	0.01612	0.01780	0.00546	69.33%	10.42%
106	0.042	28.1466	0.6342	0.6062	0.02028	0.02575	0.00665	74.17%	26.97%
107	0.032	26.7588	0.6196	0.6465	0.01950	0.02800	0.00706	74.79%	43.59%
108	0.04	31.6889	0.6471	0.6901	0.02116	0.02580	0.00681	73.60%	21.93%
109	0.045	41.6000	0.6163	0.6585	0.01762	0.01834	0.00619	66.25%	4.09%
110	0.032	31.8526	0.5927	0.6512	0.01894	0.02166	0.00625	71.14%	14.36%
111	0.039	23.8261	0.7299	1.0422	0.02115	0.02656	0.00760	71.39%	25.58%
113	0.032	16.0949	0.6218	0.7497	0.01876	0.02332	0.00525	77.49%	24.31%
114	0.035	32.6873	0.6519	0.8105	0.02102	0.02447	0.00828	66.16%	16.41%
115	0.038	38.6346	0.6843	0.9684	0.02283	0.02600	0.00868	66.62%	13.89%
116	0.027	16.2095	0.5877	0.5229	0.01617	0.02342	0.00581	75.19%	44.84%
117	0.04	56.4879	0.6219	0.8006	0.02385	0.02556	0.00800	68.70%	7.17%
118	0.045	57.2592	0.6352	0.7503	0.02377	0.02483	0.00808	67.46%	4.46%
119	0.044	35.7709	0.6195	0.5680	0.01570	0.01815	0.00492	72.89%	15.61%
120	0.044	41.2968	0.6428	0.6864	0.02189	0.02356	0.00678	71.22%	7.63%
121	0.037	54.5093	0.5977	0.7331	0.02516	0.02530	0.00782	69.09%	0.56%
122	0.045	32.7198	0.6766	0.7072	0.02037	0.02401	0.00668	72.18%	17.87%
123	0.04	46.7933	0.6526	0.8123	0.02665	0.02895	0.00846	70.78%	8.63%
124	0.046	46.8620	0.6543	0.7695	0.02177	0.02351	0.00671	71.46%	7.99%
125	0.039	37.4273	0.6211	0.6361	0.01787	0.02050	0.00563	72.54%	14.72%
126	0.044	44.5050	0.5816	0.6154	0.01846	0.02042	0.00601	70.57%	10.62%
127	0.043	39.2148	0.5860	0.5839	0.01732	0.01925	0.00631	67.22%	11.14%
128	0.046	50.2143	0.6261	0.7461	0.02168	0.02240	0.00601	73.17%	3.32%
129	0.038	18.6666	0.7040	0.7376	0.01437	0.01661	0.00456	72.55%	15.59%

130	0.045	46.3564	0.6417	0.7545	0.01967	0.02045	0.00664	67.53%	3.97%
131	0.046	50.2062	0.5860	0.6815	0.01977	0.02042	0.00633	69.00%	3.29%

Table 7 (cont.)

132	0.043	48.4188	0.6481	0.8814	0.02499	0.02632	0.00793	69.87%	5.32%
133	0.036	41.7288	0.6038	0.6522	0.02052	0.02181	0.00647	70.33%	6.29%
134	0.044	58.6704	0.5824	0.6777	0.02126	0.02208	0.00750	66.03%	3.86%
135	0.045	43.7454	0.6563	0.7392	0.02153	0.02323	0.00715	69.22%	7.90%
136	0.038	40.9824	0.6417	0.7389	0.02536	0.03001	0.00847	71.78%	18.34%
137	0.045	44.4755	0.6555	0.7573	0.02174	0.02273	0.00667	70.66%	4.55%
138	0.046	49.1013	0.6616	0.8178	0.02147	0.02272	0.00775	65.89%	5.82%
139	0.045	46.8620	0.5993	0.6411	0.02042	0.02107	0.00655	68.91%	3.18%
140	0.033	37.6432	0.5961	0.7826	0.02544	0.02990	0.00858	71.30%	17.53%
141	0.039	33.5299	0.5875	0.5814	0.01783	0.01872	0.00596	68.16%	4.99%
142	0.043	22.9986	0.5720	0.4491	0.01411	0.01505	0.00427	71.63%	6.66%
143	0.037	40.5880	0.6197	0.7759	0.02290	0.02612	0.00813	68.87%	14.06%
144	0.045	24.5931	0.5545	0.4342	0.01554	0.01654	0.00504	69.53%	6.44%
146	0.045	44.5139	0.5908	0.7088	0.02006	0.02129	0.00735	65.48%	6.13%
147	0.039	42.4388	0.6245	0.8032	0.02509	0.02880	0.00910	68.40%	14.79%
148	0.037	49.5821	0.5701	0.7717	0.02376	0.02528	0.00982	61.16%	6.40%
Avg	**0.040**	**38.4046**	**0.6255**	**0.7050**	**0.02047**	**0.02299**	**0.00683**	**70.16%**	**12.44%**
Std. Dev.	**0.005**	**10.7872**	**0.0371**	**0.1165**	**0.00320**	**0.00391**	**0.00125**	**3.13%**	**9.65%**

Appendix B: Chapter 2 Raw Data

Table 1. Mechanical data for all rabbits

Group	Rabbit	Load N	time to peak msec
time zero	M54	621.16	3.2
	M57	529.94	2.1
	BU63	575.8	2.4
	BU62	744.43	5.4
	BB3	939.64	3.1
	BU64	863.48	4.9
ave		**712.41**	**3.52**
stdev		**164.78**	**1.34**
4 Days No Poloxamer	M40	738.44	3.2
	M72	912.19	4.1
	481BF	550.45	3.1
	BU66	525.07	2.3
	BU60	595.65	3.8
	BU61	600.54	5.1
ave		**653.72**	**3.60**
stdev		**146.56**	**0.96**
4 Days Poloxamer	M74	730	4
	M78	641	3
	M90	741	4.2
	M82	579.1	2.6
	480BF	510.68	3.7
	BU65	764.3	2.2
ave		**661.01**	**3.28**
stdev		**101.52**	**0.81**
Total Average		**675.7**	**3.5**
Total St Dev		**134.4**	**1.0**

Table 2. Matrix Damage (total surface fissure length) Data for all rabbits

Matrix Damage (mm)			
		Un-impacted	Impacted
time zero	BU62	3.904468085	26.15521277
	BU63	0	8.226702128
	BU64	0.942659574	2.036914894
	BB3	0	8.365744681
	Average	**1.211781915**	**11.19614362**
	St Dev	**1.84930766**	**10.40022374**
4 Days No Poloxamer	481BF	0.796702128	6.747659574
	BU66	0	4.297765957
	BU60	0	2.558617021
	BU61	5.112978723	16.67085106
	Average	**1.477420213**	**7.568723404**
	St Dev	**2.452631496**	**6.306694917**
4 Days Poloxamer	M74	13.95170213	26.6543617
	M90	11.07319149	19.24531915
	480BF	0.620212766	5.912234043
	BU65	2.878085106	18.76308511
	Average	**7.130797872**	**17.64375**
	St Dev	**6.391152389**	**8.614668203**

Table 3. Time Zero group cell viability counts

	Controls Super	% Dead Middle	Deep	Total		test Super	% Dead Middle	Deep	Total
6jc1a	7.67	9.63	8.20	8.54	6jt1a	23.71	33.82	44.32	31.70
6jc2a	19.77	21.71	11.00	17.70	6jt2b	21.35	22.35	29.58	23.60
6jc3a	8.37	12.54	0.00	9.45	6jt3a	58.79	41.52	16.67	41.29
6jc4a	8.66	6.21	14.94	8.78	6jt4a	22.99	29.91	32.37	28.97
6jc5a	2.94	5.47	9.34	5.51	6jt5a	32.96	23.40	31.32	28.01
6jc6a	16.32	18.90	8.33	15.39	6jt6a	8.40	9.29	19.12	11.43
6jc7a	8.31	11.51	11.06	10.27	6jt7a	25.48	16.92	19.97	19.84
					6jt8a	7.72	13.10	25.00	13.29
avg	8.71	12.28	10.48	9.66		20.37	23.79	24.86	24.77
std dev	4.30	6.11	2.51	3.24		9.19	10.86	6.38	9.89
6jc1a	12.00	6.83	26.87	11.88	6jt1b	34.02	25.20	33.33	29.68
6jc3a	14.83	16.61	37.35	18.81	6jt2b	13.14	22.18	14.57	16.99
6jc4a	16.78	15.50	13.99	15.36	6jt3a	41.10	34.64	22.02	31.01
6jc5b	10.94	8.53	6.96	8.68	6jt4b	21.66	16.55	24.58	19.69
					6jt5a	9.65	20.26	28.54	20.83
					6jt6a	55.84	37.40	35.92	40.89
avg	13.64	11.87	15.94	13.68		29.24	26.04	28.88	23.64
std dev	2.66	4.91	10.10	4.37		17.73	8.27	5.81	6.30
BU62La	1.32	16.32	9.23	12.13	BU62Ra	41.10	48.65	28.10	38.63
BU62Lb	6.02	3.15	14.51	6.96	BU62Rb	36.29	58.79	37.75	46.20
BU62Lc	4.84	15.34	21.64	12.89	BU62Rc	4.70	14.25	20.22	13.84
BU62Ld	17.72	10.21	16.07	13.51	BU62Rd	22.42	2.54	20.39	11.53
BU62Le	4.12	6.49	19.39	8.88	BU62Re	57.55	61.76	44.90	55.36
BU62Lf	7.09	4.03	34.72	11.81	BU62Rf	16.67	10.24	14.17	11.95
BU62Lg	3.80	3.98	12.40	5.63	BU62Rg	44.44	31.17	21.20	29.42
BU62Lh	13.33	4.88	7.39	7.66					
Average	5.79	8.05	14.37	9.93		31.88	32.49	23.64	29.56
St Dev	3.79	5.28	5.16	3.01		18.17	24.28	8.21	17.83
BU63La	14.47	18.90	8.81	15.45	BU63Ra	28.46	12.48	5.87	12.19
BU63Lb	2.53	9.66	5.71	7.62	BU63Rb	49.66	9.40	19.70	18.40
BU63Lc	2.17	2.29	4.56	3.14	BU63Rc	59.47	39.85	25.45	41.66
BU63Ld	3.87	0.88	3.57	2.33	BU63Rd	84.31	36.67	18.23	34.37
BU63Le	14.81	7.59	8.83	8.74	BU63Re	75.29	35.49	33.91	45.41
BU63Lf	1.69	6.63	9.79	6.91	BU63Rf	89.16	46.12	47.95	56.35
BU63Lg	13.16	6.19	29.13	14.32	BU63Rg	58.82	15.29	27.66	29.62

BU63Lh	6.81	5.87	3.09	5.39	BU63Rh	55.94	25.59	11.30	30.60
Average	7.44	5.59	6.34	7.99		67.52	27.61	20.30	33.57
St Dev	5.79	3.03	2.77	4.78		15.30	13.90	9.66	14.33
BU64La	5.93	3.92	11.41	6.72	BU64Ra	37.86	41.87	27.59	38.10
BU64Lb	16.33	3.00	1.65	4.04	BU64Rb	27.35	36.60	19.58	31.71
BU64Lc	5.13	7.65	7.35	7.38	BU64Rc	58.33	25.52	15.91	30.96
BU64Ld	22.22	5.28	14.02	9.96	BU64Rd	65.27	38.10	23.36	41.02
BU64Le	17.65	7.01	7.28	8.43	BU64Re	48.98	35.61	17.74	31.48
BU64Lf	3.96	9.31	12.23	9.32	BU64Rf	4.17	27.06	16.38	21.65
BU64Lg	14.68	5.43	7.33	7.42					
BU64Lh	11.57	11.79	12.20	11.83					
Average	12.18	5.94	10.26	8.72		47.56	34.13	18.59	34.65
St Dev	6.66	2.19	2.86	1.79		15.28	6.45	3.02	4.60
BB3La	24.01	11.99	25.76	18.05	BB3Ra	58.18	33.05	26.92	40.00
BB3Lb	31.95	25.74	10.77	23.20	BB3Rb	96.94	79.41	21.43	75.51
BB3Lc	20.69	11.48	26.86	17.52	BB3Rc	70.65	35.94	14.61	33.33
BB3Ld	15.63	24.79	7.50	17.74	BB3Re	69.00	47.97	15.25	45.10
					BB3Rf	76.50	42.97	6.83	38.38
					BB3Rg	48.00	39.52	31.30	38.13
					BB3Rh	87.39	48.33	15.23	41.73
Average	20.11	18.50	17.72	17.77		72.38	41.30	18.80	39.45
St Dev	4.22	7.82	10.01	0.27		16.61	6.27	8.32	3.94

Table 4. 4 Day No Poloxomer cell viability counts

	Controls	% Dead				test	% Dead		
	Super	Middle	Deep	Total		Super	Middle	Deep	Total
M406jc1a	14.80	15.09	12.08	14.43	M406jt1a	15.15	21.50	14.29	18.02
M406jc2a	8.45	8.89	7.95	8.60	M406jt4a	27.88	29.29	20.43	27.23
M406jc3a	12.28	20.00	13.66	15.51	M406jt5a	18.87	20.11	20.14	19.81
M406jc4a	36.67	22.08	8.68	18.37	M406jt6a	34.53	27.97	17.34	25.63
M406jc5a	16.37	11.52	16.04	14.23					
Average	12.98	15.52	11.68	15.63		20.63	24.72	19.30	22.67
St Dev	3.45	5.55	3.39	1.91		6.55	4.59	1.70	4.45
M72La2	58.06	40.61	27.82	43.68	M72Ra	13.04	5.24	11.97	9.00
M72Lb	16.33	11.89	25.24	16.15	M72Rb	25.89	27.01	22.52	25.34
M72Lc	18.37	10.48	28.22	17.68	M72Rc	33.03	51.69	49.67	46.05
M72Ld	7.94	11.53	46.89	20.07	M72Rd	84.73	64.17	31.97	60.68
M72Le	2.47	2.77	7.04	3.93	M72Re	53.39	43.21	49.74	48.01
M72Lf	16.67	8.52	10.69	10.90	M72Rf	59.52	50.89	1.96	48.43
M72Lg	6.74	13.71	12.78	11.05	M72Rg	18.13	5.76	6.92	8.70
M72Lh	10.66	11.21	29.57	15.91	M72Rh	40.00	25.40	23.32	27.72
M72Li	16.51	4.51	6.32	7.77	M72Ri	6.03	15.04	41.07	16.77
Average	11.96	9.33	18.46	12.93		31.13	32.04	26.57	32.30
St Dev	5.83	3.82	10.16	5.45		19.04	21.40	17.82	19.08
481BFLa	5.29	6.01	2.72	5.00	481BFRa	94.00	47.33	5.80	41.77
481BFLb	12.93	0.99	6.40	4.79	481BFRb	42.16	59.00	37.93	49.86
481BFLc	6.45	8.00	11.34	8.73	481BFRc	61.45	14.51	8.21	22.69
481BFLd	7.92	14.04	13.77	12.50	481BFRd	64.13	25.09	29.30	37.05
481BFLe	5.02	4.13	9.63	5.52	481BFRe	40.54	15.69	28.02	22.50
481BFLf	12.66	7.69	12.07	9.84	481BFRf	85.09	14.79	10.34	26.36
Average	8.38	5.36	10.64	6.78		64.56	23.48	19.93	33.37
St Dev	3.57	2.89	2.80	2.34		21.80	14.03	13.46	11.29
BU66La	17.13	11.11	7.63	12.01	BU66Ra	28.38	34.76	25.00	31.16
BU66Lb	5.00	1.55	6.32	3.65	BU66Rb	29.24	22.86	27.98	25.94
BU66Lc	3.74	3.39	2.71	3.32	BU66Rc	63.25	16.82	33.17	33.04
BU66Ld	3.80	2.47	8.20	3.89	BU66Rd	32.20	18.87	9.94	20.30
BU66Le	9.20	2.83	6.02	4.83	BU66Re	52.30	28.27	11.99	28.08
BU66Lf	2.70	6.97	1.55	4.98	BU66Rf	42.11	29.97	46.75	36.35
BU66Lg	9.77	6.87	17.82	9.72	BU66Rg	48.47	27.05	19.62	32.37
BU66Lh	25.29	15.75	10.53	15.26	BU66Rh	43.51	15.21	14.84	21.27
Average	7.33	5.03	6.14	6.06		39.46	24.23	20.36	28.56
St Dev	5.13	3.42	3.12	3.40		9.57	6.92	8.69	5.74
BU60La	60.00	20.30	13.27	27.85	BU60Ra	57.24	29.10	8.70	31.60
BU60Lb	21.90	9.72	9.68	13.74	BU60Rb	76.83	25.24	5.30	28.12
BU60Lc	6.25	4.17	15.73	7.96	BU60Rc	40.37	16.90	14.38	19.84
BU60Ld	37.38	23.81	21.65	27.52	BU60Rd	66.15	27.32	9.09	32.82
BU60Le	20.75	8.85	9.28	11.41	BU60Re	47.97	26.25	3.29	28.22

BU60Lf	14.29	3.66	4.55	5.54	BU60Rf	38.81	29.92	10.19	26.49
					BU60Rg	88.74	30.80	27.68	44.93
					BU60Rh	65.56	43.04	80.91	56.50
Average	20.11	11.75	10.50	15.67		60.21	26.50	11.23	30.29
St Dev	11.49	8.42	4.26	9.72		17.59	4.68	8.07	7.69
BU61La	3.85	9.19	12.02	9.35	BU61Ra	8.57	18.09	3.74	11.87
BU61Lb	12.50	18.32	27.54	20.26	BU61Rb	5.26	8.33	14.17	8.94
BU61Lc	0.00	10.47	15.89	11.51	BU61Rc	0.00	0.99	12.77	3.56
BU61Ld	5.41	11.39	29.67	15.66	BU61Rd	18.53	10.63	21.05	14.86
BU61Le	28.89	17.96	31.67	23.18	BU61Re	16.77	17.13	7.89	13.58
BU61Lf	2.78	7.66	6.11	6.72	BU61Rf	6.45	9.68	7.89	8.85
BU61Lg	4.65	7.64	5.33	6.62	BU61Rg	9.21	7.99	23.53	13.42
					BU61Rh	10.90	17.63	33.19	20.87
Average	4.86	11.80	18.32	13.33		9.46	12.78	13.01	10.73
St Dev	4.19	4.54	11.22	6.56		6.03	4.61	7.25	3.91

Table 5. 4 Day Poloxomer Group cell viability counts

	Controls	% Dead				test	% Dead		
	Super	Middle	Deep	Total		Super	Middle	Deep	Total
M74LFT1a	3.82	5.19	6.29	5.10	M74RT1a	25.97	14.63	9.22	15.54
M74LFT2a	14.63	30.15	6.08	21.93	M74RT2a	38.76	8.10	26.28	20.09
M74LFT3a	2.04	1.48	0.00	1.46	M74RT3a	9.06	9.76	38.00	15.61
R74LFT4a	9.22	12.70	9.38	11.08					
Average	5.03	6.46	7.25	5.88		24.60	10.83	24.50	17.08
St Dev	3.74	5.72	1.84	4.86		14.90	3.39	14.47	2.61
M82L1	13.97	9.66	10.71	11.28	M82R1	7.27	3.43	8.65	5.51
M82L2	65.85	45.96	32.84	45.68	M82R2	13.66	8.74	20.71	13.33
M82L3	2.31	3.00	15.55	6.85	M82R3	7.77	5.41	13.16	7.54
M82L4	4.62	5.21	19.64	8.07	M82R4	32.57	20.05	19.05	23.29
M82L5	6.43	7.47	4.73	6.54	M82R5	30.52	11.20	5.50	17.41
M82L6	1.05	0.79	10.64	2.61	M82R6	70.18	31.17	6.41	35.59
M82L7	9.78	2.95	13.86	7.68					
Average	6.36	4.85	12.52	7.17		18.36	9.77	12.25	13.42
St Dev	4.84	3.27	5.08	2.80		12.32	6.48	6.50	7.26
M78LFT1a	1.60	0.24	0.00	0.40	M78RT1a	2.34	0.77	1.69	1.47
M78LFT2a	2.78	3.07	7.54	4.26	M78RT4a	21.52	13.89	10.63	15.57
M78LFT4a	17.91	12.88	16.75	15.05	M78RT5a	27.61	7.86	4.17	10.89
M78LFT5a	2.41	4.99	1.38	3.57	M78RT6a	1.33	5.33	6.60	4.83
M78LFT6a	4.39	3.93	5.59	4.46					
Average	2.79	3.06	3.63	3.17		13.20	4.65	4.15	8.19
St Dev	1.17	2.03	3.53	1.89		13.36	3.59	2.46	6.27
M90L1	31.15	15.73	7.84	16.06	M90R1	55.38	21.48	25.56	27.15
M90L2	0.00	0.22	0.00	0.17	M90R2	89.33	95.80	77.27	91.29
M90L3	82.72	38.03	24.22	44.06	M90R3	35.85	32.25	21.27	29.66
M90L5	80.79	54.98	28.22	55.23	M90R4	14.29	12.75	7.78	11.95
M90L6	11.68	4.14	3.77	6.70	M90R5	50.98	61.27	12.93	40.70
Average	41.27	14.53	12.81	24.44		39.12	31.94	16.88	27.36
St Dev	38.60	17.00	12.63	24.02		18.55	21.12	8.02	11.84
480BFLa	19.13	9.56	2.52	10.18	480BFRa	35.09	15.24	23.62	24.69
480BFLb	17.47	4.72	3.61	7.90	480BFRb	27.59	6.09	8.87	11.59
480BFLc	10.39	2.16	5.26	3.79	480BFRc	8.49	3.47	5.07	5.16
480BFLd	29.79	13.03	7.10	12.71	480BFRd	15.38	11.68	9.68	11.62
480BFLe	31.46	2.47	3.53	6.27	480BFRe	16.59	9.45	4.72	9.99
480BFLf	16.07	13.66	7.53	13.09	480BFRf	4.55	2.19	5.88	3.99
480BFLg	13.04	6.79	3.49	6.41	480BFRg	27.19	3.98	9.45	10.77

480BFLh	3.67	1.18	4.43	2.61	480BFRh	15.79	9.72	7.58	11.22
Average	17.63	6.70	4.68	7.87		18.83	7.73	7.32	9.19
St Dev	9.35	4.92	1.81	3.87		10.34	4.54	2.10	3.22
BU65La	5.94	8.04	2.53	5.91	BU65Ra	40.28	34.47	5.47	27.05
BU65Lb	3.16	4.35	6.14	4.73	BU65Rb	44.67	24.54	11.41	24.08
BU65Lc	21.52	9.50	7.33	9.96	BU65Rc	64.90	29.22	4.47	24.07
BU65Ld	25.00	7.35	15.18	13.19	BU65Rd	60.30	44.71	12.90	38.97
BU65Le	1.35	0.93	7.64	3.34	BU65Re	48.78	23.61	3.16	20.00
BU65Lf	13.51	4.55	8.66	7.06	BU65Rf	12.12	4.56	3.79	5.88
BU65Lg	7.98	2.78	10.45	6.86	BU65Rg	40.33	23.71	1.99	22.03
BU65Lh	2.35	3.50	26.82	10.70	BU65Rh	30.07	23.65	5.30	19.35
Average	10.10	5.13	8.28	7.72		47.05	29.13	5.08	22.76
St Dev	9.03	2.91	3.90	3.31		12.13	7.98	3.04	2.88

Appendix C: Chapter 3 Raw Data

Table 1. Mechanical data for the high rate of loading "with GlcN" (1-28) and "no GlcN" (29- 56) explants

Specimen	Time to Peak	Peak Stress	Peak Strain	Thickness
	[s]	*[MPa]*		*[mm]*
1	0.034	28.954	0.374	0.615
2	0.032	28.479	0.397	0.638
3	0.031	28.529	0.606	0.593
4	0.033	28.830	0.539	0.550
5	0.04	28.411	0.526	0.545
6	0.036	28.404	0.573	0.556
7	0.032	28.299	0.481	0.634
8	0.04	28.319	0.539	0.590
9	0.028	28.918	0.532	0.597
10	0.037	28.784	0.681	0.793
11	0.031	28.760	0.515	0.814
12	0.034	28.852	0.568	0.663
13	0.029	28.692	0.483	0.659
14	0.038	28.670	0.479	0.617
15	0.034	28.705	0.528	0.735
16	0.033	28.749	0.479	0.856
17	0.029	28.952	0.529	0.738
18	0.033	28.620	0.625	0.742
19	0.026	29.024	0.571	0.789
20	0.036	28.462	0.445	0.678
21	0.027	28.010	0.525	0.634
22	0.039	27.408	0.491	0.687
23	0.039	27.454	0.468	0.777
24	0.036	28.061	0.508	0.906
25	0.039	27.346	0.442	0.725
26	0.04	27.261	0.469	0.512
27	0.034	28.090	0.605	0.931
28	0.037	27.379	0.523	0.690
Average	**0.034**	**28.315**	**0.517**	**0.681**
Std. Dev.	**0.004**	**0.575**	**0.065**	**0.112**

Specimen	Time to Peak	Peak Stress	Peak Strain	Thickness
	[s]	*[MPa]*		*[mm]*
29	0.039	29.128	0.676	0.530
30	0.031	28.849	0.559	0.566
31	0.034	28.840	0.457	0.603
32	0.036	28.777	0.504	0.338
33	0.030	28.921	0.617	0.548
34	0.031	29.183	0.536	0.609
35	0.031	28.630	0.483	0.657
36	0.032	28.764	0.471	0.715
37	0.029	28.858	0.610	0.546
38	0.025	28.620	0.569	0.685
39	0.034	28.986	0.475	0.698
40	0.034	28.960	0.563	0.722
41	0.029	29.060	0.529	0.677
42	0.033	29.032	0.530	0.597
43	0.037	28.579	0.494	0.695
44	0.032	28.865	0.509	0.587
45	0.025	29.339	0.537	0.787
46	0.029	29.550	0.676	0.732
47	0.032	28.918	0.664	0.601
48	0.026	28.192	0.647	0.871
49	0.034	28.757	0.514	0.688
50	0.033	28.405	0.524	0.696
51	0.038	28.069	0.582	0.604
52	0.033	28.444	0.608	0.987
53	0.036	28.514	0.543	0.763
54	0.037	28.011	0.480	0.725
55	0.039	27.789	0.539	0.612
56	0.040	27.808	0.613	0.549
Average	**0.033**	**28.641**	**0.551**	**0.661**
Std. Dev.	**0.004**	**0.473**	**0.062**	**0.116**

Table 2. Mechanical data for the low rate of loading "with GlcN" (57-84) and "no GlcN" (85-112) explants

Specimen	Time to Peak	Peak Stress	Peak Strain	Thickness
	[s]	*[MPa]*		*[mm]*
57	0.901	29.372	0.576	0.437
58	0.879	29.370	0.637	0.425
59	0.797	29.452	0.588	0.648
60	0.800	29.471	0.686	0.687
61	0.875	29.367	0.569	0.534
62	0.858	29.390	0.664	0.548
63	0.878	29.391	0.697	0.585
64	0.833	29.449	0.716	0.744
65	0.830	29.396	0.722	0.696
66	0.883	29.413	0.639	0.638
67	0.954	28.931	0.525	0.606
68	0.954	28.945	0.628	0.561
69	0.948	28.918	0.651	0.571
70	0.948	28.893	0.622	0.383
71	0.941	28.934	0.687	0.585
72	0.955	28.905	0.499	0.642
73	0.936	28.914	0.571	0.616
74	0.948	28.939	0.546	0.553
75	0.941	28.939	0.608	0.802
76	0.947	28.941	0.595	0.723
77	0.878	28.075	0.536	0.776
78	0.866	28.247	0.659	0.973
79	0.840	28.162	0.579	0.818
80	0.912	28.038	0.570	0.713
81	0.823	28.169	0.692	0.914
82	0.895	28.223	0.521	0.721
83	0.837	28.087	0.582	0.590
84	0.903	28.205	0.564	0.646
Average	**0.890**	**28.833**	**0.615**	**0.653**
Std. Dev.	**0.049**	**0.521**	**0.062**	**0.135**

Specimen	Time to Peak	Peak Stress	Peak Strain	Thickness
	[s]	*[MPa]*		*[mm]*
85	0.823	29.467	0.619	0.574
86	0.828	29.529	0.715	0.747
87	0.874	29.432	0.625	0.583
88	0.886	29.452	0.578	0.552
89	0.880	29.409	0.556	0.523
90	0.861	29.452	0.636	0.681
91	0.886	29.411	0.540	0.452
92	0.840	29.452	0.605	0.708
93	0.826	29.524	0.655	0.949
94	0.852	29.426	0.645	0.649
95	0.941	28.882	0.413	0.569
96	0.945	28.916	0.536	0.700
97	0.945	28.868	0.612	0.550
98	0.946	28.882	0.550	0.468
99	0.943	28.880	0.481	0.411
100	0.983	28.927	0.569	0.592
101	0.946	28.895	0.491	0.627
102	0.942	28.939	0.584	0.653
103	0.934	28.921	0.631	0.675
104	0.910	28.973	0.712	0.889
105	0.870	28.306	0.572	0.839
106	0.867	28.260	0.644	0.908
107	0.857	28.156	0.622	0.720
108	0.925	28.208	0.600	0.713
109	0.866	28.188	0.685	0.875
110	0.854	28.151	0.628	0.597
111	0.916	28.113	0.485	0.642
112	0.912	28.139	0.556	0.623
Average	**0.895**	**28.851**	**0.590**	**0.662**
Std. Dev.	**0.043**	**0.529**	**0.068**	**0.133**

Table 3. Total length of surface fissures for the high rate of loading "with GlcN" (1-28) and "no GlcN" (29-56) explants

Specimen	Surface Fissure Length
	[mm]
1	11.574
2	12.575
3	47.798
4	21.272
5	32.920
6	37.343
7	36.256
8	45.666
9	30.735
10	45.101
11	40.625
12	27.741
13	29.936
14	13.609
15	26.345
16	49.226
17	35.766
18	48.512
19	48.906
20	11.126
21	17.861
22	16.551
23	29.659
24	30.885
25	7.417
26	32.238
27	47.488
28	37.865
Average	**31.480**
Std. Dev.	**13.315**

Specimen	Surface Fissure Length
	[mm]
29	40.615
30	53.915
31	35.265
32	14.622
33	56.803
34	40.966
35	50.718
36	25.471
37	48.885
38	54.458
39	54.458
40	29.659
41	39.005
42	15.741
43	38.888
44	72.107
45	46.870
46	59.243
47	56.750
48	13.460
49	17.542
50	63.176
51	37.716
52	47.989
53	53.339
54	53.670
55	55.247
56	48.107
Average	**42.787**
Std. Dev.	**15.273**

Table 4. Number of dead cells per fissure, per millimeter of fissure depth, and percentage of dead cells in each zone for the high rate of loading "with GlcN" (1-28) and "no GlcN" (29-56) explants

Spec	Dead Cells per Depth	Dead Cells per fissure	Superficial	Middle	Deep
			% Dead cells	% Dead cells	% Dead cells
1	271.244	45.5	47.57%	9.30%	9.23%
2	589.093	79	74.68%	14.90%	17.29%
3	395.119	69	25.61%	21.90%	4.76%
4	576.166	54	38.33%	9.45%	12.50%
5	740.307	67	28.09%	13.13%	3.88%
6	165.768	72	44.64%	23.41%	19.35%
7	203.675	23	28.99%	3.67%	7.84%
8	103.434	10.5	20.00%	14.47%	3.45%
9	344.611	59	37.50%	15.19%	9.03%
10	167.447	27	32.99%	8.66%	4.61%
11	492.672	61	57.07%	14.10%	14.77%
12	656.843	28	15.79%	21.22%	2.60%
13	763.862	121	52.19%	7.65%	5.56%
14	867.998	187	35.00%	76.66%	30.51%
15	621.828	45	53.49%	49.02%	58.87%
16	252.752	32	14.25%	1.44%	0.64%
17	494.330	43	38.52%	30.18%	5.59%
18	50.331	10	6.56%	8.39%	30.26%
19	52.011	11	8.21%	27.74%	31.71%
20	195.570	12	4.72%	4.39%	3.94%
21	485.298	76	23.08%	37.58%	18.37%
22	411.184	50	28.28%	13.40%	94.95%
23	76.046	6.5	13.85%	9.18%	23.08%
24	364.015	70	42.86%	12.59%	7.74%
25	877.514	144	51.85%	15.64%	23.53%
26	295.421	18.5	34.88%	12.56%	8.96%
27	288.147	48	36.59%	16.04%	18.26%
28	92.807	25.5	31.31%	6.78%	3.64%
Average	**384.036**	**52.083**	**32.81%**	**17.57%**	**16.75%**
Std. Dev.	**242.015**	**40.722**	**16.46%**	**15.34%**	**19.51%**

Spec	Dead Cells per Depth	Dead Cells per fissure	Superficial	Middle	Deep
			% Dead cells	% Dead cells	% Dead cells
29	1343.968	39.5	87.64%	30.51%	4.30%
30	1111.769	30	76.83%	18.09%	1.89%
31	506.197	38	60.40%	42.13%	10.23%
32	715.533	62	41.67%	64.03%	16.83%
33	229.293	21	88.64%	23.23%	6.50%
34	778.702	81	56.90%	19.49%	0.82%
35	640.310	67	64.20%	19.65%	21.24%
36	849.974	89	36.36%	11.50%	21.97%
37	625.101	43.5	53.70%	53.52%	38.10%
38	1294.306	138	23.33%	27.37%	39.51%
39	1000.114	90	44.93%	49.46%	21.78%
40	403.560	98	87.64%	83.08%	20.00%
41	631.756	153	26.76%	17.33%	2.13%
42	384.203	58	77.08%	86.73%	32.26%
43	1075.168	120	74.53%	59.23%	8.00%
44	1451.708	254	63.30%	56.44%	11.71%
45	1036.651	199	35.65%	11.88%	0.00%
46	910.239	89	55.56%	72.88%	62.64%
47	850.355		77.50%	75.59%	43.17%
48	1965.854	205	48.59%	43.50%	17.50%
49	766.297	84	44.87%	7.54%	16.89%
50	243.619	17.5	48.62%	26.36%	14.04%
51	823.129	121	60.38%	29.33%	24.00%
52	431.722	92	32.89%	17.91%	22.81%
53	568.862	88.5	63.77%	14.93%	10.26%
54	615.385	36	75.31%	21.01%	26.62%
55	1919.585	82	49.69%	8.77%	17.46%
56	994.941	61	40.16%	25.00%	15.15%
Average	**831.779**	**90.150**	**56.30%**	**35.08%**	**18.31%**
Std. Dev.	**438.445**	**55.038**	**18.50%**	**23.85%**	**14.09%**

Table 5. Number of dead cells per fissure, per millimeter of fissure depth, and percentage of dead cells in each zone for the low rate of loading "with GlcN" (57-84) and "no GlcN" (85-112) explants

Spec	Dead Cells per Depth	Dead Cells per fissure	Superficial	Middle	Deep
			% Dead cells	% Dead cells	% Dead cells
57	729.990	44.5	59.76%	21.51%	12.61%
58	1285.474	98	74.32%	26.29%	16.42%
59	276.380	28.5	52.17%	18.11%	6.33%
60	502.623	47	68.09%	9.31%	9.68%
61	406.038	31.5	30.83%	4.92%	4.27%
62	244.451	42	26.67%	10.34%	5.26%
63	338.911	47	50.65%	12.05%	2.86%
64	101.608	11	39.13%	3.80%	1.67%
65	250.448	29	46.91%	22.73%	13.95%
66			18.03%	13.28%	15.71%
67	712.474	158	58.46%	30.19%	6.73%
68	1849.571	127	47.44%	25.29%	97.70%
69	1238.857	102	43.30%	12.50%	5.13%
70	1602.702	214	66.09%	54.25%	8.64%
71	305.938	73	41.38%	21.70%	12.24%
72	917.397	72	37.69%	7.42%	2.78%
73	667.539	113	27.71%	63.56%	27.56%
74	1003.215	160	36.73%	41.48%	23.39%
75	729.990	44.5	57.80%	22.03%	16.82%
76	1285.474	98	46.58%	23.74%	6.77%
77	276.380	28.5	64.00%	14.46%	17.86%
78	502.623	47	72.73%	12.82%	7.96%
79	406.038	31.5	58.76%	35.03%	17.91%
80	244.451	42	25.00%	6.25%	23.21%
81	1096.694	121	41.18%	11.01%	14.00%
82	338.911	47	57.35%	23.67%	8.18%
83	101.608	11	66.67%	14.58%	8.16%
84	250.448	29	53.45%	26.67%	22.62%
Average	**664.740**	**72.103**	**48.89%**	**21.04%**	**14.87%**
Std. Dev.	**467.848**	**50.385**	**15.20%**	**14.13%**	**17.68%**

Spec	Dead Cells per Depth	Dead Cells per fissure	Superficial	Middle	Deep
			% Dead cells	% Dead cells	% Dead cells
85	1164.815	160	61.76%	59.04%	19.80%
86	621.316	70	78.38%	64.00%	37.04%
87	1065.220	182	81.82%	56.68%	29.71%
88	1488.102	67.5	77.06%	25.96%	14.71%
89	708.396	89	83.56%	32.38%	12.50%
90	809.758	126	64.08%	16.67%	17.48%
91	930.205	108	58.33%	33.74%	26.27%
92	990.388	84	72.34%	49.22%	16.16%
93	1209.386	87	38.54%	20.91%	2.60%
94	1298.088	274	64.08%	46.41%	34.33%
95	652.543	94	43.48%	25.40%	4.23%
96	946.971	72.5	67.95%	11.58%	10.62%
97	931.217	62.5	44.26%	19.67%	6.58%
98	896.670	142	66.00%	34.29%	21.71%
99	808.595	109.5	64.84%	22.86%	12.33%
100	1286.551	244	80.56%	54.01%	9.85%
101	703.538	149	44.23%	69.09%	23.31%
102	662.031	216	68.18%	53.42%	22.40%
103	398.012	77	50.00%	9.17%	13.75%
104	646.105	62	87.50%	28.24%	11.96%
105	522.482	54	66.67%	29.02%	9.62%
106	1360.639	131	72.15%	30.57%	16.67%
107	611.612	72	41.94%	15.61%	8.70%
108	645.588	50.5	57.14%	6.09%	3.15%
109	907.029	80	51.30%	25.48%	28.21%
110	479.660	35	37.96%	2.27%	0.88%
111	1151.738	92	64.37%	34.66%	19.67%
112	925.558	162	61.36%	54.12%	16.85%
Average	**898.920**	**110.794**	**62.49%**	**33.23%**	**16.11%**
Std. Dev.	**290.508**	**58.817**	**14.25%**	**18.41%**	**9.41%**

Table 6. Material property values for the theoretical model

	"no GlcN"	"with GlcN"
E_1 (MPa)	7.835	7.835
E_3 (MPa)	1.53	1.53
k_1 ($*10^{-13}$ m^2)	5.95	3.149
k_3 ($*10^{-13}$ m^2)	1.222	0.858

RABBIT PATELLOFEMORAL IMPACT SOP

What to bring with you:
1.) Portable computer w/ A2D board, 2.) LPS lubricant, ethanol, 3.) meter stick, 4.) rabbit data sheets (a copy is attached to the end of this SOP), 5.) blank IBM formatted disks

Pre-test set up: (* Leave portable computer off until all cables are connected)

1. Plug in Valadyne strain gauge amplifier (SGA) to the wall. Turn on the SGA and insure that the trigger release switch (see figure 1) is turned off (down position) to protect from accidental triggering.
2. The SGA will need to be on for 15 minutes in order to allow the electronics to stabilize.
3. Assure that all electronic connections are in place. Figures 2 through 4 carefully detail where all connections should be made.
4. Once you have made all the necessary connections, turn on and start up computer. Computer will give a list of possible configurations, choose "Ethernet configuration".
5. Spray some LPS greaseless lubrication on a rag and wipe down the steel rod and gray rails of the impact cart (see figure 5). Do this very sparingly.
6. Use alchohol to clean the sides of the cart (see figure 5) i.e., the portion of the cart where the brakes act. Keep rabbit hair off the rubber brake pads.
7. After the 15 minutes are up, run the program "rabinsur.vi" located on the portable computers desktop. If the program is running (hit small arrow in the top left of screen in Labview) you will see a readout for the load.
8. Using the small screwdriver, zero the load cell on the SGA. Use the opening to the top left of the black dial (see figure 1). Use the readout in Labview.
9. Calibrate the load cell by depressing and holding the shunt cal switch on the Valadyne strain gauge amplifier. If needed readjust the set point to **3349 N on Labview (or 7.53 Volts on the voltmeter)** by using the Gain knob (See figure 1). **** The values in step 9 are susceptible to change whenever the load cell is changed. Always double check these values with the load cell specifications.

10. Double check to make sure the load cell is still zeroed, adjust if necessary.

Rabbit preparation:

1. On the Data Sheet, record the Rabbit name, weight (kg), and sex.
2. Once the rabbit is fully sedated, pull the left hind foot through the very bottom hole of the leather strap of the holding chair and tuck the rest of the strap under the rabbit so it can be fixated to the underside of the chair.
3. Position the right leg so that the femur is pointing vertical and the impactor is directed to hit the middle of the patella.
4. Place the black strap around the right hind foot and pull tight to insure the foot is fully constrained. It is important that the femur remain vertical, but the tibia can be horizontal in order to flatten the patella. Fix the end of the strap, as well as the leather strap, to the Velcro pad on the underside of the chair.
5. Move the clamping bar into position and attach the free end to the distal clamp.
6. Slowly apply even pressure to both clamps until the clamps lock in place.
7. Slide the chair into position so the patella is directly under the head of the impacting cart.
8. Lower the cart so the head of the impacting cart is just above the patella, checking to insure the patella is centered under the head.
9. Raise the impact cart to the desired height. Measure from top of patella to the bottom of the impactor head using the meter stick (see figure 6)
10. The position of the beam holding the upper brake may need repositioning to accommodate the desired height. Do this by removing the screws of the beam and moving the beam to the desired height above the patella.
11. The height and weight of the sled should be:

Energy	Height	Mass
6 J	0.46meters	1.33kg
10 J	1 meter	1 kg

- figure 5 shows 6 J set-up
- 6 J impacts should see between 500 and 600 N as to where 10 J impacts should see from 900 to 1200 N

Impacting the rabbit:

1. Turn on the trigger enable switch on the Valadyne strain gauge amplifier.
2. Click the arrow at the top left of the Labview interface (the "run" arrow) (see figure 7). This should enable the load readout to be constantly changing (if load readout is already constantly changing then the arrow has already been hit). Then click on the large green START button below the graph area on Labview (button that reads "disabled" in figure 7). WAIT AT LEAST 5 SECONDS BEFORE PROCEEDING.
3. Press the red trigger button on the Valadyne SGA to drop the impact cart.
4. Impact cart will drop and the A/D board will trigger and save the data.
5. Labview will prompt user for a filename and location.
6. Switch the trigger enable switch to disable (down position) before removing the rabbit.
7. Excel will automatically run and a macro will plot the data. Note the peak load and time to peak on the data sheet. Also sketch the graph and note any comments.
8. Choose "save as" from the file menu. Save the file as an Excel Worksheet i.e., ".xls" format. Back up all data files to a floppy disk.
9. ***FOLLOWING IMPACTION OF ALL ANIMALS, REMOVE DISK FROM DRIVE (a:\) AND COPY ALL FILES TO THE (g:\user\bimgrad) DIRECTORY FOR PERMANENT DOCUMENTATION!***
10. When testing is done shut down computer before disconnecting cables.
11. Turn off voltmeter and leave on SGA if more testing is going to be done in the next week.

Figures

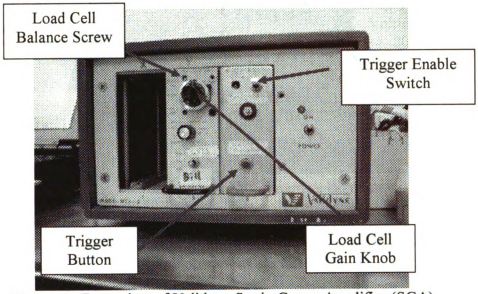

Figure 1. Front view of Validyne Strain Gauge Amplifier (SGA)

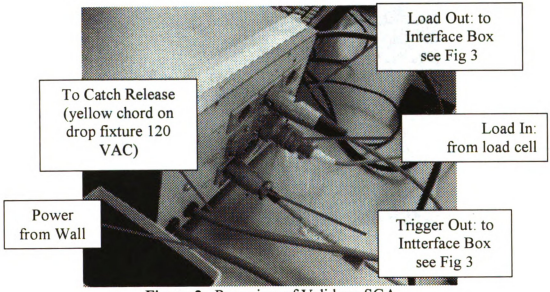

Figure 2. Rear view of Validyne SGA

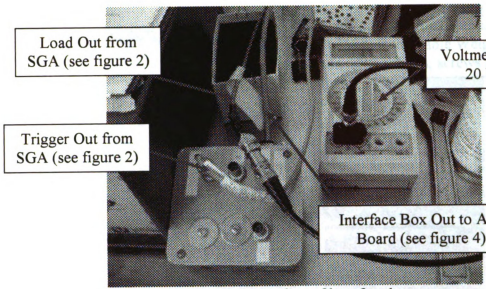

Figure 3. Top view of interface box

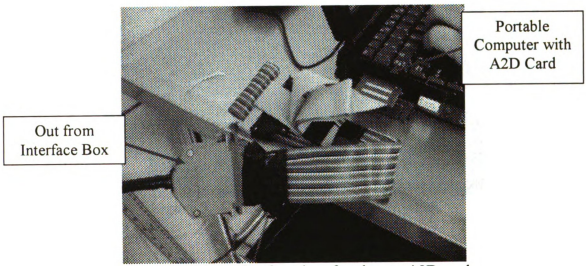

Figure 4. Connection from interface box to A2D card

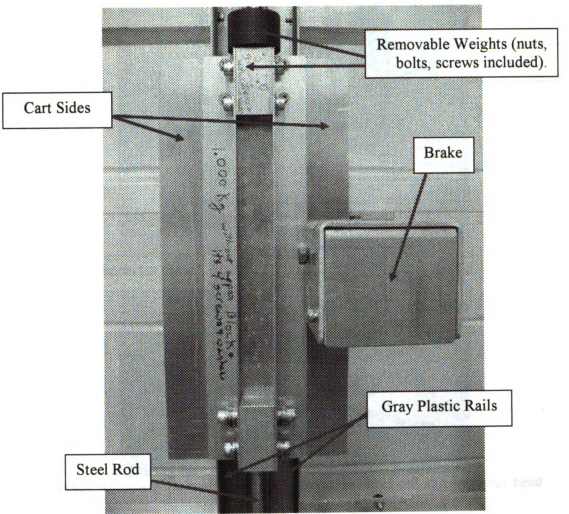

Figure 5. Cart with 1.33 Kg (6 Joule) set up

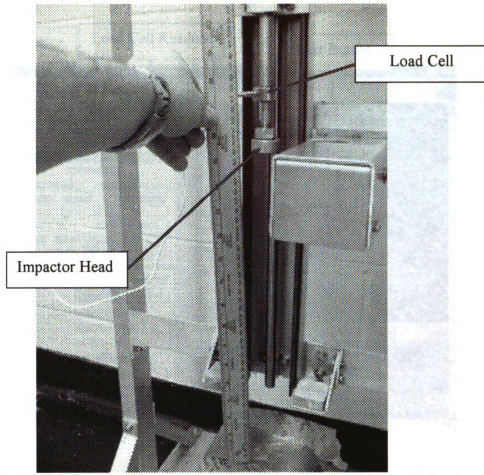

Figure 6. Lower view of impact drop fixture w/ load cell and impactor head

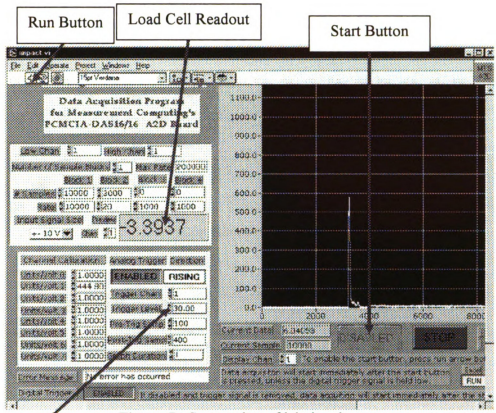

Figure 7. Screen shot of labview layout

**Trigger Value has been changed to 50 in order to prevent accidental triggering